The Influence of Musicianship on Background Neuronal Oscillations: Novel Perspectives

---

Dissertation

zur

Erlangung der naturwissenschaftlichen Doktorwürde
(Dr. sc. nat.)

vorgelegt der

Mathematisch-naturwissenschaftlichen Fakultät

der

Universität Zürich

von
Carina Klein

aus
Deutschland

Promotionskomitee

Prof. Dr. rer. nat. Lutz Jäncke (Vorsitz & Leitung der Dissertation)
Prof. Dr. rer. nat. Stephan Neuhauss
Prof. Dr. sc. nat. Thomas Koenig

Zürich, 2015

Acknowledgements

I would like to express my deepest gratitude to Prof. Dr. Lutz Jäncke for his trust, his motivating and enthusiastic character and giving scientific support in several challenging situations during my Ph.D. Thank you for providing me an environment in which I had the opportunity to follow my ideas and got to acquire a vast knowledge in the field of neuroscience. At this point I would also like to thank Prof. Dr. Stephan Neuhauss for support and co-examination of my dissertation.

I am also very grateful to the whole Sinergia team: Prof. Dr. Thomas Koenig, Prof. Dr. Peter Achermann, Prof. Dr. Daniel Brandeis, Dr. Mara Kottlow, Laura Tüshaus, Anthony Schläpfer, Anja Bänninger and Laura Díaz Hernàndez for support in every way, scientific guidance and mentoring throughout the past three years.

Further, I would like to thank all my colleagues at the Division Neuropsychology for their encouraging support, scientific inputs and especially for many hilarious moments. In particular, I would like to express my gratefulness to Jürgen, Franz and Stefan for their help and many scientific discussions. Thank you Volker, Jürg, Yolanda and Reneé for many profound conversations on various topics and backing. Thank you everybody for providing me such a warm and stimulating working atmosphere.

Thanks also to Dr. Roger Lüchinger for his permanent helpfulness in MR-related problem solving any time when needed and the great cooperation in one of my projects.

The most important thanks go to my family, Fabian and friends for their ongoing support, tremendous encouragement and love.

This work was supported by the Swiss National Science Foundation (SNSF).

Abstract

To date, there is a vast body of literature suggesting that intensive musical training has a profound influence on the functional and structural organization of the human brain. In fact, playing a musical instrument at a professional level constitutes a complex multimodal task that requires the coordinated integration of sensory, motor, haptic, and cognitive functions. Numerous studies have previously shown expertise-related neuronal adaptations during task-based experiments. However, even though results clearly indicate that activation patterns during a task-free resting state (RS) condition do not reflect noise per se, it remains largely unknown whether these specific plastic adaptations are also mirrored during rest and whether neuronal activity is predictive of behavior as a function of musical expertise. In order to shed light on these open questions, three studies were performed constituting this Ph.D. thesis.

In study I we compared whole-brain electroencephalographic functional connectivity during rest between musicians and non-musicians by using a graph-theoretical approach. Based on previous literature, we expected to find that musical training imprints the functional coupling in specific brain regions that have previously been shown to be involved in music perception and production, namely the auditory-related cortex, the somatosensory and motor cortex, as well as cognitive control instances supporting executive functions. Results revealed increased functional connectivity within the obtained network in musicians compared to non-musicians. Most interestingly, functional network characteristics were predictive of musical aptitude.

In study II we went a step further and addressed the question whether neuronal activity prior to stimulus presentation during a working memory task (Sternberg paradigm) is predictive of behavioral performance as reflected by reaction time (RT). In this context, we used electroencephalography (EEG) in combination with a covariance-mapping pro-

cedure in order to examine putative brain-behavior relationships. As a main result, our findings provide clear evidence for a general influence (independent of musical expertise) of neuronal activity across different frequency ranges on performance in RT. In addition, even though musicians and laymen did not differ in terms of response speed, we revealed an expertise-dependent modulation of pre-stimulus activity being predictive for working memory performance.

Study III was not directly related to the influence of musical expertise on neural plasticity, but more likely constitutes a methodological prerequisite for improving future study protocols in the frame of multimodal brain imaging (i. e., the simultaneous acquisition of EEG and magnetic resonance imaging (MRI)). In this context, we examined putative detrimental effects of a high-density EEG setup on MRI data quality (T1- and $T2^*$-weighted images). Taken together, our results revealed a strong sequence-dependent influence on the magnetic resonance (MR) images. In contrast to the functional data that delivered reliable results independent of whether the subjects wore the EEG cap in the scanner or not, morphometric measures of the anatomical images were strongly influenced by the EEG setup.

In summary, professional musical training does not only strongly affect the malleability of brain regions involved in perception, production, and cognitive control. Rather, even during a task-free condition, it seems to shape intrinsic functional connectivity patterns, representing a 'fingerprint' of the respective networks. Furthermore, we found initial evidence for an expertise-related modulation of pre-stimulus neuronal activity having a predictive influence on how the brain entrains itself for solving a working memory task. Finally, future multimodal imaging studies will integrate the knowledge we accumulated from studies I and III with the current idea of functional connectivity during rest, i. e. at least to a certain degree, reflecting a neurophysiological marker for the underlying anatomical connections.

Zusammenfassung

Ein musikalisches Instrument auf professionellem Niveau zu beherrschen, setzt die Integration verschiedenster Gehirnfunktionen voraus. Sowohl während des Musizierens als auch des Zuhörens werden auditorische, somatosensorische und motorische Areale sowie Gehirngebiete, welche kognitive Funktionen steuern, aktiviert. Im Rahmen zahlreicher Quer- und Längsschnittstudien wurde über die letzten Jahrzehnte wiederholt gezeigt, dass intensives musikalisches Training einen Einfluss auf die funktionelle wie auch strukturelle Organisation des menschlichen Gehirns hat. Im Gegensatz zu diesen Erkenntnissen, welche primär aus aufgabenbasierten Studien stammen, bleibt bis heute jedoch weitgehend unbeantwortet, ob Musiker und Nichtmusiker eine unterschiedliche Gehirnaktivität während eines Ruhezustandes aufweisen, oder ob neuronale Aktivität gar prädiktiv für künftiges Verhalten ist. Um diesen Fragen auf den Grund zu gehen, setzt sich die vorliegende Dissertation aus drei Studien zusammen.

In Studie I wurde untersucht, ob sich Musiker und Nichtmusiker in funktionellen Konnektivitätsmassen während eines Ruhezustandes unterscheiden. Mit Hilfe der Elektroenzephalographie (EEG) wurde anhand einer graphtheoretischen Analyse gezeigt, dass Musiker zwischen jenen Gehirnregionen, welche sowohl bei der Verarbeitung eines musikalischen Reizes als auch während des Musizierens beteiligt sind, eine erhöhte funktionelle Konnektivität aufweisen und diese positiv mit der musikalischen Fähigkeit korreliert. Betroffene Gebiete waren der auditorische Kortex, der somatosensorische, Motor- und Präfrontalkortex und das Broca-Areal.

Weiterführend zu den Befunden der ersten Studie wurde in Studie II die elektrophysiologische Aktivität während der Prästimulusperiode einer Arbeitsgedächtnisaufgabe (Sternberg-Paradigma) untersucht. Ziel war es herauszufinden, ob zum einen die Gehirnaktivität in dieser Periode prädiktiv für nachfolgendes Verhalten (Reaktionszeit) ist und zum

anderen, ob sich Musiker auf neuronaler Ebene in der Vorbereitung auf das Stimulusmaterial im Vergleich zur Kontrollgruppe unterscheiden. Die Ergebnisse der Kovarianzanalysen zeigten einen allgemeinen Zusammenhang zwischen Gehirnaktivität und nachfolgender Leistungsfähigkeit sowie ein expertise-spezifisches Aktivierungsmuster.

Im Gegensatz zu den ersten beiden Studien befasste sich Studie III nicht mit musikalischer Expertise, sondern intendierte der Verbesserung von Studienprotokollen multimodaler Bildgebungsverfahren, im Speziellen der simultanen Aufnahme von EEG und magnetresonanztomografischen (MR) Daten. Insbesondere wurde der Einfluss des EEG-Systems auf die Qualität funktioneller ($T2^*$-gewichteter) und anatomischer (T1-gewichteter) MR-Bilder untersucht. Kongruent zu bisherigen Befunden lieferten auch diese Ergebnisse eine gute Qualität der funktionellen Daten, unabhängig davon ob die Probanden eine EEG-Kappe im Magnetresonanztomographen trugen oder nicht. Morphometrische Analysen der anatomischen Bilder zeigten jedoch deutliche Inhomogenitäten.

Zusammenfassend konnte gezeigt werden, dass sich die funktionelle „Signatur“ von musikalischem Können nicht nur während der Verarbeitung eines musikalischen Reizes oder des Musizierens in neuronaler Aktivität abzeichnet, sondern sich auch in intrinsischen Aktivierungsmustern während eines Ruhezustands zeigt und sich entsprechend prädiktiv auf das Verhalten auswirkt. Mit Hilfe der Erkenntnisse aus den Studien I und III sollen weiterführende Experimente auf diesem Wissen aufbauen um herauszufinden, inwieweit das intrinsische Konnektivitätsmuster in Musikern u. a. einen neurophysiologischen Marker für die zugrundeliegenden anatomischen Verbindungen darstellt.

Contents

CHAPTER 1

General Introduction

The human brain has the capacity of being adaptable to a variety of physiological and environmental changes. This intrinsic property, commonly referred to as neural plasticity, was introduced for the first time by the Polish neurophysiologist Jerzy Konorski (Konorski, 1948) in terms of adaptations to associative learning mechanisms on the cellular level. Developing this idea further, Donald O. Hebb published his theory of Hebbian Learning, which to date represents a valid explanation for the underpinnings of neuronal adaptation and learning:

> *'When an axon of cell A is near enough to excite cell B and repeatedly or persistently takes part in firing it, some growth process or metabolic change takes place in one or both cells such that A's efficiency, as one of the cells firing B, is increased' (Hebb, 1949, p. 62).*

Thus, based on the assumption that synapses strengthen with use, animal models provided fruitful evidence for experience-driven changes of cortical organization and shed light on the molecular and neurophysiological mechanisms of learning and memory (Jenkins, Merzenich, and Recanzone, 1990; Merzenich, Recanzone, Jenkins, and Grajski, 1990; Nudo, Jenkins, and Merzenich, 1990). Contrary to the general consensus at that time that most brain regions are amenable for plastic adaptations only during development (for a review see Jäncke, 2009b), today it is well accepted that the whole human brain is highly plastic during its entire life span (Boyke, Driemeyer, Gaser, Buchel, and May, 2008). Meanwhile, numerous studies made valuable contributions on the impact of training and environmental

influences on the functional as well as the anatomical architecture of the human brain across several domains (Draganski et al., 2004, 2006; Flor et al., 1995; Jäncke, 2009a; Kelly and Garavan, 2005; Kottlow, Praeg, Leuthy, and Jäncke, 2011; Maguire et al., 2000; Muente, Altenmueller, and Jaencke, 2002). Drawing upon this knowledge, the present dissertation comprises two independent studies, expanding the current understanding of how neural plasticity is affected by long-term training, in particular in the frame of musical expertise.

While there is a steadily growing body of literature concerning neuronal and behavioral benefits of professional musical skill for solving domain-related and unrelated tasks, the first study addressed the novel question whether musical skill also has modulatory effects on neuronal activity during a task-free resting state condition, i. e. when subjects are not confronted with any stimulating items.

Conversely, the second study followed two different objectives with the help of a task-based experiment. First, it aimed at examining if spectrotemporal dynamics during a pre-stimulus period in a working memory task are predictive for future behavioral performance, in this case reaction time (RT). Second, the study investigated if these oscillatory activation patterns vary as a function of musicianship.

The third study was conducted independent of musical expertise, and it provided valuable contributions on the general improvement of experimental protocols in the field of multimodal imaging. In particular, the study focused on the impact of a high-density electroencephalography (EEG) setup on data quality of functional and structural magnetic resonance (MR) images.

1.1 Musicians–a model for human training-related plasticity

In recent decades, musicians have become a notorious human model for studying training-related plasticity because playing a musical instrument at a professional level requires the coordination and integration of various brain functions, such as auditory (Jäncke, 2009a; Kühnis, Elmer, and Jäncke, 2014), sensorimotor (Jäncke, 2012; P. Schneider et al., 2002; Zatorre, Chen, and Penhune, 2007) and higher order cognitive functions (Elmer, Hänggi, and Jäncke, 2014a; Moreno et al., 2011, 2009; Schulze, Mueller, and Koelsch, 2011; Sluming, Brooks, Howard, Downes, and Roberts, 2007; Zuk, Benjamin, Kenyon, and Gaab, 2014).

As a consequence of plasticity, both structural as well as functional adaptations have been reported.

Regarding anatomical measures, studies provided evidence for a cortical reorganization on the level of white (Bengtsson et al., 2005; Imfeld, Oechslin, Meyer, Loenneker, and Jancke, 2009; Schmithorst and Wilke, 2002) and gray matter (Abdul-Kareem, Stancak, Parkes, and Sluming, 2011; Bermudez, Lerch, Evans, and Zatorre, 2009; Schlaug, Jäncke, Huang, and Steinmetz, 1995). One of the first studies reported musicians having an increased inter-hemispheric structural connectivity thereby improving the global coupling of motor and cognitive functions (Schlaug, Jäncke, Huang, Staiger, and Steinmetz, 1995a). Alterations in the corticospinal tract (transmission of sensorimotor information; Bengtsson et al., 2005; Imfeld et al., 2009), the arcuate (connecting frontal and temporal lobe; Loui and Schlaug, 2009) and the superior longitudinal fasciculus (connecting parietal cortical fields with frontal lobe; Oechslin, Imfeld, Loenneker, Meyer, and Jäncke, 2009) have also been reported. By examining differences in gray matter, the motor hand areal was demonstrated to be enlarged as a function of the trained instrument. Professional piano players showed an expanded areal in the left, and violinists in the right hemisphere (Amunt et al., 1997; Bangert and Schlaug, 2006). Further adaptations in gray matter were found in the bilateral inferior temporal gyri (integration of visual and motor information), the bilateral precentral gyri (motor control of hand movements), the right superior parietal lobe (coordination of visual-spatial information, sight reading), the left Heschl's gyrus (HG) (processing of basal auditory information), the bilateral inferior frontal gyri (working memory, attention), and the left cerebellum (automated movements; Gaser and Schlaug, 2003).

On the functional level, the auditory system in musical experts was shown to be more sensitive to detecting fine-grained modulations of tones such as pitch (Bidelman, Krishnan, and Gandour, 2011) or timbre (Meyer, Baumann, and Jancke, 2006) and to vary in activation strength dependent on the familiarity (own or unfamiliar instrument) and intensity of the presented tones (Pantev, Roberts, Schulz, Engelien, and Ross, 2001). Elbert and colleagues (Elbert, Pantev, Wienbruch, Rockstroh, and Taub, 1995) reported comparable results to the anatomical studies and showed an enlarged sensomotoric representation of the left hand motor areal in string players. This increase seemed to be positively correlated with the age of acquisition. By comparing activation patterns in motor-related brain regions for more complex bimanual movement schemes on the piano, Haslinger and colleagues demonstrated a higher activation in the control group compared to the professional pianists, suggesting a

more efficient use of cortical and subcortical brain regions in the musicians for controlling bimanual movements (Haslinger et al., 2004).

Meanwhile, there is increasing evidence showing that musicians not only have advantages in processing musical information but also benefit in domains in which they were not explicitly trained (Besson, Chobert, and Marie, 2011; Kraus and Chandrasekaran, 2010; Milovanov and Tervaniemi, 2011; Patel, 2011; Schon and Francois, 2011). Since music and speech share physical similarities, it is not surprising that musicians show an advantage in the processing of segmental (Elmer, Meyer, and Jäncke, 2012; Marie, Magne, and Besson, 2011; Ott, Langer, Oechslin, Meyer, and Jäncke, 2011) as well as supra-segmental language information such as pitch, timbre, and rhythm (Marie et al., 2011; Marques, Moreno, Castro, and Besson, 2007; Schon, Magne, and Besson, 2004) compared to musical laymen. Further, cognitive benefits representing transfer effects of musical training have been reported for mathematical problem solving (Bilhartz, Bruhn, and Olson, 1999), mental rotation tasks (Sluming et al., 2007) or the processing of visuospatial information (Brochard, Dufour, and Després, 2004; Douglas and Bilkey, 2007).

1.2 Study I: The intrinsic activity during rest–a product of long-term training?

Across different domains of imaging techniques, such as EEG (Creutzfeldt, Watanabe, and Lux, 1966), optical imaging (Arieli, Sterkin, Grinvald, and Aertsen, 1996; Kenet, Bibitchkov, Tsodyks, Grinvald, and Arieli, 2003), single unit (A. K. Engel, Fries, and Singer, 2001), or functional magnetic resonance imaging (fMRI) (Biswal, Yetkin, Haughton, and Hyde, 1995; Fox and Raichle, 2007) recordings, the importance of intrinsic oscillatory activity during a task-free resting state condition in brain organization has repeatedly been emphasized. In this context, brain regions showing temporal correlated patterns are ascribed as regions of similar functionality (Biswal, DeYoe, and Hyde, 1996; Fox and Raichle, 2007). The temporal coupling of the oscillatory patterns between distant brain regions, reflected by the synchronized spiking of thousands of neurons, was shown to be driven by a global balance of excitatory and inhibitory synaptic currents (Haider, Duque, Hasenstaub, and McCormick, 2006). This balance represents a fundamental basis for sustaining stable brain states on one hand but also allows rapid switching from one state to the other. Thereby, the rhythmic synchronization of the neuronal activity in single frequency bands reflects functionally relevant periodic fluctuations of excitation and inhibition (Deco and Corbetta, 2011). At this point, it is worth mentioning that only

a surprisingly small percentage, roughly 10%, of all synapses are involved in processing incoming stimulus material (Peters, Payne, and Budd, 1994). This supports the assumption that the majority of neuronal activity is involved in sustaining the brain's intrinsic activity. But what exactly does this intrinsic activity reflect? To answer this question, several possibilities have been suggested. For example, endogenous neuronal oscillatory activity might represent unconstrained and spontaneous cognitive functioning, such as daydreaming (Mason et al., 2007). A further view is the initiation and maintenance of information ensuring efficient information processing. By this, the brain is not only prepared to respond to incoming stimuli, but also to predict them (Fox, Snyder, Vincent, and Raichle, 2007) and thus controls behavioral output (Haider et al., 2006). Deco and Corbetta allegorized that

> *'. . . the resting state is like a tennis player waiting for the service of his opponent. The player is not static, but continues to move with small lateral jumps left and right to be able to react more promptly to a fast ball.' (Deco and Corbetta, 2011, p. 108).*

The first study raises the question whether neuronal activity during rest can be modulated by long-term training. In fact, the influence of repetitive task-specific activations on oscillatory activity due to a behavioral action was shown for the first time by Lewis and colleagues (Lewis, Baldassarre, Committeri, Romani, and Corbetta, 2009). Meanwhile, a variety of studies have repeatedly proven this assumption across several domains. For example, training-related modulations on resting state neuronal activity have been proposed among others in badminton players (Di et al., 2012), chess (Duan et al., 2012) and Baduk (Go) experts (W. H. Jung et al., 2013). Further modifications were found in the field of cognitive functions, particularly working memory performance (Jolles, van Buchem, Crone, and Rombouts, 2013; Langer, von Bastian, Wirz, Oberauer, and Jäncke, 2013; Mackey, Miller Singley, and Bunge, 2013; Taubert, Lohmann, Margulies, Villringer, and Ragert, 2011).

Besides the acceptance that musical training leads to neuronal adaptations on the functional level for solving both music-related and unrelated tasks, it still remains unknown how expertise modulates electrophysiological oscillation patterns during a task-free resting state condition. To date, only two fMRI studies exist that focused on this research question. C. Luo et al. (2012) applied a seed-based functional connectivity analysis with seeds chosen

in the motor, the somatosensory, the auditory and the visual cortex. They found increased functional connectivity in the musical experts among the motor and multisensory cortices compared to non-musicians. In another study, Fauvel and colleagues (Fauvel et al., 2014) chose seed regions for functional data analysis based on differences in gray matter density. They reported increased connectivity values in musicians in memory- and language-related networks as well as in neuronal networks involved in the processing of sensory and motor information.

Thus, the first study of this dissertation is aimed at specifically investigating functional connectivity patterns during rest with the help of a whole head graph-theoretical approach based on intracortical electrophysiological coherence measures. This methodological procedure not only has the advantage of analyzing connectivity patterns between a priori defined seed regions and the rest of the brain but it also conveys information about any putative connections that are affected by intense music training. Based on the existing literature, we hypothesized to find increased connectivity measures between brain regions, which are typically known to be involved in processing as well as in producing music, such as the auditory, the somatosensory, the motor and prefrontal cortex, and Broca's area.

1.3 Study II: Neuronal activity as a predictor for behavioral performance

Both long-term repetitive training and the single exposure of a task have been shown to modulate the occurrences of spatiotemporal oscillation patterns during a resting state condition. For example, a speed reading training resulted in decreased connectivity measures between brain regions involved in speech production and processing in the subsequent resting state (Ferguson, Nielsen, and Anderson, 2014). Changes in the temporal coupling between the hippocampus and the striatum in response to a visual learning task persisted even until the next day (Urner, Schwarzkopf, Friston, and Rees, 2013). It was also reported that the neuronal activity during rest has a modulatory effect on the forthcoming task-evoked activity and thus indirectly shapes behavior (Hamann, Dayan, Hummel, and Cohen, 2014; Sala-Llonch et al., 2012; Wu, Srinivasan, Kaur, and Cramer, 2014), even on the single-trial level (Noh, Herzmann, Curran, and de Sa, 2014).

Going one step further, previous studies suggested that behavioral performance varies as a function of neuronal activity during a short pre-stimulus period (in the range of a few seconds) in a cognitive task. Specifically, it was shown that the successful encoding

of information is influenced by the neuronal activity that precedes it rather than only being dependent on the activity during the encoding and consolidation process (Otten, Quayle, Akram, Ditewig, and Rugg, 2006; Park and Rugg, 2010; Peller and Wagner, 2002). Hence, it can be suggested that the neuronal activity appearing several seconds before item representation does not solely reflect a level of attention or alertness but is also shaped by the preparation of neuronal sources involved in stimulus processing, motivation or anticipatory processes (Otten, Henson, and Rugg, 2002, 2006).

The oscillatory activity during the pre-stimulus period was reported to be tightly coupled with response speed (Babiloni, Vecchio, Bultrini, Luca Romani, and Rossini, 2006; Britz and Michel, 2010). Thereby, a broad frequency spectrum, ranging from theta (Gladwin, Lindsen, and de Jong, 2006) to beta (Achim, Bouchard, and Braun, 2013) was shown to be associated with performance. However, although these frequency bands have been suggested to modulate the intrinsic neuronal dynamics engaged in preparatory processes, their exact functional roles seem to vary in a task-dependent manner.

As indicated above, the ability to play a musical instrument at a professional level entails cognitive advantages across a variety of different domains i. a. in processing visuospatial information (Brochard et al., 2004; Douglas and Bilkey, 2007; Sluming et al., 2007) and letter processing (Proverbio, Manfredi, Zani, and Adorni, 2013). Based on this evidence as well as the present inconsistency in ascribing a clearly defined role of the pre-stimulus oscillatory dynamics and their influence on response speed, the intention of the second study was twofold. First, it sought to increase the current understanding of the interplay between frequency spectral power and its impact on RT in general, i. e. independent of musical expertise. Second, it investigated whether there is a difference in the spectrotemporal activation patterns during this time period as a function of musicianship.

1.4 Study III: Constraints in multimodal imaging

In the last two decades, fMRI has become one of the most often used techniques in the field of human brain imaging. Compelling advantages are that it is non-invasive, delivers a good spatial resolution in the millimeter range, covers the whole brain and does not need to deal with interferences of spatially correlating activation sites (Ritter and Villringer, 2006). Its main limitations are a poor temporal resolution and the need to measure neuronal activity on an indirect level via the blood oxygenation level dependent (BOLD) response. To

benefit from the advantages but to overcome the limitations, the simultaneous acquisition of fMRI and EEG data has gained increasing attention. Additional advantages of the combined recording are to gain a deeper understanding of neurovascular coupling processes (Herrmann and Debener, 2008; Logothetis, Pauls, Augath, Trinath, and Oeltermann, 2001) and to further particular knowledge of i. a. the functional role of EEG oscillations underlying cognitive functions, for which a technique-dependent occurrence sensitivity has been reported (Ritter and Villringer, 2006).

There exist two possible ways for integrating EEG and fMRI data: the separate EEG-fMRI recording and analysis with a subsequent combination of the results, as well as the simultaneous recording of the two imaging techniques. To avoid any perturbing interaction effects on data quality, the separate recording of both data sets seems to be promising. However, by the twofold recording of an experimental condition, session and/or repetition effects cannot be ruled out. This is supported by the fact that it is nearly impossible that an individual would show the exact corresponding activation patterns twice. Thus, to overcome the disadvantages of the separate recording of EEG and fMRI, a concurrent acquisition of both techniques seems to be a fruitful solution. Regarding putative destructive effects on EEG data quality caused by the MRI environment, mathematical algorithms were developed for successfully reducing the three main scanner-related artifacts. These constitute 1) the gradient artifact, caused by the consistently applied radio frequency pulses (Allen, Josephs, and Turner, 2000), 2) the ballistocardiological artifact, originating from cardiac or pulsatile activity (Debener, Mullinger, Niazy, and Bowtell, 2008; Tenforde, Gaffey, Moyer, and Budinger, 1983), and 3) artifacts caused by the MR cryogen helium pump. As proven by several studies, the combined acquisition of EEG and functional MR images seem to deliver reliable results (Bonmassar, Hadjikhani, Ives, Hinton, and Belliveau, 2001; Q. Luo and Glover, 2012; Mullinger, Debener, Coxon, and Bowtell, 2008). Quite in contrast, although the simultaneous recording of anatomical MR images and EEG appears questionable in a first step, the everyday experience in a neuroscientific working environment has highlighted need for considering possible destructive interaction effects. In this context, the relatively short structural sequences are also often recorded in functional study paradigms allowing an individualized and thereby improved fMRI preprocessing. And once recorded, it further opens the possibility of applying a separate analysis of the anatomical images. However, in practice, it is desirable to avoid spending additional time to take the subject out of the scanner, remove the EEG net and properly reposition the subject to then record the structural data. Driven by this goal, the third study was

conducted to examine the influence of a high-density EEG on functional ($T2^*$-weighted) and anatomical (T1-weighted) MR images, as well as on B_0 and B_1 field maps, to gain detailed information about which magnetic fields, the static or the gradient field, might be affected.

CHAPTER 2

Empirical Part Study I: The 'silent' imprint of musical training

Carina Klein[1], Franziskus Liem[1], Jürgen Hänggi[1], Stefan Elmer[1§], Lutz Jäncke[1-5§]

Under review.

[§]shared last authorship

[1] Division Neuropsychology, Institute of Psychology, University of Zurich, Zürich, Switzerland

[2] International Normal Aging and Plasticity Imaging Center (INAPIC), University of Zurich, Zürich, Switzerland

[3] Center for Integrative Human Physiology (ZIHP), University of Zurich, Zürich, Switzerland

[4] University Research Priority Program (URPP), Dynamic of Healthy Aging, University of Zurich, Zürich, Switzerland

[5] Department of Special Education, King Abdulaziz University, Jeddah, Saudi Arabia

2.1 Abstract

Playing a musical instrument at a professional level is a complex multimodal task requiring information integration between different brain regions supporting auditory, somatosensory, motor, and cognitive functions. These kinds of task-specific activations are known to have a profound influence on both the functional and structural architecture of the human brain. However, until now it is widely unknown whether this specific imprint of musical practice can still be detected during rest when no musical instrument is used. Therefore, we applied high-density EEG and evaluated whole-brain functional connectivity as well as small-world topologies during resting state in a sample of fifteen professional musicians and fifteen non-musicians. As expected, musicians demonstrate increased intra- and interhemispheric functional connectivity between those brain regions that are typically involved in music perception and production, such as the auditory, the sensorimotor and prefrontal cortex as well as Broca's area. In addition, mean connectivity within this specific network was positively related to musical skill. Thus, we conclude that musical training distinctively shapes intrinsic functional network characteristics in such a manner that its signature can still be detected during a task-free condition.

2.2 Introduction

One of the most distinctive signatures of musical training are functional (Elmer et al., 2012; Ohnishi et al., 2001; Tervaniemi, Just, Koelsch, Widmann, and Schroger, 2005) and structural (Bermudez et al., 2009; Elmer, Hänggi, Meyer, and Jäncke, 2013; Gaser and Schlaug, 2003; Hyde et al., 2009; Schlaug et al., 1995a) changes in brain regions involved in processing auditory information, coordinating fast motor movements (Muente et al., 2002), supporting cognitive control (Moreno et al., 2011; Schulze et al., 2011; Sluming et al., 2007; Zuk et al., 2014) as well as sensory-to-motor coupling mechanisms (Ellis et al., 2012; Pantev, Lappe, Herholz, and Trainor, 2009; Zatorre et al., 2007). Functional and structural alterations of the HG (P. Schneider et al., 2002, 2005; Seither-Preisler, Parncutt, and Schneider, 2014) and the planum temporale (PT) (Elmer et al., 2013; Ohnishi et al., 2001) have repeatedly been shown to correlate fairly well with the ability of musicians to identify spectrotemporal acoustic variations (Elmer et al., 2013, 2012; Seither-Preisler et al., 2014). Furthermore, the degree of malleability of the sensorimotor cortex is associated with finger tapping speed (Jäncke et al., 1998) and manual dexterity (Krings et al., 2000; Schlaug et al., 2009). Additionally, in particular violinists were reported to show functional

(Elbert et al., 1995) as well as structural adaptations (Bangert and Schlaug, 2006) in the left hand motor area. Even the ventro- and dorsolateral prefrontal cortex (PFC), both regions involved (among other functions) in sight-reading (Sergent, Zuck, Terriah, and MacDonald, 1992) and contributing in excerpting cognitive control functions (MacDonald, Cohen, Stenger, and Carter, 2000; Zuk et al., 2014), are affected by musical training.

During music production, acoustic cues have to be integrated into a multimodal processing stream via feedforward and feedback loops. These loops are principally mediated by intra- and interhemispheric fiber tracts conveying excitatory and inhibitory signals (Lotze, Scheler, Tan, Brain, and Birbaumer, 2003). In this context, the arcuate fasciculus constitutes the most eligible candidate enabling impulse transmission between the auditory-related cortex (ARC) and frontal brain regions (Catani, Jones, and ffytche, 2005, 2008). In addition, transcallosal fibers crossing the isthmus of the corpus callosum are fundamentally involved in the synchronization of brain activity between bilateral ARCs. Meanwhile, there is even evidence showing that musical training has an influence on the functional-structural (Elmer, Klein, et al., 2014; A. Engel et al., 2014; Halwani, Loui, Ruber, and Schlaug, 2011; Kühnis et al., 2014; Steele, Bailey, Zatorre, and Penhune, 2013) skeleton of both pathways.

In the last decades, the investigation of resting state networks has gained increasing attention. Today, it is widely accepted that neuronal activity during rest reflects functional meaningful activity rather than noise per se (Damoiseaux et al., 2006; Deco and Corbetta, 2011; Otten et al., 2006; Sadaghiani and Kleinschmidt, 2013; Scheeringa, Petersson, Kleinschmidt, Jensen, and Bastiaansen, 2012; Weissman-Fogel, Moayedi, Taylor, Pope, and Davis, 2010). In fact, functional connectivity during rest has been shown to be shaped by repetitive training in different domains (Langer et al., 2013; Urner et al., 2013; Vahdat, Darainy, Milner, and Ostry, 2011), to mirror prior task-related neuronal activity (Deco and Corbetta, 2011) as well as to be predictive of behavioral performance (Noh et al., 2014; Otten et al., 2006). In addition, resting state functional connectivity seems to constitute, at least partially, a physiological marker of the underlying structural skeleton (Deco and Corbetta, 2011; Greicius, Supekar, Menon, and Dougherty, 2009; W. H. Jung et al., 2013; Taubert et al., 2011).

Based on this current state of knowledge, the present work aimed at examining the influence of musical training on functional network characteristics during rest by using a graph-theoretical approach, without defining any a priori seed regions. In particular, we reasoned

that the imprint of intense musical training should even be manifested during task-free periods, in terms of increased functional connectivity in networks typically involved in musical performance. By measuring a homogeneous group of string players, we specifically expect to find altered connectivity measures between the right sensorimotor cortex, and the prefrontal and ARC.

2.3 Material and methods

2.3.1 Subjects

Fifteen professional string players (all graduates from local music conservatories; five males; mean age = 24.2 years, standard deviation (SD) = 3.21; mean cumulative number of training hours = 10831, SD = 5797.99) and fifteen control subjects without musical training (all students from local universities; seven males; mean age = 26.07 years, SD = 4.98) participated in the study. All participants were consistently right-handed as revealed by the Annett Handedness Inventory (Annett, 1970). None of the subjects reported taking any medication or drugs, nor suffered from any past or present neurological or psychiatric disease. Subjects gave written informed consent and were paid for participation. The present study was approved by the local ethics committee, according to the Helsinki declaration.

2.3.2 Cognitive capability and musical aptitude

To exclude between-group differences in intelligence, all subjects performed three subtests of the German 'Wechsler Adult Intelligence Scale–3rd edition' (WAIS-III) (Wechsler, 1997), namely the subtests necessary to calculate the *Working Memory Index* (Number Sequencing and Repetition), the *Perceptual and Organization Index* (Mosaic Test), and the *Processing Speed Index* (Digit-Symbol Coding; Waldmann, 2008). Musical aptitude was quantified with the 'Advanced Measures of Music Audition' (AMMA) test (Gordon, 1989). In this test, subjects have to decide if two short piano sequences are equal or rhythmically/tonally different. Group differences in biographical data (intelligence quotient (IQ), age, and musical aptitude) were evaluated in Statistical Package for the Social Sciences (SPSS) 21 (`http://www-01.ibm.com/software/ch/de/analytics/spss/`) by using t-tests for independent samples (two-tailed). To test for a relationship between training hours and musical aptitude,

a partial correlation analysis (corrected for age) was performed within the musicians group (one-tailed t-test, false discovery rate (FDR) corrected).

2.3.3 Experimental procedure, EEG recording, and data processing

High-density electroencephalography (EEG) (256 channels) was recorded for 7 min (eyes open) with a sampling rate of 1000 Hz by using the Geodesic Netamp system (Electrical Geodesics, Eugene, Oregon). During EEG recording, data were band pass filtered between 0.1 Hz and 100 Hz, electrode Cz was used as recording reference, and impedances were kept below 30 kΩ. Data were preprocessed offline with the BrainVision Analyzer software (BrainVision Analyzer 2.2; http://www.brainproducts.com/downloads.php). Thereby, artifact-affected electrodes (in the outermost circumference, chin and neck) were removed, resulting in a 204-electrode array (Langer et al., 2013). An independent component analysis was applied to correct remaining eye movement artifacts (T. P. Jung et al., 2000). Data were band-pass filtered between 0.1 Hz and 15 Hz to remove remaining muscle artifacts. After preprocessing, data were recomputed against an average reference, segmented into single sweeps of 2 s, and subjected to network analyses. The presentation of the resting state modality (a fixation cross to minimize muscle artifacts in the EEG) was controlled by the Presentation software (Neurobehavioral Systems, USA, http://www.neurobs.com).

2.3.4 Connectivity analyses in the intracranial space

Functional connectivity was evaluated with the standardized low resolution brain electromagnetic tomography (sLORETA) toolbox (http://www.uzh.ch/keyinst/loreta.htm; see Pascual-Marqui, 2002), by using intracranial instantaneous coherence measures (De Vico Fallani et al., 2010; Jäncke and Langer, 2011; Langer et al., 2012, 2013; Pascual-Marqui, 2007b). We calculated the connectivities between the centroid voxels of 84 regions of interest related to the Brodmann areas (BAs) (Brodmann, 1909) in sLORETA (42 in each hemisphere) in the theta (6.5 Hz to 8 Hz), alpha 1 (8.5 Hz to 10 Hz), and alpha 2 (10.5 Hz to 12 Hz) frequency bands (Kubicki, Herrmann, Fichte, and Freund, 1979; Langer et al., 2012, 2013). We specifically focused on 'low frequency' oscillations because they are relatively uncontaminated by artifacts and have previously been shown to contribute to the propagation and integration of information across long-range brain circuits (Ward, 2003). The Juelich Histological and the Harvard-Oxford cortical atlases (http://fsl.fmrib.ox.ac.uk/fsl/fslwiki/Atlases;

implemented in functional magnetic resonance imaging of the brain (FMRIB) Software Library (FSL): http://fsl.fmrib.ox.ac.uk/fsl/fslwiki/FSL) were used for a more detailed specification of brain regions underlying the coordinates of the BAs (i. e., centroid voxel; see Table 2.1). Coordinates are depicted for the BAs, obtained from the NBS analysis (see below).

Table 2.1: Specification of the brain regions underlying the centroid voxel of the BAs obtained from the NBS analysis. Planum temporal = PT, primary auditory cortex = A1, primary motor cortex = PM, the primary somatosensory cortex = SS, ventromedial prefrontal cortex = vmPFC.

BA	MNI coordinate (x, y, z)	Brain structure
BA41	(45, -30, 10)	A1
BA41	(55, -20, 5)	A1
BA42	(-60, -25, 10)	PT
BA42	(-60, -10, 15)	A1
BA42	(65, -25, 10)	PT
BA3	(35, -25, 50)	PM/SS
BA25	(-10, 20, -15)	vmPFC
BA44	(-50, 10, 15)	Broca's area

2.3.5 Network-based statistics

For evaluating between-group differences in functional connectivity, we applied a statistical approach called network-based statistic (NBS) (Zalesky, Fornito, and Bullmore, 2010). NBS is a whole-brain and non-parametrical randomization technique where mass-univariate statistical testing is performed on every pairwise association between the single BAs, by controlling for familiywise error (FWE) rate. Brain-behavior relationships (i. e., mean functional connectivity values and total AMMA score) were further assessed separately within the two groups (one-tailed t-tests, FDR corrected).

2.3.6 Graph-theoretical small-worldness and regional node analysis

To obtain the best small-world network topology (high cluster coefficient (C) and short path length (L) compared to a random network; after Bullmore and Sporns, 2009), the averaged weighted connectivity matrix across all subjects was thresholded from $r = 0.65$ to 0.95 in increments of 0.05. C and L were calculated with the MATLAB-based Brain Connectivity Toolbox (`http://www.brain-connectivity-toolbox.net`; Rubinov and Sporns, 2010) for the real and a random network (100 randomizations) for the evaluation of the small world indices γ ($C_{\text{real}}/C_{\text{rand}}$), λ ($L_{\text{real}}/L_{\text{rand}}$) and σ (λ/γ) (Humphries, Gurney, and Prescott, 2006; Sporns, Honey, and Kötter, 2007), separately for each threshold. Best small world characteristics ($\sigma \gg 1$) were obtained for the highest threshold $r = 0.95$. Thus, only this particular threshold was applied for further analyses steps.

Subsequently, to evaluate efficiency in information transmission of the BAs involved in the functional network obtained from the between-group NBA analysis (see Table 2.2), the node degree (regional node index, a measure of local connectivity) was calculated with the Brain Connectivity Toolbox for the individual thresholded ($r = 0.95$) matrices. Thereby, the number of connections of a particular node in a network to other nodes was calculated. To test for group differences, Mann-Whitney U tests (according to a deviation from a normal distribution) were computed in SPSS and corrected for multiple comparisons by using FDR (Benjamini and Hochberg, 1995; Yekutieli and Benjamini, 1999). In addition, correlation analyses separately within the two groups were calculated to examine putative relationships between node degree and musical skill (i. e., total AMMA score, FDR corrected).

2.4 Results

2.4.1 Autobiographical and behavioral data

The two groups did not differ in terms of age ($T_{(28)} = 1.22$, $p = 0.23$; two-tailed) and cognitive capability ($T_{(28)} = -1.68$, $p = 0.1$; two-tailed). In addition, as expected, musicians outperformed the controls in the AMMA test (total score: $T_{(28)} = -5.87$, $p < 0.001$; tonal score: $T_{(28)} = -5.29$, $p < 0.001$; rhythm score: $T_{(28)} = -5.23$, $p < 0.001$; two-tailed). Partial correlation analysis within the musicians revealed a positive relation between the cumulative training hours during life and musical skill. This implies that the more hours musicians

have trained the higher was the total AMMA score ($r = 0.754$, $p = 0.013$; one-tailed t-test; FDR corrected; see Fig. 2.2 A).

2.4.2 Network-based statistics

Musicians showed significantly increased functional connectivity in the theta (Fig. 2.1 A) and alpha 1 (Fig. 2.1 B) frequency range (theta: $p = 0.049$; alpha 1: $p = 0.01$, FWE corrected) compared to the controls. In particular, results revealed increased inter-hemispheric connectivity between the bilateral PT (theta, alpha 1), left PT and right sensorimotor cortex (theta, alpha 1), right PT and left ventromedial prefrontal cortex (vmPFC) (theta, alpha 1). Increased intra-hemispheric connectivity was also revealed within left (theta, alpha 1) and right (alpha 1) PT and primary auditory cortex (A1), between left PT and left Broca pars opercularis (theta), between right A1 and right sensorimotor cortex (alpha 1). A detailed summary of these results is shown in Table 2.2. Comparison between the two groups did not deliver any increased functional connections in the non-musicians compared to the expert group across all examined frequency bands.

Table 2.2: Mean functional connectivity measures for each pairwise association identified with the Network-based Statistic toolbox ($p < 0.05$) for both groups in the theta and alpha 1 frequency range. Listed are the averaged coherence values across all subjects separated for the two groups (FWE corrected) and the t statistics for the single associations.

Frequency	Network connection (MNI x, y, z)	Mean coherence non-musicians ± SD	Mean coherence musicians ± SD	t stats
6.5 - 8 Hz	BA42 (-60, -25, 10) – BA41 (45, -30, 10)	0.18 ± 0.10	0.43 ± 0.22	3.84
	BA42 (-60, -25, 10) – BA42 (65, -25, 10)	0.21 ± 0.11	0.47 ± 0.22	4.01
	BA25 (-10, 20, -15) – BA42 (65, -25, 10)	0.24 ± 0.12	0.49 ± 0.23	3.66
	BA42 (-60, -25, 10) – BA42 (-60, -10, 15)	0.26 ± 0.12	0.53 ± 0.23	3.85
	BA42 (-60, -25, 10) – BA44 (-50, 10, 15)	0.30 ± 0.13	0.56 ± 0.23	3.69
	BA42 (-60, -25, 10) – BA3 (35, -25, 50)	0.18 ± 0.12	0.43 ± 0.21	3.80
8.5 - 10 Hz	BA25 (-10, 20, -15) – BA41 (45, -30, 10)	0.24 ± 0.16	0.54 ± 0.19	4.37
	BA41 (55, -20, 5) – BA41 (45, -30, 10)	0.32 ± 0.15	0.58 ± 0.17	4.41
	BA42 (-60, -25, 10) – BA41 (45, -30, 10)	0.23 ± 0.17	0.52 ± 0.20	4.30
	BA25 (-10, 20, -15) – BA42 (65, -25, 10)	0.29 ± 0.19	0.57 ± 0.18	4.06
	BA41 (55, -20, 5) – BA42 (65, -25, 10)	0.38 ± 0.18	0.66 ± 0.13	4.68
	BA42 (-60, -25, 10) – BA42 (65, -25, 10)	0.27 ± 0.20	0.56 ± 0.19	4.07
	BA41 (55, -20, 5) – BA3 (35, -25, 50)	0.38 ± 0.17	0.66 ± 0.12	4.89
	BA42 (-60, -25, 10) – BA3 (35, -25, 50)	0.26 ± 0.18	0.53 ± 0.18	4.01

2.4.3 Network-based statistics: brain-behavior relationships

By investigating putative interrelationships between the AMMA test and mean functional connectivity within the expert group, we consistently found positive correlations (theta (Fig. 2.2 B): $r = 0.586$, $p = 0.047$; alpha 1 (Fig. 2.2 C): $r = 0.674$, $p = 0.019$; one-tailed t-test; FDR corrected). Within-group correlation analyses for the non-musicians did not deliver significant results.

2.4.4 Regional node degree analysis

The node degree measures were compared between the two groups. Thereby, we only selected the nodes (i. e., BAs) of the network showing increased connectivity in musicians compared to non-musicians (NBS analysis; see Table 2.2). Results revealed increased node degree values for the alpha 1 frequency band in musicians in two nodes residing in the right ARC (see Fig. 2.1 C; musicians: BA41 (Montreal Neurological Institute (MNI) coordinates: 45, -30, 10; A1): mean = 20.4, SD = 12.96; BA42 (65, -25, 10; PT): mean = 25.46, SD = 14.42; non-musicians: BA41 (45, -30, 10; A1): mean = 8.73, SD = 4.68; BA42 (65, -25, 10; PT): mean = 13.37, SD = 7.47; Mann-Whitney U test BA41: $p = 0.018$; BA42: $p = 0.045$, FDR corrected). Correlation analyses between musical aptitude and node degree values of BA41 and BA42 did not show significant relationships neither in the musicians nor in the control group.

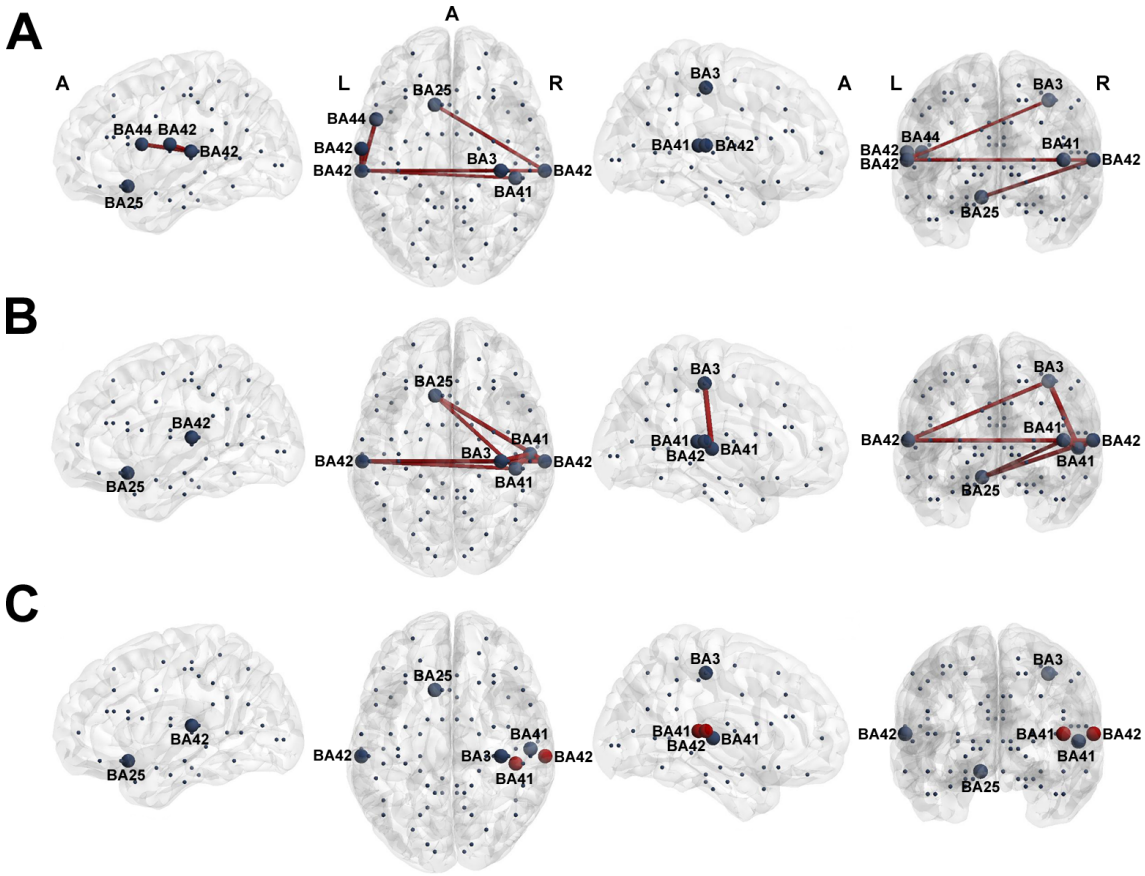

Figure 2.1: Network-based statistics between musicians and musical laymen. Increased functional connectivity (depicted in red) in musicians in A) the theta and B) the alpha 1 frequency band between the BAs depicted with enlarged size ($p < 0.05$, FWE corrected). C) The node degree measures of the nodes for the alpha 1 frequency band between which the musicians showed an increased functional connectivity (NBS analysis). In the right auditory cortex (BA41 and 42; visualized in red) the musicians show an increased node degree value compared to the non-musicians ($p < 0.05$, FDR corrected). Intra- and interhemispheric connectivities are shown in the sagittal, horizontal and coronal views. A = anterior, L = left hemisphere, R = right hemisphere.

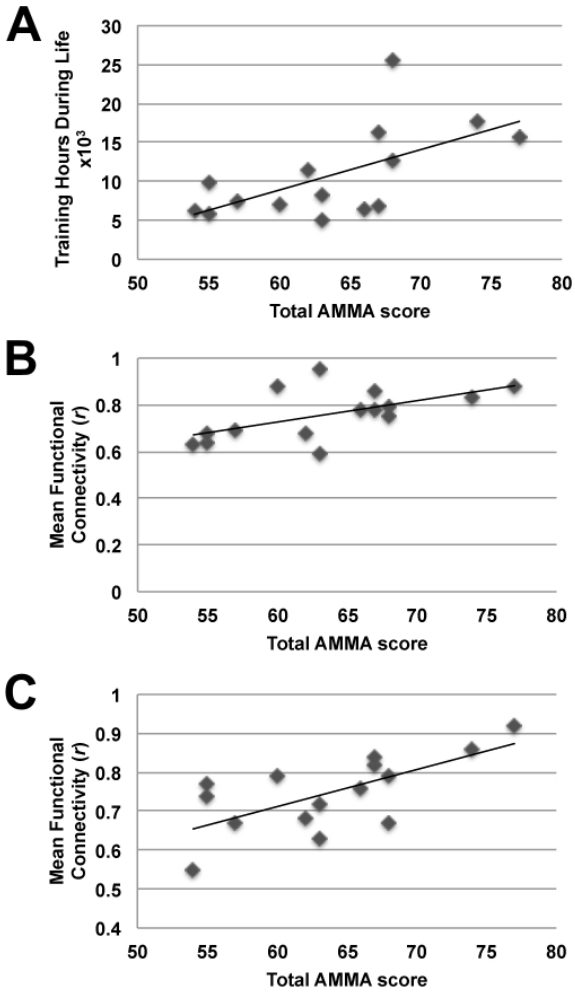

Figure 2.2: Correlations within the musicians ($p < 0.05$, FDR corrected) between the total AMMA score and A) the cumulative number of training hours during life, B) the mean value of functional connectivity in the theta and C) the alpha 1 frequency band.

2.5 Discussion

The aim of the present study was to determine whether the distinctive neurophysiological and anatomical fingerprint often observed in musicians can still be detected during task-free conditions. In line with our hypothesis, results showed that brain regions which are synchronously activated during musical performance build a functional unit that is also detectable during rest. Our findings support this point of view and additionally indicate that the right ARC constitutes a hub (i. e., increased local connectedness) within this network (comparable to Jäncke, Langer, and Hänggi (2012) with absolute pitch musicians).

Notably, we also revealed robust brain-behavior relationships suggesting a training-related intertwining between resting state activity, musicianship and training. Therefore, we propose that long-term musical training facilitates the functional interrelationship of distinct brain areas in such a manner that the characteristic electrophysiological signature can still be detected during short resting state periods.

The resting state network we identified consists of the same brain regions that have repeatedly been shown to be altered as a function of musical expertise (for an overview consider for example Muente et al., 2002). More precisely, at least two previous studies provided evidence for an increased representation of the left hand area in the somatosensory (Elbert et al., 1995) and motor cortex (Bangert and Schlaug, 2006) of violinists compared to pianists or non-musicians. In addition, there is also a convergence of findings pointing to a strong influence of musical training on the functional (Pantev et al., 2001; Schon et al., 2004; Tervaniemi, Castaneda, and Knoll, 2006) and structural (Bermudez et al., 2009; Hyde et al., 2009) architecture of the ARC as well as on functional (Kühnis et al., 2014) and structural (Elmer, Klein, et al., 2014; Steele et al., 2013) connectivity between bilateral ARCs. Such plastic adaptations might not only favor the processing of a variety of spectrotemporal acoustic cues (Besson et al., 2011; Kühnis et al., 2014), but also promote an interhemispheric division of labor (Elmer, Klein, et al., 2014; Kühnis et al., 2014; Steele et al., 2013). Thereby, it is assumed that the right ARC is preferably engaged in processing spectral information, whereas the left counterpart is more likely sensitive to fast changing acoustic cues (Griffith and Warren, 2002; Poeppel, 2003; Thierry, Giroud, and Prica, 2003; Zatorre and Belin, 2001). This framework is even in line with findings reported by P. Schneider et al. (2002) who detected a relationship between instrument-dependent pitch perception preference and functional and structural asymmetry of the HG. In particular, in string players this trait is more pronounced in the right hemisphere, whereas musicians playing fast and reactive instruments (i. e., piano) more likely show plasticity effects in the contralateral homologue. Finally, our findings are even consistent with an EEG study showing that musical training does not only influence the architecture of auditory and motor cortices per se, but also the communication between these two brain regions (Ellis et al., 2012; Jäncke, 2012).

To date, there is a growing body of literature reporting musical training-related adaptations within Broca's area (Sergent et al., 1992) and in particular within the pars opercularis (Maess, Koelsch, Gunter, and Friederici, 2001). The latter can be considered as being a

part of the so-called motor territory (Binkofski et al., 2000), is a point of convergence of the arcuate fasciculus and has repeatedly been shown to be involved in sensory-to-motor coupling mechanisms (Pantev et al., 2009), sight reading (Parsons, Sergent, Hodges, and Fox, 2005; Sergent et al., 1992) and language-selective processing (Fedorenko, Duncan, and Kanwisher, 2012; Makuuchi and Friederici, 2013). Furthermore, based on the assumption that the concept of functional connectivity implies, at least in part, being a neurophysiological fingerprint of the underlying anatomical architecture (Deco and Corbetta, 2011; Greicius et al., 2009; W. H. Jung et al., 2013; Taubert et al., 2011), we propose that the increased functional coupling we revealed between the left PT and Broca's region might originate from altered structural properties of the arcuate fasciculus found in professional musicians (A. Engel et al., 2014; Halwani et al., 2011; Wan and Schlaug, 2010).

Currently, it is also widely accepted that music has a strong emotional impact on human beings (Blood, Zatorre, Bermudez, and Evans, 1999; Grewe, Kopiez, and Altenmüller, 2009, 2005; Koelsch, 2014; Koelsch, Fritz, v. Cramon, Muller, and Friederici, 2006) and represents a crucial prerequisite for playing a musical instrument in an expressive manner. Hence, the vast interdependencies we revealed between the vmPFC and ARC, Broca's region, and the sensorimotor cortex, possibly indicate that music perception and production are tightly coupled with emotions (Koelsch et al., 2006) and cognitive functions (Fedorenko et al., 2012), even during rest. In this context, it cannot be ruled out that the obtained connectivity patterns are a result of music-related mentation. Although subjects reported after the measurement to not have been focusing on a particular thought during data recording, a complete omission of mental rehearsal of practiced music passages cannot be excluded.

To date, to the best of our knowledge, only two fMRI studies evaluated the influence of musical expertise on functional connectivity during rest (Fauvel et al., 2014; C. Luo et al., 2012). In the first study, C. Luo et al. (2012) selected a priori defined seed regions (i. e., left primary motor cortex (PM), left ARC, left primary somatosensory cortex (SS), and left visual cortex) for computing connectivity analyses. Results consistently revealed increased connectivity between the a-priori defined seeds and the contralateral homolog regions. By contrast, Fauvel and co-workers (Fauvel et al., 2014) selected the seed regions based on between-group differences in gray matter density, and reported increased functional connectivity in musicians between prefrontal, temporal, inferior-parietal, and premotor areas. However, one critical aspect that is worth mentioning is that both studies used

fMRI in combination with a seed-based analysis approach. The precarious aspect of this procedure is that it leads to the disadvantage of reductionism, meaning that it only enables to make a statement about the interrelationship between a-priori defined nodes while completely neglecting residual whole-brain dynamics. A further shortcoming is that data are often contaminated by the detrimental effects of scanner noise, which induces activations within the auditory system. Therefore, fMRI does not provide an optimal environment for measuring pure resting state activity (even more in musicians).

The fact that we found increased connectivity patterns in musical experts in the theta and lower alpha frequency ranges might be explained by the evidence that low frequency oscillatory activity is involved in the propagation of information across long-distanced brain regions (Ward, 2003), as it is the case in our findings. Furthermore, theta and alpha oscillatory activity is involved in various brain functions crucial for music processing and production, such as for example memory (George and Coch, 2011; Schulze and Koelsch, 2012; Ward, 2003), inhibitory functions (Klimesch, Sauseng, and Hanslmayr, 2007; Moreno, Wodniecka, Tays, Alain, and Bialystok, 2014), or attention (Baumann, Meyer, and Jäncke, 2008; Klimesch, 1999; Zuk et al., 2014). However, regarding the fact that we only found differences in the lower but not in the upper alpha band remains an unsolved issue since there is not at all clarity about the exact functional meaning of the different oscillations.

In summary, based on our results we propose that the pattern of increased resting state connectivity we found constitutes an idiosyncratic signature of musical training. In fact, here we show that the same brain regions that have repeatedly been shown to be functionally and structurally altered in musicians are indeed hyper-connected on a functional level, even during a 'task-free' condition. Hence, our results constitute an important step towards a holistic and integrative understanding of the 'silent' imprint of musical training on the human brain. Certainly, future studies using multimodal imaging techniques (i. e., simultaneous EEG and magnetic resonance imaging (MRI) measurements) are strictly required in order to achieve a deeper understanding of the functional-structural compliance of neuronal network organization.

CHAPTER 3

Empirical Part Study II: The influence of pre-stimulus EEG activity on reaction time during a verbal Sternberg task is related to musical expertise

Carina Klein[1], Laura Diaz Hernandez[2], Thomas Koenig[2], Mara Kottlow[2, 3], Stefan Elmer[1§], Lutz Jäncke[1, 4-7§]

Accepted for publication in Brain Topography, doi: 10.1007/s10548-015-0433-7.

[§]shared last authorship

[1] Division Neuropsychology, Institute of Psychology, University of Zurich, Zürich, Switzerland

[2] Translational Research Center, University Hospital of Psychiatry, Bern, Switzerland

[3] Center of Cognition, Learning and Memory, University of Bern, Bern, Switzerland

[4] Institute of Pharmacology and Toxicology, University of Zurich, Zürich, Switzerland

[5] International Normal Aging and Plasticity Imaging Center (INAPIC), University of Zurich, Zürich, Switzerland

[6] Center for Integrative Human Physiology (ZIHP), University of Zurich, Zürich, Switzerland

[7] University Research Priority Program (URPP), Dynamic of Healthy Aging, University of Zurich, Zürich, Switzerland

[8] Department of Special Education, King Abdulaziz University, Jeddah, Saudi Arabia

3.1 Abstract

Previous work highlighted the possibility that musical training has an influence on cognitive functioning. The suggested reason for this influence is the strong recruitment of attention, planning, and working memory functions during playing a musical instrument. The purpose of the present work was twofold, namely to evaluate the general relationship between pre-stimulus electrophysiological activity and cognition, and more specifically the influence of musical expertise on working memory functions. With this purpose in mind, we used covariance mapping analyses to evaluate whether pre-stimulus electroencephalographic activity is predictive for reaction time during a visual working memory task (Sternberg paradigm) in musicians and non-musicians. In line with our hypothesis, we replicated previous findings pointing to a general predictive value of pre-stimulus activity for working memory performance. Most importantly, we also provide first evidence for an influence of musical expertise on working memory performance that could distinctively be predicted by pre-stimulus spectral power. Our results open novel perspectives for better comprehending the vast influences of musical expertise on cognition.

3.2 Introduction

The ability of the human brain to undergo structural and functional changes relies on its specific adaptability to training or environmental changes (Draganski et al., 2004; Kelly and Garavan, 2005; Maguire et al., 2000). In this context, musicians have been proposed to constitute a promising group for studying experience-driven structural as well as functional plasticity (Herholz and Zatorre, 2012; Jäncke, 2009a, 2009b; Muente et al., 2002; Peretz and Zatorre, 2005). In fact, mastering a musical instrument requires the integration of widespread neuronal networks supporting the functional coordination of auditory (Jäncke, 2009a; Kühnis et al., 2014), sensorimotor (Jäncke, 2012; P. Schneider et al., 2002; Zatorre et al., 2007) as well as higher order cognitive functions (Elmer, Klein, et al., 2014; Moreno et al., 2011, 2009; Schulze et al., 2011; Sluming et al., 2007; Zuk et al., 2014).

Today, there is some evidence showing cognitive advantages in musicians across a variety of cognitive functions, including auditory-verbal (Besson et al., 2011; Kühnis, Elmer, Meyer, and Jäncke, 2013; Moreno et al., 2011), visuospatial (Brochard et al., 2004; Douglas and Bilkey, 2007), short-term memory (George and Coch, 2011; Schulze and Koelsch, 2012;

Williamson, Baddeley, and Hitch, 2010), long-term verbal memory (Groussard et al., 2010; Ho, Cheung, and Chan, 2003; Huang et al., 2010), and inhibition of irrelevant responses (Moreno et al., 2014). Based on the fact that musical training strongly engages executive functions (Jäncke, 2009a), one may expect that it further entails advantages in cognitive demanding tasks, including music-related and unrelated tasks (Besson et al., 2011), even across life span (Amer, Kalender, Hasher, Trehub, and Wong, 2013; Jäncke, 2013).

Meanwhile, there is increasing evidence showing that successful encoding of information into memory is also dependent on the neuronal activity that precedes an item, rather than only on the activity during the encoding and consolidation process (Otten et al., 2006; Park and Rugg, 2010; Peller and Wagner, 2002). For example, mnemonic functions are strongly dependent on how a subject is prepared to encounter and encode information as well as on the neuronal processes initiated by stimulus presentation (Otten, Quayle, and Puvaneswaran, 2010). The modulatory role of pre-stimulus neuronal activity, i. e. the measured neuronal activity prior to a stimulus presentation in a second or millisecond range, does not solely reflect a state-related level of attention or alertness but also the tuning of neuronal populations engaged in proper stimulus processing, anticipatory processes (Otten et al., 2002, 2006), motivation as well as reward and emotional processes (Adcock, Thangavel, Whitfield-Gabrieli, Knutson, and Gabrieli, 2006; Gruber and Otten, 2010; Meeter, Murre, and Talamini, 2004). Thus, the averaged neuronal activity across pre-stimulus trials reflects the efficiency with which the information is encoded and consolidated into memory. In contrast to the above-mentioned studies that rely on averaged pre-stimulus neuronal activations, single-trial pre-stimulus activity has been proposed to constitute a more sophisticated measure of preparatory processes for encoding. For example, Noh and colleagues (Noh et al., 2014) were even able to successfully predict memory performance from single-trials, suggesting that such analyses can be used as a salient electrophysiological predictive marker for memory performance.

Notably, previous work also provided evidence for a relationship between pre-stimulus neuronal activity and response speed that varied as a function of congruency in a Stroop (Britz and Michel, 2010) or a visuospatial task (Babiloni et al., 2006). In this context, alpha power has been shown to reflect the level of preparedness, and to be inversely correlated with cortical excitability (Haegens, Handel, and Jensen, 2011). Furthermore, an increased pre-stimulus vigilance state has previously been suggested to be reflected by faster RTs, and associated with overall increased alpha amplitudes (Volberg, Kliegl, Hanslmayr, and

Greenlee, 2009) during a visual detection task. Shorter RTs have also been associated with increased theta (Gladwin et al., 2006) and beta band oscillatory activity. Therefore, it has been proposed that these three frequency bands play a pivotal role in modulating intrinsic neuronal dynamics before stimulus presentation. Recently, Achim and colleagues (Achim et al., 2013) reported that decreased pre-stimulus amplitudes in frequency bands ranging from 2 Hz to 24 Hz were associated with shorter RTs during a near threshold visual detection task. Thus, these findings lead us to conclude that pre-stimulus spectral power and behavioral performance are tightly coupled but seem to vary in a task-dependent manner.

Our interest was to expand the knowledge about pre-stimulus influences upon stimulus processing into the context of higher order brain functions that are susceptible to expertise-related plastic changes. In particular, we wanted to know if the preparatory allocation of neuronal resources before stimulus presentation is predictive for performance in a complex task that demands prolonged sensory, memory, basal language processing (single letter processing) and executive functions. Furthermore, we were interested in finding out, if these preparatory processes are modulated by musical training. We therefore investigated the influence of the pre-stimulus state (assessed by EEG spectral power) on reaction time in a visual Sternberg task in control subjects and professional musicians. In this context it is worth mentioning that visual and visual-spatial related brain areas play crucial roles in sight-reading and in the integration of multimodal sensory (auditory, visual and somatosensory) information during music processing and production (Gaser and Schlaug, 2003; Proverbio, Calbi, Manfredi, and Zani, 2014). It was even shown that musical training leads to a bilateral letter/notes processing in contrast to untrained subjects for whom strong left-lateralized activations are found (Proverbio et al., 2013).

Based on previous evidence indicating a putative relationship between musicianship and cognition as well as on inconsistent findings regarding the influence of pre-stimulus oscillatory dynamics on RTs, we specifically addressed the following two research questions:

1. Does pre-stimulus spectral EEG power predict working memory performance during a visual Sternberg task, irrespective of expertise?

2. Are musicians and laymen characterized by distinct pre-stimulus EEG spectra that are predictive for the different behavioral outcome of experts and non-experts?

These two research questions are specifically addressed by exploiting the excellent temporal resolution of the EEG technique and by evaluating single-trial covariance matrices between pre-stimulus spectral power and RTs. This specific methodological approach will provide fruitful insights into the temporal dynamics of attentional modulation as a function of expertise.

3.3 Material and methods

3.3.1 Subjects

Fifteen professional musicians (four males; mean age = 24.33 years, SD = 5.15 ($T_{(28)} = 0.892$, $p = 0.38$; two-tailed); mean age of practice commencement = 5.46, SD = 1.62; mean total number of instrumental training hours during live = 10507, SD = 4052.94) and fifteen control subjects, students of the local universities, who had never learned to play an instrument (seven males; mean age = 26.5 years, SD = 9.75), participated in this study. The history of musical training was assessed using an in-house questionnaire (Elmer et al., 2012). In this questionnaire, age of commencement of musical training, estimated amount of hours played during single age ranges (0-7 years (age), 8-10, 11-13, etc.) per day and per week, and the respective instrument(s) played are assessed. All musicians were string players, started with their musical training before the age of ten years and were recruited from local classical orchestras and music academies. All participants were consistently right-handed, as supported by the Annett handedness inventory (Annett, 1970). None of the subjects reported any past or present neurological or psychiatric disease, nor used any medication or drugs. Informed consent was obtained from all individual participants included in the study and they were paid for participation. The present study was approved by the local ethics committee, according to the Helsinki declaration.

3.3.2 Cognitive capability and musical aptitude

To rule out a significant difference in cognitive capability, all subjects performed three subtests of the German language edition WAIS-III (Wechsler, 1997). In particular, the subjects were tested in the subtests of verbal and performance intelligence, namely on the *Working Memory Index* (Number Sequencing and Repetition), the *Perceptual and Organization Index* (Mosaic Test), and on the *Processing Speed Index* (Digit-Symbol Coding;

Waldmann, 2008). Because the subjects did not perform the entire WAIS-III test due to reasons of time, the obtained scores for the single subtests were z-transformed and a T-value was evaluated, which entered statistical analysis to test for group differences. Analyses revealed that the two groups did not differ in cognitive capability (T-value controls: 53.12, SD = 5.37, musicians: 55.55, SD = 2.99; $T_{(28)}$ = -1.278, p = 0.212; two-tailed).

All subjects performed the AMMA test (Gordon, 1989) in order to examine their developmental and stabilized musical aptitude. Thereby, the subjects had to compare 30 pairs of short melodies and rate whether the single melody pairs were exactly the same, or whether there were rhythmical or tonal differences. As expected, musicians outperformed the control group in the music test ($T_{(28)}$ = -6.584, $p < 0.001$; two-tailed).

3.3.3 Task and procedure

The EEG recording took place in a dimmed and sound shielded Faraday cage. The subjects were instructed to sit in a comfortable chair in front of a table with a computer screen at a distance of about 110 cm. Presentation of all stimulus material and the recording of the given responses was controlled by the Presentation software (Neurobehavioral Systems, USA, http://www.neurobs.com).

At the beginning of the EEG session a resting state period consisting of 7 min eyes open, 2 min eyes closed, 2 min eyes open, 2 min eyes closed was recorded (details below). During the eyes open periods, a fixation cross was presented on a computer screen. At the transition from eyes open to eyes closed and vice versa, the black screen switched to white for 2 s and a sine tone ramp (750 Hz to 1350 Hz) was presented to the subject via hi-fi-headphones (Sennheiser CX271, 70 dB sound pressure level) in order to ensure that subjects do not miss the switch from eyes closed to eyes open.

In the second part of the experiment, the subjects had to perform a visual Sternberg task, which was adapted from a previous study by Michels and colleagues (Michels et al., 2010). As shown in Figure 3.1, the Sternberg task consisted of a period of stimulus presentation during which either two or five letters (here named from now on as load level (LL) LL2 and LL5) were presented for 2.5 s on a screen. Stimulus presentation was followed by a retention period with a fixation cross, during which the subjects had to remember the presented letters for 3.5 s. Afterwards, a probe stimulus was displayed for 2 s and the

subjects had to decide by button press with their right index and middle finger whether the probe letter had been part of the stimulus presented before or not as fast and as correct as possible. Whether the 'yes' or 'no' response was assigned to the index or middle finger was randomized across subjects. The probe period was followed by an inter-trial-interval (ITI), ranging from 1.8 s to 2.7 s. This ITI was used as the pre-stimulus period, which entered data analysis. Each load level condition consisted of 32 trials that were presented in eight four-trial-blocks, pseudo randomized across LL2 and LL5. In between, after every fourth trial, a fixation cross was presented for the duration of 24.5 s, six times in total.

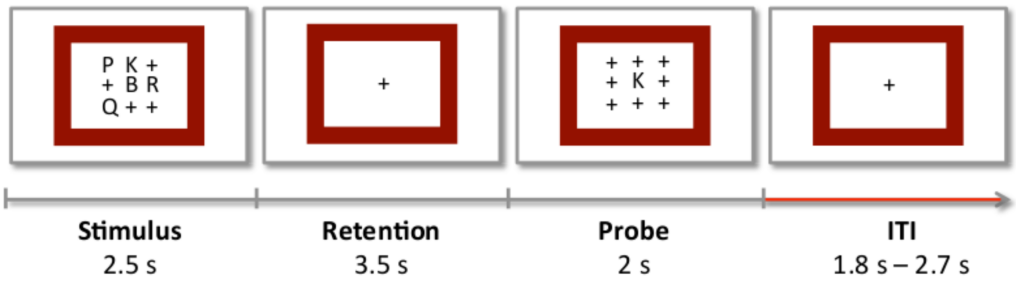

Figure 3.1: Schematic presentation of the verbal Sternberg working memory task. Depending on the load level condition (LL2 or LL5), two or five letters were presented on the screen for 2.5 s, followed by a retention period of 3.5 s. After a probe letter had been displayed, subjects had to indicate by button press, whether the letter had been presented before or not. The LL conditions were separated by an ITI, ranging from 1.8 s to 2.7 s, respectively. The red part of the arrow indicates the time period, which entered data analysis (1.8 s before stimulus presentation).

After the visual Sternberg paradigm, a second resting state of 7 min with eyes open was recorded, followed by an auditory stimulation of 6 min 28 s (first movement of 'A little night music' by W. A. Mozart) and a third resting state period of 7 min with eyes open. Analyses and result interpretations of these additional experimental conditions will be considered in further publications. All in all, the experiment lasted for around 2.5 h to 3 h.

3.3.4 Behavioral and biographical data

RTs were only calculated for the correct responses (i. e., correct 'yes' and 'no' responses), measured by the time window between onset of probe letter presentation and the response button press. To evaluate group differences in behavioral performance (RT and number of correct responses) and biographical data (IQ and musical aptitude), analysis of variance

(ANOVA) for repeated measures and independent t-tests were applied, using SPSS (http://www-01.ibm.com/software/ch/de/analytics/spss/).

3.3.5 EEG recording and data processing

High-density EEG (256-channels) was recorded using a Geodesic Netamp system (Electrical Geodesics, Eugene, Oregon) with a sampling rate of 1000 Hz by using an online band pass filter (0.1 Hz to 100 Hz). During recording, Cz (vertex of head) was used as reference electrode and impedances were kept below 30 kΩ. For offline data preprocessing with the BrainVision Analyzer software (BrainVision Analyzer 2.2; http://www.brainproducts.com/downloads.php), the electrodes in the outermost circumference were removed, resulting in a 204-channel array. Data were high and low pass filtered between 0.1 Hz and 49 Hz, including a Notch filter (50 Hz). Eye movement artifacts were removed by using an independent component analysis (T. P. Jung et al., 2000). Remaining muscle and movement artifacts were excluded by an automated raw data inspection and visually verified afterwards. Artifact free EEG data were then recomputed against the average reference. The pre-stimulus period (from -1800 ms until stimulus presentation) was segmented and band pass filtered into the following spectral frequency bands: theta (4 Hz to 8 Hz), alpha (8 Hz to 12 Hz), beta 1 (12 Hz to 18 Hz), and beta 2 (18 Hz to 30 Hz) based on previous studies (S. S. Chen et al., 2008; Geller et al., 2014). In order to obtain the time-varying power envelope of the signal, the EEG data were then squared and again low pass filtered for the single frequency bands with 2 Hz, 4 Hz, 6 Hz, 9 Hz, and 15 Hz, respectively, to obtain a smooth envelope of the time varying power envelope. Using MATLAB (the MathWorks, Natick, MA, Version R2011b), these single trial power envelopes were then combined with the reaction time measured in the corresponding trial by computing the covariance of single trial power envelopes and reaction time for each subject, electrode, and time point. These individual matrices of covariance values can thus be considered as a fingerprint of brain processes that co-vary with reaction time in a linear fashion (Koenig, Melie-Garcia, Stein, Strik, and Lehmann, 2008).

In addition, to assess putative expertise-related influences already present during a baseline resting state condition, we calculated a fast Fourier transform (FFT) based on power values in the BrainVision Analyzer software for the resting state period with eyes open of equal length as the pre-stimulus segments (32 trials per LL of 1.8 s duration each) and averaged the single trials. All data were exported for statistical analyses.

3.3.6 Statistical analyses of the EEG data

All statistical analyses were performed by using the Ragu software (Randomization Graphical User interface; http://www.thomaskoenig.ch/Ragu.htm) developed by Koenig and colleagues (Koenig, Kottlow, Stein, and Melie-Garcia, 2011). This software is based on measurements of scalp-field data (here the covariance maps) using unbiased and assumption-free randomization statistics. The threshold for statistical testing was set to $p < 0.05$, based on 5000 randomizations for all types of randomization tests. To correct for false positives due to multiple testing across time, overall significance across time and the minimal duration of significant effects were computed based on a further analysis of the data obtained by randomization (Koenig and Melie-Garcia, 2010). Briefly, each randomization run can be tested against the remaining randomization runs for reaching a p-value below the threshold ($p < 0.05$). Based on this test, one can establish the distribution of the duration of continuous periods of below-threshold p-values under the null-hypothesis. The durations of below-threshold p-values in the actual data can then be tested against this distribution.

In general, the aim of our statistical analysis was threefold, namely, we first wanted to evaluate if the two groups differ during resting state activity, being considered as a baseline condition to the working memory task. Therefore, FFT data calculated for every subject for the resting state condition entered a topographical analysis of variance (TANOVA). This analysis is based on shuffling topographical maps between subject groups and/or conditions to test if an observed topographical difference between groups/conditions can be equally well explained by the shuffled data, a procedure for calculating group and/or condition effects on the level of scalp field maps based on assumption-free randomization statistics (for details see Koenig et al., 2011).

In a second step, we wanted to evaluate time windows during the pre-stimulus period that show consistently over subjects, a linear relationship between single-trial pre-stimulus neuronal activity in specific frequency ranges and RT. To test this, we calculated topographic consistency tests (TCTs) over the whole individual covariance matrices (i. e., from -1800 ms to 0 ms) across all participants, independent of musical expertise to increase statistical power (Koenig and Melie-Garcia, 2010). This analysis is based on shuffling measurements at the individual electrode level to test if a group mean topographic distribution could equally well be explained by data with a random topography. By using TCT analyses, time windows with consistent topographical patterns were obtained, reflecting those generators

that showed, consistently across subjects, a linear relation of activation with RT. This analysis was performed for all tested frequency bands separately.

In a third step, we were interested in detecting time frames of the pre-stimulus interval that are predictive for the RTs as a function of musical expertise. Therefore, a TANOVA on the covariance matrices was performed for all frequency bands (the two groups as a between subject factor and the single frequency bands as a within subject factor). Afterwards, an averaged TCT was calculated over the time frame of the TANOVA results that displayed a significant group difference. In this manner, it was possible to evaluate the consistency of a topographic map, indicating from which group the effect in the TANOVA was coming from. At this point it is important to mention that based on our analysis, we only infer whether covariance measures between neuronal activity and RT are positive or negative.

3.4 Results

3.4.1 Behavioral data

Differences between the groups for the number of correct responses in the visual Sternberg paradigm (controls LL2: 29.07, SD = 3.67, LL5: 28, SD = 3.57; musicians LL2: 30.2, SD = 2.81, LL5: 30.27, SD = 1.65) and the RTs for both LLs (controls LL2: 0.91 s, SD = 0.18, LL5: 1.09 s, SD = 0.21; musicians LL2: 0.99 s, SD = 0.17, LL5: 1.19 s, SD = 0.18) were evaluated in two separate ANOVAs: 1. two groups × number of correct responses of the two LLs; 2. two groups × RTs of the two LLs. The first ANOVA did not reveal a significant group ($F_{(1,\ 28)} = 3.042$, $p = 0.09$) or number of correct response ($F_{(1,\ 28)} = 0.92$, $p = 0.43$) main effect, nor an interaction ($F_{(1,\ 28)} = 0.61$, $p = 0.61$). The results of the second ANOVA showed a main effect of RT (within subject contrast, $F_{(1,\ 28)} = 98.78$, $p < 0.001$) with a mean RT across groups of 0.95 s for LL2 (SD = 0.17) and a mean RT of 1.14 s for LL5 (SD = 0.2). Since we did not reveal a main group effect ($F_{(1,\ 28)} = 941.82$, $p = 0.29$) nor a group × RT interaction ($F_{(1,\ 28)} = 0.47$, $p = 0.48$), EEG data analysis was focused on finding group differences on the averaged RT for both LLs. This has further the advantage of increasing the signal-to-noise ratio.

3.4.2 EEG data

Statistical analyses of the resting state FFT data did not reveal between-group differences in any of the examined frequency bands (all p values > 0.05).

Expertise-independent analysis

For this analysis step, we calculated a TCT across all subjects, to test for a linear relationship between performance in RT and the pre-stimulus neuronal activity (-1800 ms to 0 ms), separately for the single frequency bands theta, alpha, beta 1 and beta 2. In Figure 3.2, the results of the TCT analyses over all subjects (expertise-independent analysis) for the four frequency bands are displayed. A consistency in the appearance of the time windows that were significantly predictive for performance in RT (highlighted in green) is visible in the TCT graphs for the four frequency bands.

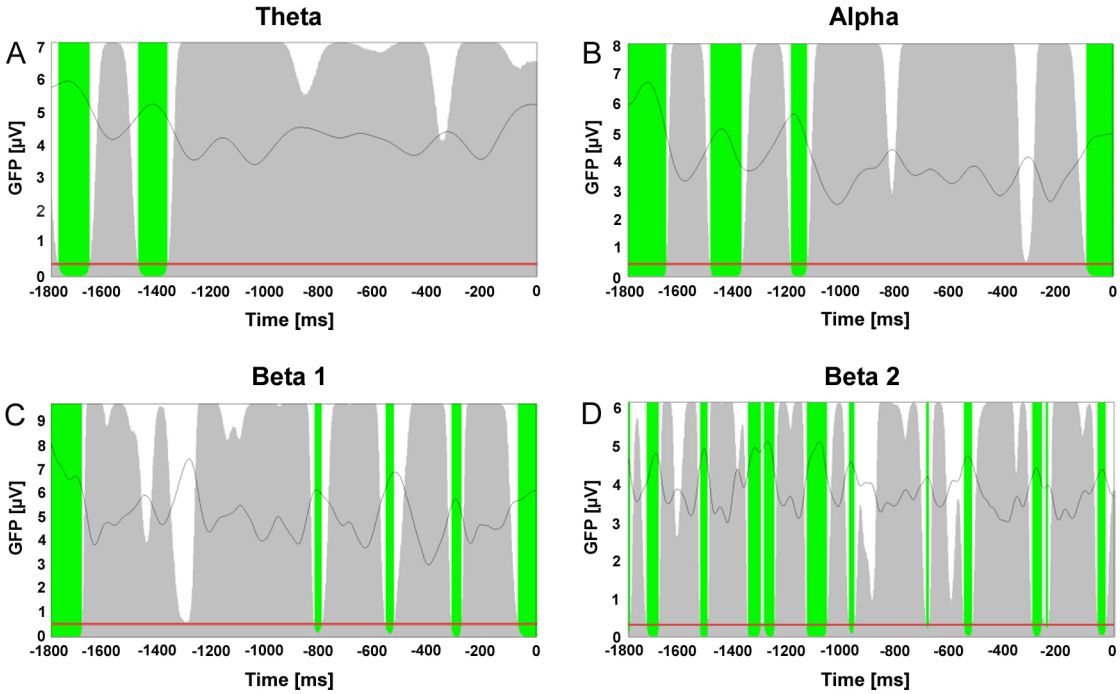

Figure 3.2: TCTs for the single frequency bands A) theta, B) alpha, C) beta 1, and D) beta 2 across all subjects. The red line indicates the uncorrected statistical threshold for significant consistency (p-value fluctuations are displayed by the gray area): A) overall significance: $p = 0.0002$ (min. duration: 4 ms), B) overall significance: $p = 0.0002$ (min. duration: 4 ms), C) overall significance: $p = 0.0002$ (min. duration: 2 ms), D) overall significance: $p = 0.0002$ (min. duration: 2 ms). Significant time frames with consistent scalp topographies, which are predictive for RT are depicted in green. The curved line in the graphs depicts the envelope of the global field power (GFP). X-axis depicts time from -1800 ms until stimulus onset (0 ms) and the y-axis depicts GFP [µV].

Figure 3.3 depicts the covariance maps (t-values; upper row), averaged for the single significant TCT time windows from Figure 3.2, and the corresponding maps of the t-tests (against zero; lower row). Very narrow adjacent time frames of the TCTs were pooled to one time window. Notably, independent of the frequency band, all maps show an anterior-posterior scalp distribution for positive covariance between the EEG data and RTs. Negative covariance was found over more lateral regions, with increasing involvement of more centro-posterior regions from theta to beta 2. In this context, a positive covariance appears if a fast RT is related to low brain activity and a slow RT to relatively increased brain activity, respectively. In contrast, a negative covariance reflects a significant relationship between fast RT and an increased brain activity as well as a significant linear relationship between slow RT and a proportionally low brain activity.

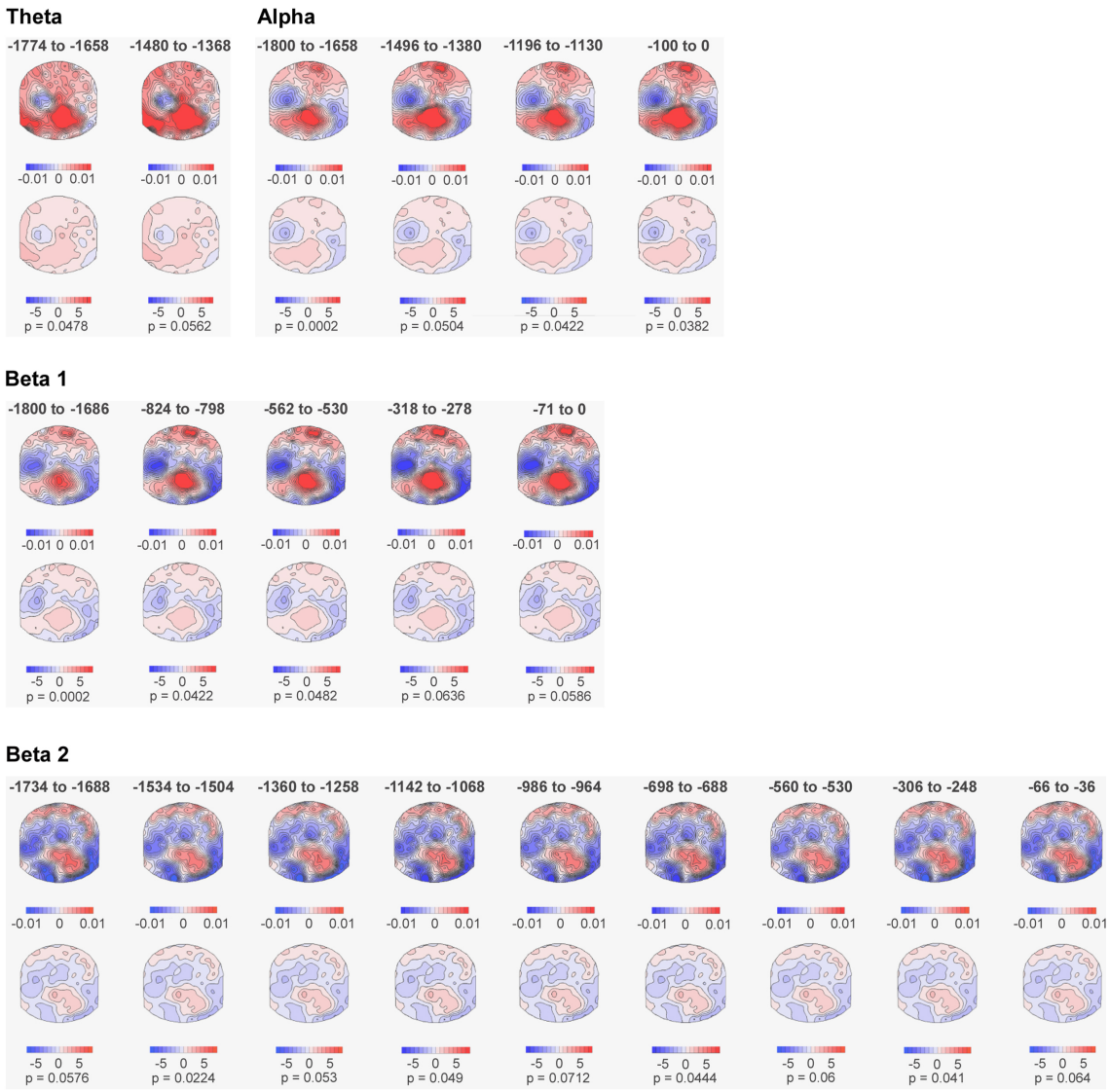

Figure 3.3: Averaged covariance (upper row) and t-maps (lower row; positive covariance: red, negative covariance: blue) for the significant predictive time windows of the TCT time frames for the single frequency bands theta, alpha, beta 1, and beta 2 and the respective p-values. Time is shown in [ms].

Expertise-dependent analysis

To test for statistical significant group differences in time frames, which were predictive for RT, a TANOVA was performed between the two groups separately for the four single frequency bands. In Figure 3.4, the results of the between-group analyses are depicted.

Significant group differences were obtained for the alpha (-328 ms to -160 ms) and the beta 1 (-382 ms to -310 ms and -252 ms to -152 ms) and beta 2 (-412 ms to -202 ms) frequency bands but not for theta (see Figure 3.4 A-C).

In a second step, TCT analyses were examined for the single groups separately for alpha, beta 1 and beta 2. In this case, a consistent scalp topography covering the time frame of the TANOVA during which groups differ significantly enabled us to reliably interpret the data. Consistent scalp topographies were only found in the musicians in the alpha frequency range (Fig. 3.4 E) but not in the non-musicians (Fig. 3.4 D).

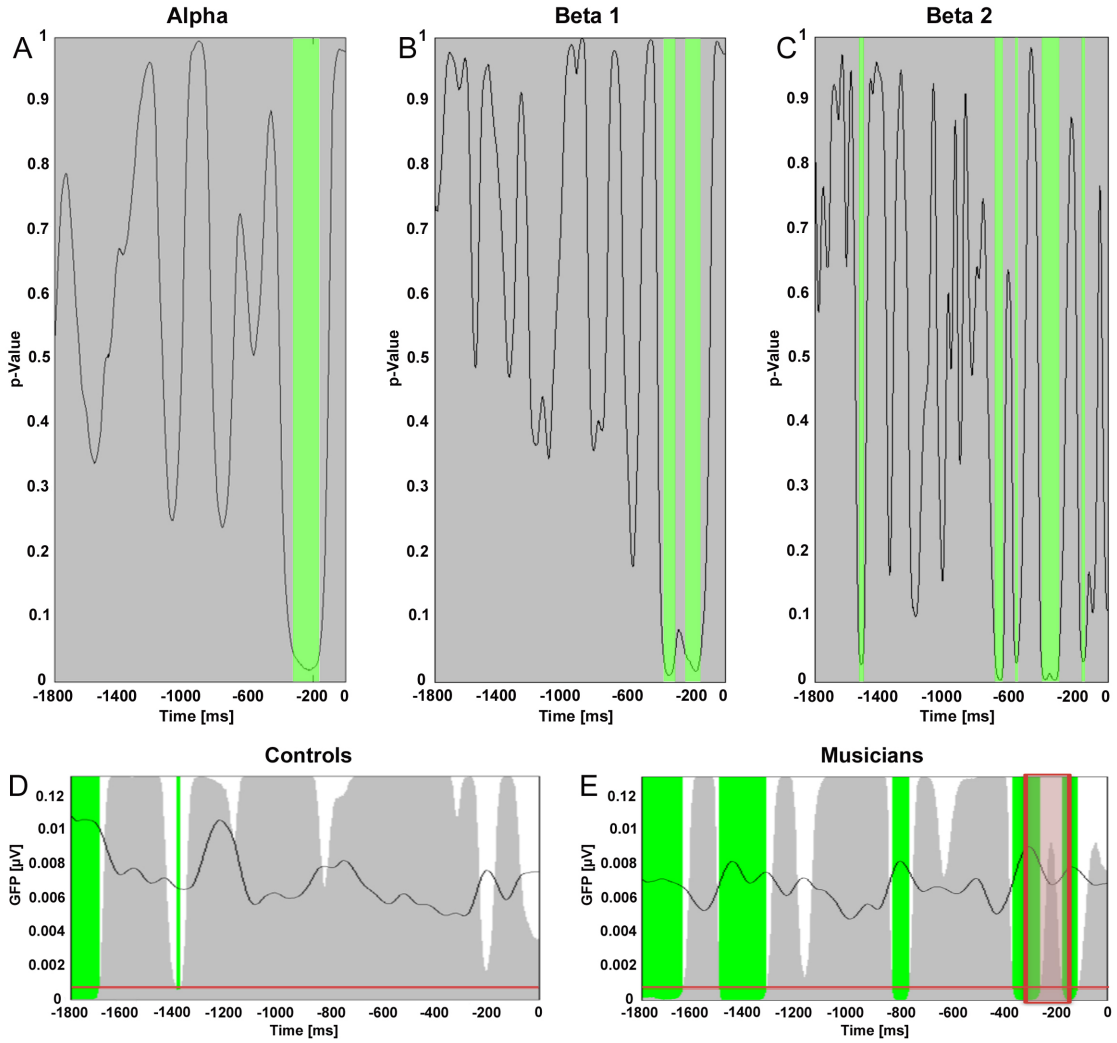

Figure 3.4: Results of the TANOVA between the control group and the musical experts for the pre-stimulus interval -1800 ms until stimulus onset (0 ms; $p < 0.01$) for A) alpha, B), beta 1, and C) beta 2. Results of the TCTs of the alpha frequency band are shown in panel D) for the controls and E) for the musicians. The red frame in E) indicates the significant time window of the TANOVA between the two groups. The red line displays the uncorrected statistical threshold (with D) overall significance: $p = 0.0014$ (min. duration: 2 ms) and E) overall significance: $p = 0.0002$ (min. duration: 4 ms)). Significant time frames with consistent scalp topographies, which are predictive for RT are depicted in green. The curved line in the graphs depicts the envelope of the GFP. X-axis depicts time from -1800 ms until stimulus onset (0 ms) and the y-axis depicts GFP [μV].

To get an idea about group-specific covariance patterns and variance across the two groups, in a third step, averaged covariance maps were created for the time frames during which

groups differed significantly in the TANOVA. The obtained covariance maps (upper row) and the respective t-maps (t-tests against zero; lower row) are shown in Figure 3.5 A-C in the left panel. The control group showed a slight anterior-posterior distributed pattern of negative covariance with a slight left-lateralized centro-parietal positive covariance distribution, whereas the musicians displayed a comparable anterior-posterior pattern distribution but with the opposite relation. The clarity of the anterior-posterior scalp pattern disappeared more and more with an increasing frequency. In the right panel of Figure 3.5, the electrodes displaying the highest t-value of both the controls and the musicians are depicted for giving a more quantitative impression about the group variances.

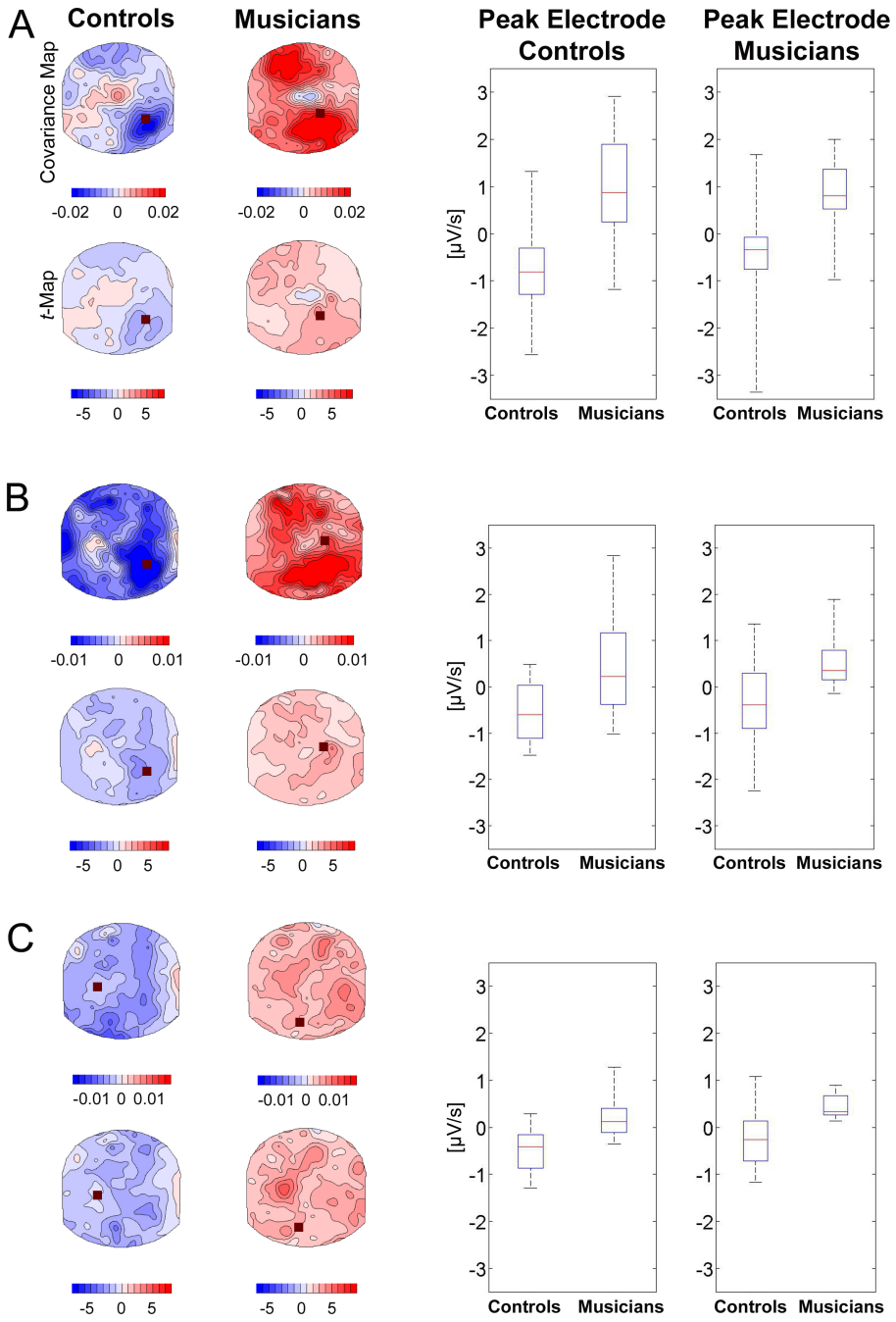

Figure 3.5: Averaged scalp topographies (upper row; t-values) for the time windows during which groups differ significantly and the corresponding *t*-maps (lower row; *t*-tests against zero) in the left panel for A) the alpha, B) the beta 1 and C) the beta 2 frequency band. Red indicates a positive and blue a negative covariance between the brain activity and performance in RT. In the right panel, group variances of the electrodes displaying the highest t-value are depicted [μV/s].

3.5 Discussion

3.5.1 General discussion

To the best of our knowledge, no previous study has specifically addressed a putative relationship between pre-stimulus activity and RTs in the context of a Sternberg paradigm, neither in a general population nor in musicians. Therefore, here we explicitly performed statistical analyses both within the whole sample of subjects as well as between the two groups. Within-group analyses constituted a first approach for validating the sensitivity of TCT applications in conjunction with our experimental design. Afterwards, we used this methodological approach in combination with TANOVA analyses for addressing the influence of musical expertise on pre-stimulus activity and behavior. Based on the distinct covariance patterns we revealed for the two groups (principally in the alpha and beta frequency-ranges), we propose that musical expertise not only affects stimulus-related cognitive activity (Baumann et al., 2008; Koelsch et al., 2009; Moreno et al., 2011; Zuk et al., 2014) but notably also pre-stimulus physiological entrainment to attentional functions during a visual Sternberg paradigm. In the following, we will discuss these results in a more comprehensive manner.

3.5.2 Behavioral data

Statistical analyses did not reveal a main effect of group nor a group by performance interaction effect. Thus, it is conceivable that the presented LLs were not demanding enough for capturing group-specific cognitive traits. In line with our findings, comparable behavioral performances between musicians and non-musicians have previously already been reported by other groups during tasks testing executive functions and working memory (Schulze and Koelsch, 2012). Although we did not identify behavioral differences between musical experts and non-musicians, we found substantial neurophysiological activation differences between the two groups. Thus, the identified activation differences are not due to performance differences rather than to specific neurophysiological organization patterns of the two groups.

3.5.3 Expertise-independent EEG analysis

Statistical analyses within the whole sample of subjects provided clear evidence for the sensitivity of TCT applications in detecting neuronal activity predicting RTs occurring six to seven seconds later in response to the probe stimulus. Our results are concordant with prior literature suggesting that trial-by-trial neuronal dynamics during pre-stimulus periods do not reflect noise per se or unspecific activations, but neurophysiological processes influencing perceptual awareness (Britz, Diaz Hernandez, Ro, and Michel, 2014), visual processing (Britz and Michel, 2011), and multisensory interaction (Gonzalez Andino, Michel, Thut, Landis, and Grave de Peralta, 2005), all in all preparatory actions involved in processing forthcoming items (for an overview on inter-individual differences also consider Kanai and Rees, 2011).

Theta oscillations

Meanwhile, there is converging evidence showing that theta oscillations (4 Hz to 8 Hz) are associated with a variety of cognitive functions, including mnemonic processes (J. Chen et al., 2013; Crespo-Garcia, Cantero, and Atienza, 2012; Ward, 2003), attention (Lara and Wallis, 2014), information integration (Ward, 2003), and neuronal communication between distinct brain regions over long-range circuits (Lara and Wallis, 2014; von Stein, Chiang, and Koenig, 2000; Ward, 2003). In addition, pre- and post-stimulus theta power has been shown to positively correlate with RTs as well as with omission errors during perceptual (Busch, Dubois, and VanRullen, 2009), discrimination (Minkwitz et al., 2011) and cognitive (Papenberg, Hammerer, Muller, Lindenberger, and Li, 2013) tasks. Thus, it is assumed that behaving slow or failing to detect a stimulus might be reflected by a down tuning of brain functions (Achim et al., 2013). Similarly, theta waves have been proposed to be related to neurophysiological activations supporting the temporal modulation of attentional functions, thereby reflecting a sensory selection mechanism (Jones and Wilson, 2005; Schroeder and Lakatos, 2009).

In line with previous literature (Busch et al., 2009), we principally revealed positive covariance patterns between pre-stimulus theta power and RTs over anterior-posterior regions that were accompanied by a slightly lateralized negative covariance pattern (see Figure 3.3). These opposite anterior-posterior and posterior-lateral directions of the positive and negative covariance patterns lead to suggest that different brain regions influence

working memory control in an antagonistic manner. Based on the reasoning that positive covariance can originate from both long RTs/increased theta power and short RTs/reduced theta power, our data suggest that strong anterior-posterior theta manifestations have a negative influence on behavioral performance. Following this logic further in terms of negative covariance, an up-regulation of posterior-lateral theta power more likely facilitates the speed of motor response. Certainly, the methodological approach we applied does not enable us to specifically describe the neuropsychological functions beyond the observed effects. Otherwise, based on previous literature showing a relationship between theta power and phasic (entrainment to the task dynamics) attention functions (Klimesch, 1999), results are interpreted as suggesting a distinct influence of theta power on an anterior-posterior attentional system (Posner and Dehaene, 1994). Certainly, a vast part of this system is involved in supporting a variety of attentional modulations that can vary depending on the task, cognitive demands, and brain-area studied (Klimesch, 1999).

Alpha oscillations

Alpha oscillations have previously been reported to indicate neurophysiological processes that have a modulatory influence on behavior. In fact, it has repeatedly been shown that decreased alpha activity favors behavioral output during visual perception (Babiloni et al., 2006; Ergenoglu et al., 2004; Hamm, Dyckman, Ethridge, McDowell, and Clementz, 2010; Hanslmayr et al., 2007; Mathewson, Gratton, Fabiani, Beck, and Ro, 2009) and spatial attention tasks (Foxe, Simpson, and Ahlfors, 1998; Freunberger et al., 2008; Rihs, Michel, and Thut, 2007; Sauseng et al., 2005; Thut, Nietzel, Brandt, and Pascual-Leone, 2006). By contrast, studies applying working memory paradigms more likely showed a divergent relationship between alpha power and performance (Hanslmayr et al., 2005).

As already described for the theta frequency band, a positive covariance between pre-stimulus alpha power and RTs was most clearly detectable at anterior-posterior scalp sites, leading to suggest that oscillatory activity in a variety of frequency bands are modulated by similar neuronal generators. Based on the fact that previous work consistently revealed activations in fronto-parietal networks during a Sternberg paradigm (Michels et al., 2010; Zakrzewska and Brzezicka, 2014), it is more likely that the topological distribution underlies neuronal activity originating from frontal and parietal brain regions, supporting a variety of attentional functions (Cabeza and Nyberg, 2000; Katsuki and Constantinidis, 2012). In this context, an increased alpha oscillatory activity could reflect a disengagement of attentional

control mechanisms (Mazaheri, DiQuattro, Bengston, and Geng, 2011), whereas a study by Meltzer and colleagues (Meltzer, Negishi, Mayes, and Constable, 2007) leads to assume that reduced alpha activity may demonstrate an up-regulation of attentional functions in fronto-parietal systems enabling faster response speed by modulating alpha-induced cortical inhibition mechanisms (Freunberger, Fellinger, Sauseng, Gruber, and Klimesch, 2009; Strauss, Wostmann, and Obleser, 2014). This leads us to speculate whether the positive alpha-to-behavior relationship we found may reflect a modulation of attentional functions in that alpha plays the role of an 'attentional gatekeeper' by reducing possible interferences with non-relevant information (Freunberger, Werkle-Bergner, Griesmayr, Lindenberger, and Klimesch, 2011). Furthermore it is worth mentioning that attentional functions are mediated by a relative amplification of brain activity in the cortical areas that contribute to a specific task (Posner and Dehaene, 1994).

In the present work, we also revealed a negative covariance between alpha power and RT at lateral scalp positions. Even though this result seems to be somehow counterintuitive, it is compatible with a putative association between alpha activity and cortical inhibitory functions just described above. Since previous neuroimaging studies provided strong evidence for a functional contribution of fronto-parietal brain regions to working memory in general (Cabeza and Nyberg, 2000) and to the Sternberg task (Michels et al., 2010), we propose that increased lateral alpha oscillations contribute to inhibit task-irrelevant neuronal populations. Such an inhibition can be particularly efficient in that it enables the reduction of neuronal noise and therefore the interference of task-unrelated neuronal activity. Certainly, further research is needed to completely understand how the excitatory-inhibitory balance is modulated through alpha oscillations during the pre-stimulus period in the context of a visual Sternberg task.

Beta oscillations

To date, the specific functional role of beta oscillations is still controversial and not completely understood (A. K. Engel and Fries, 2010). Otherwise, there is at least some evidence showing that this specific frequency band is sensitive to numerous cognitive functions, such as memory (Senkowski, Molholm, Gomez-Ramirez, and Foxe, 2006) and attention (Basile et al., 2007; Gross et al., 2004; Kaminski, Brzezicka, Gola, and Wrobel, 2012). Studies on both humans (A. K. Engel et al., 2001; Fries, 2009) and animals (Buschman and Miller, 2009, 2007) reported that tasks involving a strong engagement of

endogenous top-down components such as attention, are linked to increased activity in the beta band along frontal and parietal regions (Buschman and Miller, 2009, 2007).

It is important to mention that our analyses revealed a shift from positive to negative covariance patterns as a function of frequency-range increase (i. e., from theta to beta 2). In particular, the positive covariance at anterior-posterior scalp sites became less prominent and tended to be superseded by an increased propagation of negative covariance at central, posterior and lateral scalp sites. Since negative covariance can originate from a combination of increased power values/shorter RTs or decreased power values/longer RTs, data are interpreted as suggesting response facilitation that is mediated by increased beta oscillatory activity. A comparable relationship has previously been described by Kaminski and colleagues who evaluated pre-stimulus beta activity during a visuospatial discrimination task (Kaminski et al., 2012). They showed that faster RTs are coupled with increased beta band activity over central-posterior scalp regions prior to target presentation. The authors interpreted their findings by taking into account a bottom-up modulation of attentional functions that is mediated by beta oscillatory power. Our data complement these findings and provide additional insights into the functional meaning of different frequency bands and its relationship to behavior.

3.5.4 Group-related effects in the alpha frequency range as a function of musical expertise

Due to the fact that TCT analyses did not reveal temporally stable topographic maps in the beta frequency band, here we exclusively focus on the interpretation of between-group differences in the alpha range. The TANOVA calculated on the covariance profiles yielded significant group differences in the alpha frequency band, this result leading to suggest an expertise-dependent modulation of alpha-to-behavior relationship. As visible from Figure 3.5 A, non-musicians were principally characterized by primarily negative covariance over anterior and posterior scalp sites with a slight positive covariance distribution at the left-lateralized centro-parietal scalp site, whereas musicians more likely showed widespread positive covariance patterns at anterior and posterior loci. As suggested above, data are interpreted as indicating an expertise-dependent phasic brain state that is driven by a differential recruitment of attentional resources that might be mediated by alpha-related inhibitory activity (Foxe and Snyder, 2011). In particular, based on the distinctive positive and negative covariance maps observed in the two groups, we propose that the attentional modules are differentially influenced by expertise, namely a task-related (anterior-posterior

network) and a task-unrelated (left lateralized centro-parietal network) one. Building on the reasoning that alpha oscillations promote inhibitory functions (Foxe and Snyder, 2011; Jensen and Mazaheri, 2010; Strauss et al., 2014) and that working memory is principally dependent on fronto-parietal brain regions (Cabeza and Nyberg, 2000; Michels et al., 2010), a down-tuning of anterior-posterior alpha power (i. e., less inhibition) is presumed to facilitate response speed, principally in musicians. Otherwise, increased alpha power may possibly reflect a parsimonious strategy to circumvent excessive cognitive demands. In contrast to the musicians, the non-musicians more likely showed negative covariance patterns at anterior-posterior electrodes possibly reflecting the inhibitory influence of alpha on task-related networks but also unrelated networks (left-lateralized centro-parietal positive covariance pattern distribution).

Playing a musical instrument several hours per day has previously been shown to facilitate cognitive control mechanisms, such as attention (Baumann et al., 2008; Zuk et al., 2014) and working memory (George and Coch, 2011; Schulze and Koelsch, 2012). In addition, in order to focus on their instrument and to avoid environmental interferences, musicians have to inhibit task-irrelevant information. Currently, there is some evidence supporting the notion that the training of such filter mechanisms favors inhibitory functions (Moreno et al., 2014) that can even be transferred to non-specifically trained domains (Besson et al., 2011; Kühnis et al., 2013). Consequently, this leads us to speculate whether the positive covariance observed over posterior-lateral scalp sites in musicians may reflect the inhibition of task-irrelevant information in the task-related network, thereby enabling a more efficient functioning of the neuronal resources required for preparing the solving of the task.

3.6 Conclusion

To summarize, here we examined expertise-related and unrelated influences of pre-stimulus oscillatory activity on behavioral performance during a verbal Sternberg task. We found evidence for an overall influence of pre-stimulus activity across all analyzed frequency bands on RTs, irrespective of expertise. Notably, we identified an expertise-specific processing mode possibly reflecting the inhibition of task-irrelevant information in the task-related network thereby enabling a more efficient tuning of the neuronal resources necessary for dealing with the visual Sternberg task. We conclude that both pre-stimulus oscillatory activity and musical expertise have a predictive influence on how the brain entrains itself for managing cognition. However, our findings not only allow an implication for a better

understanding of the electrophysiological signature of musicianship but also open novel insights into the relevance of neuronal preparatory processes in association with a cognitive task. In particular, our results open new perspectives for pragmatic applications in the domains of predictive coding, oscillatory entrainment and neurofeedback. Furthermore, it is conceivable to assume that a meticulous training-related intervention on the pre-stimulus neuronal dynamics may constitute a fruitful approach for ameliorating behavioral performance during a cognitive task.

3.7 Limitations

Due to methodological constraints of the approach applied in the present study and the sparse literature available, it was not possible to infer a putative relationship between the temporal dynamics of cognitive processing stages and the significant time frames obtained from the TCTs and the TANOVA (Figure 3.2 and Figure 3.4 A-E). Therefore, further work is necessary to fully answer this open question. Another shortcoming is the fact that the LLs we applied were apparently not demanding enough for enabling us to discriminate between the two groups at a behavioral level. To pinpoint the cognitive advantages that have previously been reported in musicians, future studies should apply a more demanding task, i. e. with increased LLs. But to summarize, it can be said that the advantage of measuring different performance scores between two different groups of subjects is that it allows characterizing the functional correlates of a distinctive behavioral performance. However, this specific approach is weakened by the fact that it becomes impossible to disentangle whether the distinctive brain modulations more likely reflect cognitive effort or rather efficiency. This means that brain activity is contaminated by the different levels of performance. Otherwise, to keep behavioral performance constant across the groups has the advantage of capturing expertise-specific as well as task-related cognitive mechanisms.

CHAPTER 4

Empirical Part Study III: MRI with and without a high-density EEG cap–what makes the difference?

Carina Klein[1]*, Jürgen Hänggi[1]*, Roger Luechinger[2], Lutz Jäncke[1, 3-6]

Published in NeuroImage (2015), 106:189-97, doi: 10.1016/j.neuroimage.2014.11.053.

*authors contributed equally to this work

[1] Division Neuropsychology, Institute of Psychology, University of Zurich, Zürich, Switzerland

[2] Institute for Biomedical Engineering, University and ETH Zurich, Zürich, Switzerland

[3] International Normal Aging and Plasticity Imaging Center (INAPIC), University of Zurich, Zürich, Switzerland

[4] Center for Integrative Human Physiology (ZIHP), University of Zurich, Zürich, Switzerland

[5] University Research Priority Program (URPP), Dynamic of Healthy Aging, University of Zurich, Zürich, Switzerland

[6] Department of Special Education, King Abdulaziz University, Jeddah, Saudi Arabia

4.1 Abstract

Besides the benefit of combining EEG and MRI, much effort has been spent to develop algorithms aimed at successfully cleaning the EEG data from MRI-related gradient and ballistocardiological artifacts. However, there are also studies showing a negative influence of the EEG on MRI data quality. Therefore, in the present study, we focused for the first time on the influence of the EEG on morphometric measurements of T1-weighted MRI data (voxel and surfaced-based morphometry). Here, we demonstrate a strong influence of the EEG on cortical thickness, surface area, and volume as well as subcortical volumes due to local EEG-related inhomogeneities of the static magnetic (B_0) and the gradient field (B_1). In a second step, we analyzed the signal-to-noise ratios for both the anatomical and the functional data when recorded simultaneously with EEG and MRI and compared them to the ratios of the MRI data without simultaneous EEG measurements. These analyses revealed consistently lower signal-to-noise ratios for anatomical as well as functional MRI data during simultaneous EEG registration. In contrast, further analyses of $T2^*$-weighted images provided reliable results independent of whether including the individuals' T1-weighted image with or without the EEG cap in the fMRI preprocessing stream. Based on our findings, we strongly recommend against using the structural images obtained during simultaneous EEG-MRI recordings for further anatomical data analysis.

4.2 Introduction

MRI as well as EEG techniques are well established and widely used in the field of clinical and cognitive neuroscience. In order to exploit the strengths of both measurements, which is the high spatial resolution of the MRI and the high temporal resolution of the EEG, more and more studies use simultaneous EEG-MRI recordings. In this context, much work has been conducted so far to develop algorithms for cleaning EEG data from MRI-related ballistocardiological and gradient artifacts (Herrmann and Debener, 2008; Ritter and Villringer, 2006). However, previous studies have shown that the EEG electrodes and even the composition of EEG equipment such as the electrode paste exert negative influences on MRI data quality (Bonmassar et al., 2001). In particular, the interaction of the magnetic field and the EEG channels lead to susceptibility artifacts, which create magnetic field inhomogeneities and hence cause signal loss in the MRI data. In this context, Mullinger et al. (2008) showed that an increasing number of electrodes (32 and 64 channel net) as well as an increasing magnetic field strength (1.5, 3, and 7 Tesla) lead to both B_0 and B_1

field perturbations that result in decreasing signal intensity of the functional images in the affected regions. In addition, the strongest perturbations of the B_1, B_0, and the anatomical sequences were reported to be mainly driven by the electrocardiography (ECG) and the electrooculography (EOG) leads passing along the head (Mullinger et al., 2008).

Today, the usage of high-density EEG systems has become increasingly popular due to the benefit in source localization (Michel et al., 2004). Recently, Q. Luo and Glover (2012) tested the influence of a dense-array EEG system with 256 electrodes (the same system as used in the present study) on data quality of $T2^*$-weighted functional and T2-weighted structural MRI sequences. Their findings reveal a significant reduction of the T2-weighted anatomical signal due to a shielding effect of the conducting wires, especially over occipital regions where all the wires of the net come together. However, the signal-to-noise ratio (SNR) of the functional data with and without the EEG cap was comparable.

To the best of our knowledge, here we provide first evidence for the influence of a high-density EEG net on T1- and $T2^*$-weighted (echo planar) images at 3 Tesla. In particular, the influence of EEG electrodes on structural data analysis such as surface- and voxel-based morphometry was tested. In addition, B_0 and B_1 maps were recorded to examine whether a putative destructive effect on data quality arises from magnetic inhomogeneities of the static magnetic field or of perturbations of the radio frequency (RF) pulse. Furthermore, we tested whether including the individual T1-weighted image with and without the EEG cap in the spatial normalization step of the fMRI preprocessing has any influence on the localization of functional activity.

4.3 Material and methods

The present study is divided into a structural and functional part. In the structural part, the influence of a high-density EEG net (256 channels) on the quality of the T1-weighted MRI scans was investigated. First, we evaluated the influence of the EEG net on common morphometric features of T1-weighted MRI data such as cortical thickness and cortical surface area (derived from surface-based morphomety (SBM)), subcortical volumes (derived from subcortical segmentations), as well as on voxel-wise probabilistic gray matter density (derived from voxel-based morphometry (VBM)). Subsequently, we investigated the influence of the EEG net on the spatial SNR of the T1-weighted images, as well as on the homogeneity of the static magnetic (B_0) and the gradient field (B_1).

In the functional part of our study, the influence of the EEG net on the BOLD signal was investigated, of both resting-state data as well as during a simple auditory task. Here, we further assessed the influence of the EEG net on the temporal SNR. In addition, we also examined the bias onto spatial normalization of functional MRI scan time series when transformations are estimated based on the distorted T1-weighted images acquired during simultaneous EEG-MRI recording.

4.3.1 Subjects

Thirteen young subjects (seven women and six men) with a mean age of 28.2 years (SD = 3.02 years) participated in the structural part of the study. To evaluate the influence of T1-weighted images with and without the EEG cap on functional data, we additionally recorded $T2^*$-weighted images in six out of 13 subjects during 7 min resting state (without auditory stimulation, the control condition) with eyes open and a block of 6 min of auditory stimulation (here we used the first movement of 'A little night music' by W. A. Mozart). This subgroup comprised one man and five women (mean age of 23.5 years, SD = 2.69 years). A functional $T2^*$-weighted sequence (for a seed-based analysis of 5 min resting state data) and B_0 maps were recorded on five other subjects (one woman and four men with a mean age of 32.8 years, SD = 5.6 years). Five additional subjects (four women and one man with a mean age of 28 years, SD = 7.3 years) participated in the third part of data collection, with which the homogeneity of the B_1 field map was investigated. Except two men and one woman who participated in the T1 recordings, all other subjects were consistently right-handed as assessed by self-report. Table 4.1 provides an overview about the recorded sequences and how many subjects were measured. Participants did not report having any neurologic or psychiatric disease, showed no neuropsychological problems, and denied taking drugs or any illegal medication. The local ethics committee approved the study protocol and written informed consent was obtained from all participants.

Table 4.1: Overview of the recorded sequences/data processing and number of measured participants. Sequences that were applied to the same subjects are indicated with the same superscripts (either § or $^{\Lambda}$). AC = Auditory control condition, AS = auditory stimulation, R = right handed, RS-DMN = resting state (RS) data used for the seed based analysis of the default mode network (DMN).

MR sequence	# of subjects	Mean age ± SD	# of woman	Handedness
T1§	13	28.2 ± 3.02	7	10 R
T2* (AC, AS)§	6	23.5 ± 2.69	5	6 R
T2* (RS-DMN)$^{\Lambda}$	5	32.8 ± 5.60	1	5 R
$B_0{}^{\Lambda}$	5	32.8 ± 5.60	1	5 R
B_1	5	28.0 ± 7.30	4	5 R

4.3.2 Magnetic resonance imaging data acquisition

MRI scans were acquired on a 3.0 Tesla Philips Ingenia whole body scanner (Philips Medical Systems, Best, The Netherlands) equipped with a transmit-receive body coil and a commercial 15-element head coil array. Two volumetric 3D T1-weighted gradient echo sequence (turbo field echo (TFE)) scans were acquired on 13 participants, one scan when participants wore the EEG cap and one scan without wearing the cap. The spatial resolution of these T1-weighted images was $1.0 \times 1.0 \times 1.0\,\mathrm{mm}^3$ (acquisition matrix 240×240 pixels, 160 slices) and reconstructed to a resolution of $0.94 \times 0.94 \times 1.0\,\mathrm{mm}^3$ (reconstruction matrix 256×256 pixels, 160 slices). Further imaging parameters were: field of view (FOV) $= 240 \times 240\,\mathrm{mm}^2$, flip-angle $\alpha = 8°$, echo time (TE) $= 3.8\,\mathrm{ms}$, repetition time (TR) $= 8.27\,\mathrm{ms}$, sensitivity encoding (SENSE) factor R = 1.5. Total acquisition time was 8 min 23 s per scan.

A fast gradient echo echo-planar imaging (EPI) sequence was applied in the functional part of the study in order to obtain BOLD scans at rest as well as during auditory stimulation. 300 functional volumes were acquired with a measured spatial resolution of $3.0 \times 3.0 \times 3.7\,\mathrm{mm}^3$ (acquisition matrix 80×78 pixels, 35 slices) and a reconstructed

spatial resolution of $3.0 \times 3.0 \times 3.7\,\mathrm{mm}^3$ (reconstruction matrix 80×80 pixels, 35 slices). Further imaging parameters were: FOV $= 240 \times 240\,\mathrm{mm}^2$, TE $= 30.0$ ms, TR $= 1.96$ ms, flip-angle $\alpha = 83°$, SENSE factor R $= 2.2$. Total acquisition time was about 13 min (7 min auditory control condition without auditory stimulation, 6 min auditory stimulation) and 5 min (resting state), respectively.

A T1-weighted fast filed echo (FFE) sequence was used to map the B_0 field. The B_0 map (3D echo sequence) is composed of a magnitude and a phase image and was measured with a spatial resolution of $2.0 \times 4.0 \times 4.0\,\mathrm{mm}^3$ (acquisition matrix 112×56 pixels, 75 slices). Further imaging parameters were: FOV $= 224 \times 224 \times 120\,\mathrm{mm}^3$, dual TE $= 3.6/5.63$ ms, TR $= 30.0$ ms, flip-angle $\alpha = 60°$; total acquisition time was 4 min 11 s. The B_1 field was also mapped using a T1-weighted FFE sequence. The B_1 map was calculated by the MRI scanner software using a dual repetition method, the actual flip-angle imaging (AFI) method (Yarnykh, 2007), with TR $= 30.0/150$ ms and flip-angle $\alpha = 60°$. Further imaging parameters were: FOV $= 400 \times 400 \times 120\,\mathrm{mm}^3$, TE $= 2.2$ ms, spatial resolution of $5.9 \times 6.0 \times 12.0\,\mathrm{mm}^3$ (acquisition matrix 68×67 pixels, 20 slices); total acquisition time was 4 min 40 s.

4.3.3 Electroencephalographic system

MR images were recorded with and without the presence of an MR-compatible (field isolation containment) high-density EEG Geodesic Net Amp system with 256 channels (Electrical Geodesics, Eugene, Oregon). Electrode cables were placed along the subjects' back, leaving the scanner parallel to the subjects' legs. Before EEG cap application, the sponge-equipped electrodes were soaked with salted water (potassium chloride) and shampoo, as done during usual EEG recordings, to achieve best possible electrical conductivity. The distribution of the electrodes on the scalp is shown in Supplementary Figure A.1.

4.3.4 Surface-based morphometry

Differences in cortical morphological features such as cortical thickness, cortical surface area, and cortical volume between the conditions with and without the EEG cap were evaluated by using SBM. Cortical surface reconstruction, cortical parcellation, as well as subcortical volumetric segmentation were performed using the FreeSurfer image analysis suite (version

5.3.0), one of the commonly used surface-based morphometric tools, which is documented and freely available online (http://surfer.nmr.mgh.harvard.edu). The technical details of these procedures are described in prior publications (Fischl and Dale, 2000, 2001, 2002; Fischl, Salat, van der Kouwe, et al., 2004; Fischl, Sereno, and Dale, 1999; Fischl, Sereno, Tootell, and Dale, 1999; Fischl, van der Kouwe, et al., 2004). The 3D structural T1-weighted MRI scan was used to construct models of each subject's cortical surface in order to measure cortical thickness and cortical surface area. This fully automated procedure comprised segmentation of the cortical white matter (Fischl, Sereno, and Dale, 1999), tessellation of the gray/white matter junction, inflation of the folded surface tessellation patterns (Fischl, Sereno, and Dale, 1999; Fischl, Sereno, Tootell, and Dale, 1999) and an automatic correction of topological defects in the resulting manifold (Fischl et al., 2001). This surface was then used as starting point for a deformable surface algorithm designed to find the gray/white and pial (gray matter/cerebrospinal fluid (CSF)) surfaces with sub-millimeters precision (Fischl and Dale, 2000). The procedures for measuring cortical thickness have been validated against histological analysis (Rosas et al., 2002) and manual measurements (Kuperberg et al., 2003; Salat et al., 2004). This method uses both intensity and continuity information from the surfaces in the deformation procedure in order to interpolate surface locations for regions in which the MRI image is ambiguous (Fischl and Dale, 2000). For each subject, cortical thickness of the cortical ribbon was computed on a uniform grid (comprised by vertices) with 1 mm spacing across both cortical hemispheres, with the thickness being defined by the shortest distance between the gray/white and pial surface models. Cortical area was estimated by computing the area of each vertex in a standardized, spherical atlas space surface tessellation and mapped back into the individual subject space. The calculation of cortical volume is a vertex-wise multiplication of cortical thickness and cortical area. The thickness and area maps produced are not limited to the voxel resolution of the image and thus sensitive for sub-millimeter differences between groups (Fischl and Dale, 2000). The way in which the resolution of the cortical maps goes beyond the resolution of the original acquisition is conceptually similar to a (conventional) partial volume correction procedure. The cortex is smooth at the spatial scale of several millimeters, which is imposed as constraint by FreeSurfer to estimate the location of the surface with subvoxel accuracy. For instance, if a given voxel is darker than its neighboring gray matter it probably contains more CSF and so the surface model is at a slightly different position than if the neighboring voxels were brighter and therefore contain probably more white matter. Cortical thickness, surface area, and volume measures were mapped to the inflated surface of each participant's brain reconstruction, this allowing visualization of data across the entire cortical surface (gyri and sulci) without the data being obscured by cortical folding.

Data were re-sampled for all subjects and rendered onto a common spherical coordinate system (Fischl, Sereno, Tootell, and Dale, 1999). Then a surface-based vertex-wise cortical thickness, surface area, and volume map were computed for each participant. For the whole-brain vertex-wise analysis, the data were smoothed on the surface tessellation using an iterative nearest-neighbor averaging procedure with 148 iterations on the left hemisphere and 147 iterations on the right hemisphere, corresponding to a 2D surface-based diffusion smoothing kernel with a full width at half maximum (FWHM) of about 15 mm. (adapted from http://surfer.nmr.mgh.harvard.edu/fswiki/FreeSurferMethodsCitation and Hänggi, Brütsch, Siegel, and Jäncke, 2014)

In addition, the cerebral cortex was parcelled into units based on gyral/sulcal structure as implemented in FreeSurfer (Desikan et al., 2006; Destrieux, Fischl, Dale, and Halgren, 2010; Fischl, van der Kouwe, et al., 2004) and the subcortical brain structures were fully-automatically segmented into region of interests (ROIs), of which the volumes were computed.

4.3.5 Voxel-based morphometry

Differences in probabilistic gray matter volume between the cap and noncap condition were evaluated by using VBM (Ashburner and Friston, 2000; Good et al., 2001). All pre-processing steps were performed with the VBM8 toolbox (release 435, http://dbm.neuro.uni-jena.de/VBM/download/) that uses statistical parametric mapping (SPM)8 (release 4667, http://www.fil.ion.ucl.ac.uk/spm/) software. The following pre-processing steps were realized: 1) the coordinate origin of each native image was manually set on the anterior commissure. 2) Intensity inhomogeneity (bias field) correction, tissue class segmentation, and spatial normalization (affine and warping) were performed using unified segmentation (Ashburner and Friston, 2005) combined with the 'new segmentation approach' in SPM8. For spatial normalization, the diffeomorphic anatomical registration through exponentiated lie algebra (DARTEL) approach was used (Ashburner, 2007). Canonical a priori maps (International Consortium for Brain Mapping (ICBM) 452 T1-weighted) implemented in SPM8 were used as reference templates. 3) To enhance tissue class segmentation, hidden Markov random field (HMRF) modulation was applied (http://dbm.neuro.uni-jena.de/VBM/markov-random-fields/; Cuadra, Cammoun, Butz, Cuisenaire, and Thiran, 2005). 4) To investigate absolute volumes, the warped images were voxel-wise multiplied with the Jacobian determinant of the deformations

(linear as well as nonlinear terms were modulated). 5) The resulting Jacobian and HMRF modulated and segmented gray matter images were smoothed with a Gaussian kernel of FWHM = 9 mm and the additional smoothing introduced during the modulation process was about FWHM = 3 mm. (adapted from Elmer, Hänggi, and Jäncke, 2014b)

4.3.6 Preprocessing of resting state fMRI data

Functional MRI data were preprocessed with the Data Processing Assistant for Resting-State fMRI (DPARSF) toolbox (version 2.0; Chao-Gan and Yu-Feng, 2010) using functions of SPM8 (www.fil.ion.ucl.ac.uk/spm/). The following steps were realized: 1) slice timing correction, 2) realignment, 3) linear and non-linear normalization onto a standard EPI template, 4) voxel re-sampling to $2 \times 2 \times 2\,\mathrm{mm}^3$, 5) smoothing with a Gaussian kernel of 8 mm full width at half maximum, 6) detrending, 7) filtering (such that frequencies $0.01\,\mathrm{Hz} < f < 0.08\,\mathrm{Hz}$ passed the filter), 8) regressing out the variance of nine nuisance covariates: six parameters from head motion correction (three translation, three rotation parameters) as well as the global mean signal, white matter signal and cerebrospinal fluid signal based on standard masks implemented in SPM8. Local maxima MNI coordinates for the precuneus/posterior cingulate cortex (classical seed region for the default mode network) were obtained from a study published by Greicius, Krasnow, Reiss, and Menon (2003). Next, 5 mm radius spherical ROIs were created centered on the respective coordinates (MNI: 5, -51, 27 for right precuneus and -5, -51, 27 for left precuneus) using the Wake Forest University Pickatlas toolbox (Maldjian, Laurienti, Kraft, and Burdette, 2003). We used combined seed ROIs incorporating both right and left hemispheric parts of the precuneus. For both seed ROIs, mean signal time course was computed and used as regressor in a voxel-wise resting state functional connectivity (rsFC) analysis using functions of Resting-State fMRI Data Analysis Toolkit (REST) toolbox 1.6 (Song et al., 2011). For each subject and each seed ROI, one whole-brain correlation map was obtained (first-level). Next, each map was r-to-z-transformed to yield normal distribution for parametric group analysis (second-level). (adapted from Baur, Hänggi, Langer, and Jäncke, 2013)

4.3.7 Preprocessing of auditory task-related fMRI data

To find any putative influences of the anatomical image with and without the EEG cap on fMRI preprocessing, a session of auditory stimulation (block of 6 min) was contrasted

against resting state (eyes open, block of 7 min). A standard preprocessing procedure was applied on the functional data. Images were realigned and unwarped (B_0 map was calculated from the functional data) using field map to correct for motion and susceptibility artifacts and motion-by-susceptibility interactions (Andersson, Hutton, Ashburner, Turner, and Friston, 2001; Hutton et al., 2002). To investigate a putative bias of the EEG cap on spatial normalization of the functional images, spatial normalization was conducted once with the individual T1-weighted images recorded with and once without the EEG cap. For stereotactic normalization the MNI152 T1-weighted template was used combined with the unified segmentation approach by Ashburner and Friston (Ashburner and Friston, 2005). The data were spatially smoothed with a FWHM of a 8 mm Gaussian kernel. First level analysis on the individual level was performed using a general linear model (GLM). The design matrix included two conditions, namely an auditory control condition (resting state with eyes open) and an auditory stimulation. Furthermore, the standard hemodynamic response function as well as a standard high-pass filter (128 s cut-off) was applied. To test for statistical significant voxels, a second-level analysis was calculated with t-statistics against zero for within group effect. Afterwards, the resulting statistical parametric maps of fMRI data from the normalization with the different T1 images (with and without the EEG cap) were overlaid and visually inspected. In addition, a mean image was created for the T1-weighted images across all subjects separately for the conditions with and without the EEG cap to visualize anatomical differences between the two different conditions (see Figure 4.4).

4.3.8 Computation of the SNR

The spatial white matter SNR of the T1-weighted images was computed by using the 'wm-anat-SNR' function in the FreeSurfer's quality assessment (QA) tools (`http://ftp.nmr.mgh.harvard.edu/fswiki/QATools`). Voxels that have been labeled by FreeSurfer automatic segmentation procedure (see `aparc+aseg.mgz` file) as cerebral, cerebellar, and callosal white matter as well as voxels labeled as white matter hypointensities were considered for spatial SNR computation. With this tool, the spatial SNR has then been computed by dividing the mean intensity value of all voxels within the above-mentioned labels by the SD of these white matter voxels. The spatial gray matter SNR values were provided by the common FreeSurfer processing stream (as described in 4.3.4) from the `lh/rh.w-g.pct.stats` and the `aseg.stats` file. As described for calculation of the white matter SNR, voxels that has been labeled by FreeSurfer automatic segmentation procedure

(see `aparc.mgz` file) as cerebral and cerebellar gray matter entered spatial gray matter SNR computation by dividing the mean of the gray matter signals by the SD of these signals.

The temporal SNR was calculated in MATLAB with the `sd_images.m` script (http://dbic.dartmouth.edu/wiki/index.php/Noise_Detection) by dividing voxel-wisely (across the whole head) the mean of the signal by the SD of these voxels across all time series.

4.3.9 Preprocessing of B_0 field map

The following preprocessing steps were applied to the B_0 field map: 1) The magnitude images of both the cap and noncap condition, which are in the same space as the corresponding B_0 maps, were spatially normalized onto the T1-weighted template delivered with the SPM software using both linear and nonlinear transformations. 2) These transformations were applied to the B_0 map of the cap and noncap condition, respectively. 3) The B_0 maps were then smoothed using a Gaussian kernel of FWHM = 8 mm. Effect size was calculated based on Cohen's d using pooled variance of the local minimum or maximum of the cluster with the lowest and that with the highest p-value.

4.3.10 Preprocessing of B_1 field map

The following preprocessing steps were applied to the B_1 field map: 1) One of the magnitude images of the noncap condition, which is in the same space as the corresponding B_1 map, was co-registered to the subjects T1-weighted image derived from the noncap condition and these transformations were applied to the noncap B_1 map. 2) One of the magnitude images in the cap condition, which is also in the same space as the corresponding B_1 map, was co-registered to the co-registered magnitude image from the noncap condition (step 1) and these transformations were applied to the cap B_1 map. 3) The T1-weighted image was spatially normalized onto the T1-weighted template delivered with the SPM software using both linear and nonlinear transformations and these transformations were applied to both co-registered B_1 maps. 4) The B_1 maps were then smoothed using a Gaussian kernel of FWHM = 8 mm. Effect size was calculated based on Cohen's d using pooled variance of the local minimum or maximum of the cluster with the lowest and that with the highest p-value.

4.3.11 Individual B_0 and B_1 analysis

In order to investigate individual differences of the B_0 and B_1 field maps between the cap and the noncap condition, we computed voxel-wisely a mean and an SD map (whole head) across all subjects of the B_0 and B_1 field maps for the noncap and the cap condition, respectively. Afterwards, the individual B_0 and B_1 field maps of the cap condition were z-transformed using the mean and SD of the noncap condition, reflecting the cap > noncap contrast of the group analysis. The individual B_0 and B_1 field maps of the noncap condition were analyzed accordingly and z-transformed using the mean and SD of the cap condition, representing the noncap > cap contrast of the group analysis.

4.3.12 Statistical analyses

For all imaging data, vertex- or voxel-wise GLMs for repeated measures were applied using either parametric testing (SBM, resting state fMRI, B_0 and B_1 map) or permutation-based non-parametric testing (VBM) that also corrects for multiple comparisons across space. For VBM data, the threshold free cluster enhancement (TFCE) technique was used in addition (Smith and Nichols, 2009).

For the SBM data, a GLM based on parametric statistics was applied within FreeSurfer software (MRI_GLMfit tool) without using TFCE. Error probability was set at $p < 0.05$ combined with an FDR correction (see Figure 4.1, Supplementary Figure A.2 and A.3). For the VBM data, a GLM based on non-parametric statistics was applied within FSL software (randomize tool) using TFCE. Error probability was set at $p < 0.05$ combined with permutation-based corrections for multiple comparisons across space (see Supplementary Figure A.4).

For the B_0 and B_1 field maps, GLMs based on parametric statistics were applied within the SPM software (paired *t*-test) without using TFCE (see Figure 4.3). Here, we did not apply any correction for multiple comparisons for several reasons. The sample size was rather small ($n = 5$), the B_0 and B_1 field maps showed differential effect sensitivity, and also in order to decrease the beta error probability, i. e. the probability to miss an effect that is real.

For the resting state fMRI data, a voxel-wise one-sample *t*-test examining whether the

correlation coefficient (z-value) was different from zero, indicating positive rsFC was applied within the SPM software (see Figure 4.2). Furthermore, a paired *t*-test was computed between the two conditions (with versus without the EEG cap) to test for putative significant effects of the EEG cap on rsFC. In order to find significant voxels in the auditory stimulation condition, a one-sample *t*-test against zero was performed. This *t*-test was performed twice, once for the preprocessed data including the individual T1-weighted image with the EEG cap in the spatial normalization step and once for the control condition, i. e. the data with the individual anatomical image without the EEG cap included in the normalization step. For visualization, we have then overlaid the respective statistical parametric maps of the cap and the noncap condition (see Figure 4.4 A).

For the comparisons of global brain measures, volumes of subcortical structures, and the SNR of the T1-weighted images, SPSS statistics 20 was used (SPSS, an IBM company, Armonk, New York) without any correction for multiple comparisons.

4.4 Results

The measurement of cortical thickness with the T1-weighted MR data revealed an increased cortical thickness of approximately 0.14 mm in frontal regions of the left and 0.17 mm of the right hemisphere and a strong decrease over the temporal lobe of -0.25 mm in the left and -0.29 mm in the right hemisphere (paired *t*-test, FDR = 0.05), when subjects wore the EEG cap in the scanner (see Figure 4.1). These values are in the range of around 10% of the averaged cortical thickness in humans (Han et al., 2006; Sowell, 2004). The influence of the EEG cap also yields a negative effect on volumetric measurements of subcortical structures (see Supplementary Table A.2 and A.3) as well as on cortical volume and surface area measurements (data shown in Supplementary Figure A.2 and A.3). Analysis of the voxel-based morphometry delivered comparable results (see Supplementary Figure A.4). A consistent influence of the EEG cap on cortical thickness of every single subject that entered the group level surface-based analysis is depicted in Supplementary Figure A.5.

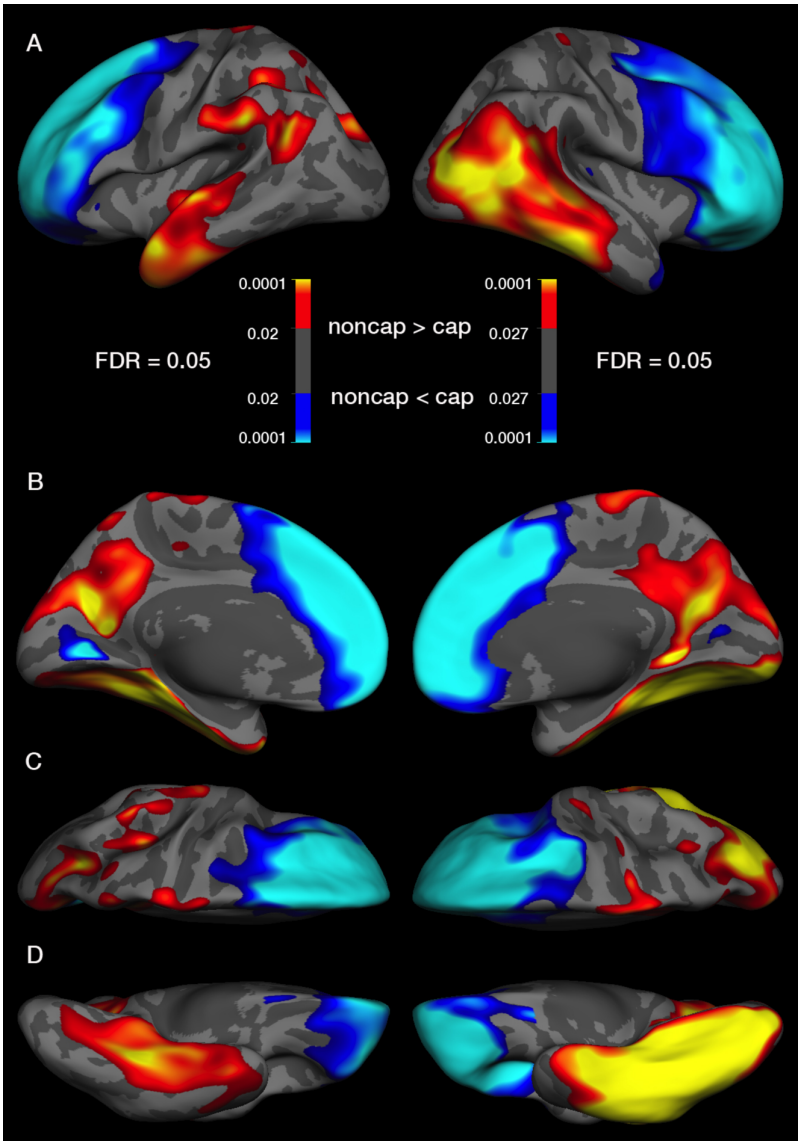

Figure 4.1: The influence of the high-density EEG net on cortical thickness measurement derived from surface-based morphometry of T1-weighted images shown on A) lateral, B) medial, C) superior, and D) inferior view of the left (left column) and right (right column) hemisphere. Cortical thickness is increased over frontal cortical areas (blue) and significantly decreased over the temporal lobe (yellow-red) when subjects wear the EEG cap (paired t-test, FDR = 0.05, false discovery rate corrected). The color bar represents FDR-corrected p-values.

In contrast to the findings reported by Q. Luo and Glover (2012), the evaluation of the SNR for both the structural (spatial SNR) and functional (temporal SNR) images revealed a significant and consistently higher value for the measurements when subjects did not

wear the EEG cap compared to when wearing the cap (T1-weighted images: mean spatial SNR of white matter without cap: 24.3, SD = 1.49; mean spatial SNR of white matter with EEG cap: 20.3, SD = 1.73; paired *t*-test, $T_{12} = 6.079$, $p < 0.001$ uncorrected; mean spatial SNR of gray matter without cap: 4.23, SD = 0.14; mean spatial SNR of gray matter with EEG cap: 4.04, SD = 0.14; paired *t*-test, $T_{12} = 8.134$, $p < 0.001$ uncorrected; $T2^*$-weighted images: mean temporal SNR without cap: 77.46, SD = 14.18; mean temporal SNR with EEG cap: 70.92, SD = 13.69; paired *t*-test, $T_4 = 2.974$, $p < 0.005$ uncorrected).

Results of the seed-based analysis of resting state activity with respect to the precuneus (MNI: 5, -51, 27 for right precuneus and -5, -51, 27 for left precuneus) as part of the default mode network (DMN) are depicted in Figure 4.2 (one-sample *t*-test against zero, $T_9 = 4.29$, $p < 0.001$ for the cap as well as the noncap condition, uncorrected). Correlations are comparable with and without the EEG cap and hemodynamic activity was found at typical DMN locations, such as the precuneus/retrosplenial cortex, the anterior cingulate cortex, the posterior cingulate cortex, and medial prefrontal regions (Raichle et al., 2001). A paired *t*-test between the two conditions did not reveal a significant difference in terms of hemodynamic fluctuations.

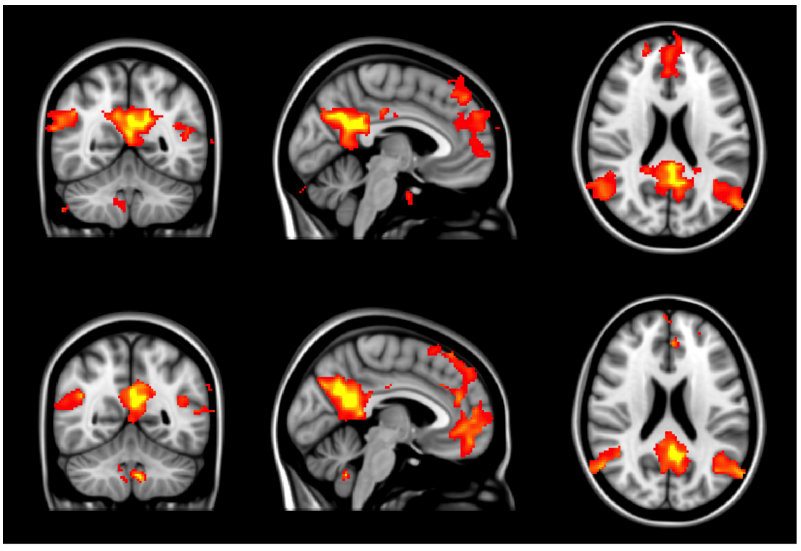

Figure 4.2: Correlations of the resting state activity with the precuneus seed hemodynamic fluctuation for the DMN with the EEG cap (upper row) and without the cap (lower row; one-sample *t*-test against zero, $T_9 = 4.29$, $p < 0.001$ uncorrected, $k > 20$ voxels for the cap as well as the non-cap condition).

As shown in Figure 4.3, analysis of B_0 and B_1 maps revealed significant local perturbations of

the field maps over frontal, fronto-temporal and parietal regions with and without the EEG net, respectively, with a stronger perturbation of the B_1 map over the right compared to the left hemisphere (B_0: paired t-test, $T_4 = 2.13$, $p < 0.05$ uncorrected, effect size according Cohen's $d \geq 0.735$ for the noncap > cap contrast and $d \geq 0.783$ for the cap > noncap contrast; B_1: paired t-test, $T_4 = 7.17$, $p < 0.001$ uncorrected, effect size according Cohen's $d \geq 3.404$ for the noncap > cap contrast and $d \geq 3.095$ for the cap > noncap contrast). Raw data of B_1 field map inhomogeneities on the example of a single subject are shown in Supplementary Figure A.6. In Supplementary Figure A.7 and A.8, z-transformed B_0 and B_1 field maps are depicted on the single-subject level.

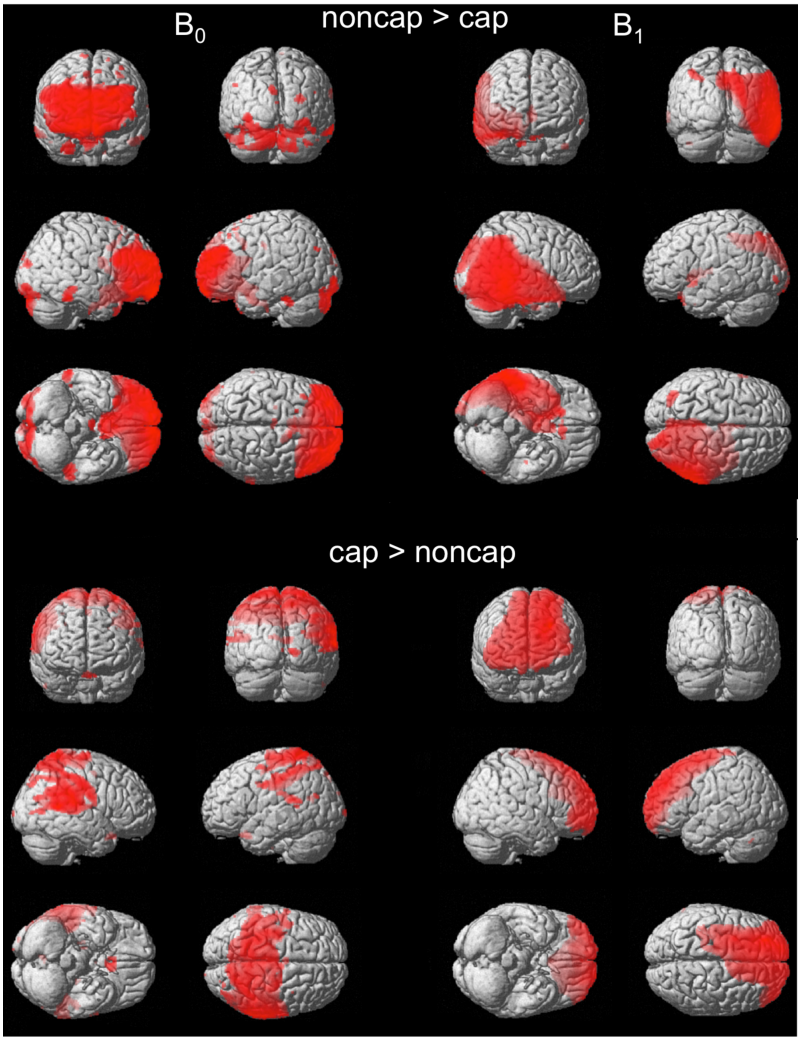

Figure 4.3: Statistical differences of B_0 (left column) and B_1 (right column) field map inhomogeneities for both contrasts noncap > cap and cap > noncap (B_0: paired *t*-test, $T_4 = 2.13$, $p < 0.05$ uncorrected, effect size according Cohen's $d \geq 0.735$ for the noncap > cap contrast and $d \geq 0.783$ for the cap > noncap contrast; B_1: paired *t*-test, $T_4 = 7.17$, $p < 0.001$ uncorrected, effect size according Cohen's $d \geq 3.404$ for the noncap > cap contrast and $d \geq 3.095$ for the cap > noncap contrast). Local field inhomogeneities are present over the frontal, parietal, and temporal lobe with an emphasis on the right hemisphere.

To understand putative differences in the analysis of the functional data due to anatomical differences caused by the EEG cap, T1-weighted images one with and one without the EEG cap were included separately in the spatial normalization step of the fMRI preprocessing (one-sample *t*-test against zero, $T_5 = 2.015$, $p < 0.05$ uncorrected; see Fig. 4.4 A). The activations in response to the auditory stimulation occurred nearly in the same brain

regions on the statistical parametric maps, with the activation slightly shifted upwards in z-direction when including the anatomical image with the EEG cap. Therefore, functional MRI seems to deliver reliable results, independent of including the individual T1-weighted image without or even with the EEG cap. Figure 4.4 B-D indicates in which brain regions the T1 images (average across group) with and without the EEG cap differ in size and shape. Therefore, with help of the 'slices' function in the FSL software, we overlaid the averaged T1 image across all participants without the EEG cap with the averaged T1 image when subjects wore the EEG cap (background image). Some slight edge effects at, for example, the corpus callosum and the outermost borders of the gray matter of the cortex are visible.

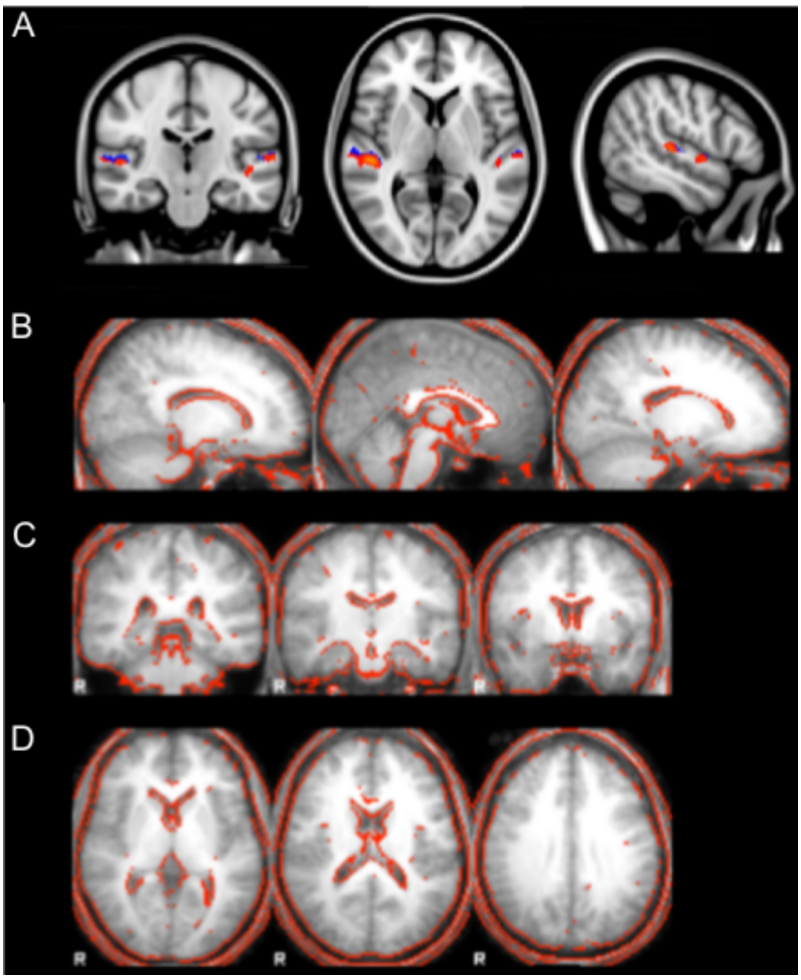

Figure 4.4: A) Overlay of the statistical parametric maps of the functional data during listening to music versus resting state activity, once using the T1-weighted image with the high-density EEG cap (blue) and once without (yellow-red) during spatial normalization on a T1-weighted template (one-sample *t*-test against zero, $T_5 = 2.015$, $p < 0.05$ uncorrected). B-D) Overlay of brain slices of averaged T1-weighted images of all subjects with (background image) and without the EEG cap of B) sagittal, C) coronal, and D) horizontal orientations. The red line indicates in which regions the T1-weighted image without the EEG cap differs in shape compared to the T1-weighted image with the EEG cap (background image).

4.5 Discussion

In order to extend the current knowledge about the influence of a high-density EEG cap on MRI data quality during simultaneous EEG-MRI scanning, we recorded T1- and $T2^*$-weighted images as well as B_0 and B_1 field maps during two conditions. In one

condition the subjects wore the EEG cap, whereas in the other they did not. To this end, we analyzed both the functional and anatomical data in conventional ways often used in the neuroscientific community (i. e., standardized fMRI preprocessing, SBM, VBM; for details see chapter 4.3).

Analysis of the SNR showed a consistent reduction for both the functional and structural data, which is in line with previous studies (Mullinger et al., 2008; Vasios et al., 2006). Therefore, we conclude that with a reduced SNR, weaker brain activation might get overlooked in simultaneous EEG-fMRI recordings in contrast to sole fMRI data acquisitions and thus, important findings might get disregarded by conservatively correcting the p-value.

Regarding the T1-weighted images, we observed a strong effect of the EEG cap on structural morphometric measurements, in particular over the frontal and temporal lobes, which was more pronounced on the right hemisphere (see Figure 4.1). The observed effect amounted to approximately 10% of the average cortical thickness in humans (Han et al., 2006; Sowell, 2004), reflecting a strong decrease in data quality. By comparing the results of cortical volume morphometric measure, which is a simple vertex-wise multiplication of cortical thickness and surface area, it becomes obvious, that the EEG cap leads to an increased vertical orientation (i. e., cortical thickness, see Figure 4.1) of disturbance of the MR signal rather than a horizontal one (i. e., surface area, see Supplementary Figure A.2). This, in turn, explains the increased influence of the cortical thickness on the volume measures (Supplementary Figure A.3) compared to the area measures.

In addition to the anatomical images, inhomogeneities of the B_0 and B_1 field maps were observed, showing that the EEG cap has a negative impact on both the static magnetic field as well as the RF pulse, as has been reported in a previous study by Mullinger and colleagues (Mullinger et al., 2008). Comparing the affected brain regions of the T1-weighted images with perturbations of the B_0 and B_1 field maps (see Figure 4.3), regional consistencies arise. In this context, inhomogeneities in the gradient field seem to lead to a decreased cortical thickness over the temporal lobe, whereas the increase in cortical thickness of frontal regions caused by the EEG cap seem to be ascribed to the frontal disruptions of both the B_0 and the B_1 field map. Thus, the interplay between the affected static magnetic field and the RF pulse seems to affect the anatomical image. A possible explanation for this finding might be that high frequencies such as the RF pulse

(128 MHz at 3 T) induce currents in the electrodes and/or electrode wires. Thereby, the resulting electromagnetic fields interact with the B_1 field, leading thus to local changes of signal intensities. On the other hand, the electrically conductive material in the EEG cap as well as eddy currents in the electrodes induced by the gradient field might also cause perturbation of the static magnetic field B_0. In the previous study by Mullinger and colleagues (Mullinger et al., 2008), frontal and parietal perturbations of the B_0 field maps appeared to be arisen by ECG and EOG leads in contrast to inhomogeneities in the B_1 maps resulting from single electrodes that increase in severity with field strength. This finding cannot be supported by our results since the EEG system used in the present study does not include extra EOG and ECG leads passing the subject's head. Moreover, the electrodes of the EEG cap are evenly distributed over the head (see Supplementary Figure A.1), not showing any left-right asymmetric arrangement of the conductive parts (electrodes/electrode wires). Consequently, the asymmetric intensity distribution of the B_0 field map induced by the gradient field is not caused by the spatial arrangement of the electrically conductive material of the EEG cap. A more plausible explanation might be the fact that the RF field is rotating (around the main magnetic field axis), which results in a left-right asymmetric alteration of the B_0 field homogeneities. Changes in the B_0 field might ultimately lead to a distorted allocation of brain tissue to the voxels during data acquisition, in particular at the borders between different tissues. As depicted in Figure 4.4 B-D, the inaccurate assignment of voxels to brain tissue types cannot be corrected by applying standard normalization processing. In order to exactly explain or to find a way to reduce or compensate the anterior-posterior and left-right asymmetry of the signal intensities of the B_1 and B_0 maps, information about the local differences in the electromagnetic field distributions are needed, which would require a full electromagnetic field simulation of the RF shield, the RF coil as well as a head model with and without the EEG cap. This is out of scope of this publication (for first steps of B_1 and B_0 map improvement see Katscher and Bornert, 2006; R. Schneider, Ritter, Haueisen, and Pfeuffer, 2013). In this context, another aspect worth to be mentioned is a putative influence of changes of the impedance of the electrodes during measurement, which might affect data quality of the MRI images. Due to ventilation in the scanner, frontal electrodes are expected to dry out first, leading to an increased impedance and thus to a worse signal quality of the EEG. Whether such changes of impedance values might lead to changes in MR signal quality was not tested here and remains an open question.

A comparison of the $T2^*$-weighted images did not reveal the EEG cap having an impact on

the localization of brain activity for either the seed-based analysis of the resting state data or on the involvement of the individual T1-weighted images with and without the EEG cap in the spatial normalization step of the fMRI preprocessing. Thus, in contrast to the anatomical data, the worse spatial resolution of the functional images ($3 \times 3 \times 3.7\,\mathrm{mm}^3$) leads to a decreased sensitivity of an inaccurate assignment of brain tissue to the respective voxel.

4.6 Conclusion

In summary, our findings reveal a strong sequence-dependent influence of high-density EEG caps on MRI data quality. Our results demonstrate decreased SNRs for both the anatomical and functional sequence during a simultaneous recording of EEG and MRI, as well as reliable results for the localization of brain activity for the functional data, but also a strong influence of the EEG cap on morphometric measurements. Based on these facts, we strongly advice against the measurement of T1-weighted images simultaneously with a high-density EEG cap, despite the benefit of time and as long as no final solution has been found for correcting the artifacts caused by the EEG setup. Even though this study provides new insights on the interaction of high-density EEG caps and MRI data, we want to emphasize that our findings are restricted to the field strength and particular EEG setup used in this work. However, as suggested by Mullinger and colleagues (Mullinger et al., 2008), a decreased destruction of anatomical images might be expected with fewer electrodes and reduced field strength. But to draw any final conclusions regarding this issue, further studies need to be performed.

CHAPTER 5

General Discussion

The present dissertation aimed at investigating the effects of musicianship on brain functions during two different conditions. First, it was tested if neuronal signatures of musical expertise are detectable during a task-free resting state condition. Second, it was examined if spectrotemporal oscillation patterns during a pre-stimulus period of a music-unrelated working memory task are predictive for later behavioral outcome. This was evaluated both dependent and independent of musicianship. Third, the last part of this dissertation focused on the research field of multimodal imaging, dealing with the problem of data quality reduction during a simultaneous EEG-MRI recording approach. Specifically, the effect of a high-density EEG setup on the reliability of MR-images (T1- and $T2^*$-weighted) was tested to optimize future study protocols.

5.1 Expertise-related changes of resting state activity

Today, it is widely accepted that spontaneous neuronal activity during rest contributes to functional activation patterns that are important for brain organization, i. e. does not reflect noise per se (Damoiseaux et al., 2006; Deco and Corbetta, 2011; Otten et al., 2006; Sadaghiani and Kleinschmidt, 2013; Scheeringa et al., 2012; Weissman-Fogel et al., 2010) and that it can be altered due to intense long-term training (Fauvel et al., 2014; Langer et al., 2013; Mackey et al., 2013; Taubert et al., 2011). Following this research, we hypothesized that functional connectivity between typical 'music-related' brain regions varies in musicians (professional string players) compared to members of a control

group, who have never learned to play a musical instrument. By applying high-density EEG, functional connectivity patterns (based on instantaneous coherence measures on the intracortical level) during a resting state period were compared between musical experts and non-musicians. As a main finding, musicians showed increased connectivity between those brain regions which are known to be involved in the production and processing of music from previous studies (for a review see Muente et al., 2002). These constitute the right motor cortex, Broca's area, the PFC and the ARC in both the theta and alpha frequency band. Thus, our results support the current idea that neuronal activation patterns during rest are shaped to a certain degree by the prior history of coactivation during intense training behavior (Deco and Corbetta, 2011; Lewis et al., 2009; Tambini, Ketz, and Davachi, 2010).

Besides the impact of musicianship on connectivity patterns on the global level, we further found enhanced local communication efficiency in the right ARC, reflected in an increased weighted node degree value. This result is in agreement with previous findings of instrument-specific functional and structural adaptations to pitch perception of the auditory cortex in the left and the right hemisphere. In this context, Schneider and co-workers (P. Schneider et al., 2005) showed a sensitivity of the left HG in musicians playing 'high pitch instruments' requiring rapid temporal processing, such as drums, guitar, or piano. In contrast, the right HG showed a tendency towards 'lower pitch melodic instruments' challenging an increased processing of spectral information, like a saxophone or string instruments.

Taken together, the findings of the first study support the idea that resting state reflects an individual imprint of the subjects' prior history of training. Thereby, the findings constitute a valuable and integrative understanding of discrete spatiotemporal network activation patterns in the field of musical expertise. Furthermore, the findings confirm previous literature examining the application of EEG as an adequate imaging technique for studying functional brain networks during rest (Jäncke and Langer, 2011; Langer et al., 2012, 2013) and that it provides promising insights in the functional signature of brain activity in the field of expertise research.

5.2 Neuronal activity as a predictor for behavioral performance

Previous research has shown that in addition to the fact that spontaneous activity during rest is affected by long-term training, even a single exposure to a task already leads to

corresponding modulations of subsequent resting state activity (Ferguson et al., 2014; Urner et al., 2013). Furthermore, the successful encoding of information during a working memory task is dependent on previous activity during rest, as well as the activity during a pre-stimulus period several seconds before item presentation (Britz and Michel, 2010; Otten et al., 2002, 2006; Park and Rugg, 2010; Peller and Wagner, 2002). Hence, the second study was designed to investigate, whether response speed can be predicted by the neuronal activation patterns during a pre-stimulus period in general, and in addition in the context of musical expertise. To figure this out, we performed a trial-by-trial topographical covariance mapping analysis by correlating the spectrotemporal activation pattern during the pre-stimulus period with the measured reaction times of the corresponding trials. The results revealed the activation patterns across all examined frequency bands, namely theta, alpha, and upper and lower beta, being predictive for behavioral outcome independent of musical training. A TANOVA between the two groups revealed that the alpha frequency band in particular has an expertise-related modulatory effect on endogenous activation patterns for processing upcoming events. In this context, the topographical covariance maps displayed a slight anterior-posterior distribution of negative covariance in the control group, whereas the experts showed the opposite relation. This finding suggests an expertise-specific processing mode possibly reflecting a down tuning of alpha activity (i. e. less inhibition) in the task-related anterior-posterior network, which presumably facilitates response speed (Freunberger et al., 2009, 2011; Strauss et al., 2014).

To summarize, the results of the second study demonstrated that the impact of neuronal activity on behavioral outcome is not restricted to a single frequency band. Rather, it is a product of the interplay of activity across various frequency ranges. Furthermore, we identified the alpha frequency band supporting an expertise-specific processing mode, possibly facilitating the brain in focusing on task-solving relevant information processing during the Sternberg paradigm. Hence, musical training not solely leads to functional and structural adaptations of the human brain for processing stimulus material, whether music related or not. It further opens a new and interesting field of research into the question of how musical training entails the brain for processing future events and in particular managing cognitive control mechanisms.

5.3 The impact of a high-density EEG setup on MRI data quality

As described in chapter 1.4, the combined acquisition of EEG and MRI data not only offers the advantage of the combined benefits of the temporal resolution of the EEG and the spatial resolution of the MRI data. It also presumes the conscious approach of successfully cleaning the data from setup-related artifacts. Since the simultaneous recording of EEG and MRI has attracted more and more attention in the field of cognitive neuroscience, it is increasingly required to ensure appropriate data handling, starting at the early stage of proper data recording. Based on this fact, the third study was aimed at particularly examining the impact of a high-density EEG system on $T2^*$- and T1-weighted MR images. To test for putative EEG cap-driven inhomogeneities of the MRI sequences, we analyzed both functional and anatomical images of subjects both with and without the EEG cap in the scanner. The analysis of the $T2^*$-weighted data revealed reliable results independent of whether the subjects were wearing the EEG cap. However, morphometric measurements (surface- and voxel-based morphometry) of the T1-weighted anatomical data showed a significantly increased cortical thickness of the frontal lobe and a reduced thickness of the temporal lobe when subjects wore the EEG cap in the scanner. In order to investigate whether the EEG electrodes themselves or the electrode wires have a destructive effect on the standard magnetic or the gradient field, B_0 and B_1 field maps were additionally measured. Data analyses revealed that the EEG setup leads to inhomogeneities of both the static as well as the radio frequency pulse. By comparing the affected regions of the perturbed anatomical image and the B_0 and B_1 field maps, regional consistencies were observed. In particular, the observed decreased cortical thickness of the temporal lobe seemed to be triggered by destructed homogeneities of the gradient field, whereas the increase in cortical thickness measures over the frontal lobe was apparently caused by disruptions of both the static and the gradient field. One explanation for the findings might be that during scanning, electrical currents are induced in the electrodes and/or electrode wires, caused by the high frequencies of the RF pulse. This results in an electromagnetic field that itself interacts with the B_1 field, which in turn might lead to reduced signal intensities in the static magnetic field.

In summary, our findings revealed a sequence-dependent influence of the EEG setup on MRI data. Regarding the practical implications of the present findings, we strongly recommend against the combined recording of anatomical and EEG data as long as no computational solution on the level of artifact rejection is found. Thus, we are convinced that the results

of the third study will enhance experimental paradigms of future simultaneous EEG-MRI studies in a wide range of research and will help especially to avoid the erroneous acquisition and analysis of destructed anatomical T1-weighted images.

5.4 Methodological constraints and implications for future work

The three studies performed comprising the present dissertation confirm and extend previous research investigating long-term training-related effects on human neuroplasticity and its multimodal imaging methods. However, some methodological issues remain to be discussed.

Regarding the first study, it is worth mentioning that although the analysis of brain networks based on electrophysiological data delivered reliable results, spatial limitations in source localization should not be neglected. However, the methodological approach applied here for data analysis has previously delivered promising results for example in the field of working memory training (Langer et al., 2013), intelligence (Langer et al., 2013), or color-hearing synaesthetes (Jäncke and Langer, 2011). Choosing intracortical ROIs for the calculation of inter-nodal associations bears the advantages that in contrast to choosing scalp electrodes, the exact ROI locations are not predefined (Pascual-Marqui, 2007a). To improve the outcome of data analysis, individual anatomical brain scans for examining the neuronal generators might improve findings compared to the common usage of an averaged standard brain. Nevertheless, the problem of volume conduction, a tissue-dependent reduction of signal transmission, still remains an unsolved question. In this context, lagged phase coherence might be a valid measure as opposed to instantaneous coherence measures. Thereby, a time shift in information transmission between brain regions is taken into account (Pascual-Marqui, 2007b). Unfortunately, comparable to previous performed studies (Jäncke, 2012; Langer et al., 2012, 2013), lagged phase coherence did not deliver proper connectivity values for the calculation of network characteristics or small-world topologies. It remains an open question whether another study design or recording system might deliver better results regarding this connectivity measure.

Furthermore, regarding the two existing MRI studies investigating the impact of musical training on resting state activity (Fauvel et al., 2014; C. Luo et al., 2012), the question arises if MRI provides an optimal technique for recording resting state data. Especially when working with a group of human subjects that are characterized by their high sensitivity

and specialized auditory processing, a scanner producing loud noise is probably not the best way for recording resting state activity. Due to the ever-growing field of state-of-the art analysis approaches in EEG research, this imaging method might provide a more appropriate way, particularly in the view of its reduced application costs.

As a future experiment, combining the findings of the first study with individual and properly recorded structural images of each subject would further the knowledge concerning the extent that resting state activity reflects a neurophysiological fingerprint of the underlying anatomical framework. In fact, functional and structural connectivity cannot be dichotomized and should rather be regarded as two interacting signatures of neuroplasticity. In this context, many studies reported a high correlation between the functional connectivity measures and the underlying structural architecture (for a review see Damoiseaux and Greicius, 2009). However, the impact of the length of the recorded resting state should not be neglected, as a long time period (several minutes) is more likely to reflect an overlap with structural connections compared to shorter time periods of measured resting state activity (milliseconds; Honey, Kotter, Breakspear, and Sporns, 2007).

With respect to the second study, it must be mentioned that the applied methodological approach accompanied by a lack of literature leads to an inability to properly interpret the affected time frames in the TCT and TANOVA analyses. With this information, even more detailed evidence could be given about the exact timing of neuronal preparation processes predictive for future performance. Nevertheless, using a covariance mapping approach brings up new perspectives in the domains of predictive coding, the entrainment of oscillatory activity in behavioral outcome and even neurofeedback paradigms in the frame of clinical applications.

5.5 Conclusion

The results reported in this Ph.D. thesis confirm on different levels that intense musical training leads to neuronal adaptations on the functional level. As the findings reveal, this expertise-related modification is not limited to the period of time during the processing of domain-specific stimulus material but is also manifested in the neuronal signature of resting state and the pre-stimulus activity during a working memory task. Even though an impressive amount of work has been done to date to understand the influence of musical

training on brain functioning and behavior, considerably more studies are required to understand the entire extent of that influence.

References

Abdul-Kareem, I. A., Stancak, A., Parkes, L. M., & Sluming, V. (2011). Increased gray matter volume of left pars opercularis in male orchestral musicians correlate positively with years of musical performance. *J Magn Reson Imaging*, *33*(1), 24–32.

Achim, A., Bouchard, J., & Braun, C. M. (2013). EEG amplitude spectra before near threshold visual presentations differentially predict detection/omission and short-long reaction time outcomes. *Int J Psychophysiol*, *89*(1), 88–98.

Adcock, R. A., Thangavel, A., Whitfield-Gabrieli, S., Knutson, B., & Gabrieli, J. D. (2006). Reward-motivated learning: mesolimbic activation precedes memory formation. *Neuron*, *50*(3), 507–17.

Allen, P. J., Josephs, O., & Turner, R. (2000). A method for removing imaging artifact from continuous EEG recorded during functional MRI. *Neuroimage*, *12*(2), 230–239.

Amer, T., Kalender, B., Hasher, L., Trehub, S. E., & Wong, Y. (2013). Do older professional musicians have cognitive advantages? *PLoS One*, *8*(8), e71630.

Amunt, K., Schlaug, G., Jäncke, L., Steinmetz, H., Schleicher, A., Dabringhaus, A., & Zilles, K. (1997). Motor cortex and hand motor skills: structural compliance in the human brain. *Hum Brain Mapp*, *5*(3), 206–15.

Andersson, J. L., Hutton, C., Ashburner, J., Turner, R., & Friston, K. (2001). Modeling geometric deformations in EPI time series. *Neuroimage*, *13*(5), 903–19.

Annett, M. (1970). A classification of hand preference by association analysis. *Br J Psychol*, *61*, 303–321.

Arieli, A., Sterkin, A., Grinvald, A., & Aertsen, A. (1996). Dynamics of ongoing activity: explanation of the large variability in evoked cortical responses. *Science*, (273), 1868–71.

Ashburner, J. (2007). A fast diffeomorphic image registration algorithm. *Neuroimage*, *38*(1), 95–113.

Ashburner, J. & Friston, K. J. (2005). Unified segmentation. *Neuroimage*, *26*(3), 839–851.

Ashburner, J. & Friston, K. J. (2000). Voxel-based morphometry–the methods. *Neuroimage*, *11*(6), 805–821.

Babiloni, C., Vecchio, F., Bultrini, A., Luca Romani, G., & Rossini, P. M. (2006). Pre- and poststimulus alpha rhythms are related to conscious visual perception: a high-resolution EEG study. *Cereb Cortex*, *16*(12), 1690–700.

Bangert, M. & Schlaug, G. (2006). Specialization of the specialized in features of external human brain morphology. *Eur J Neurosci*, *24*(6), 1832–4.

Basile, L. F., Anghinah, R., Ribeiro, P., Ramos, R. T., Piedade, R., Ballester, G., & Brunetti, E. P. (2007). Interindividual variability in EEG correlates of attention and limits of functional mapping. *Int J Psychophysiol*, *65*(3), 238–51.

Baumann, S., Meyer, M., & Jäncke, L. (2008). Enhancement of auditory-evoked potentials in musicians reflects an influence of expertise but not selective attention. *J Cogn Neurosci*, *20*(12), 2238–2249.

Baur, V., Hänggi, J., Langer, N., & Jäncke, L. (2013). Resting-state functional and structural connectivity within an insula-amygdala route specifically index state and trait anxiety. *Biol Psychiatry*, *73*, 85–92.

Bengtsson, S. L., Nagy, Z., Skare, S., Forsman, L., Forssberg, H., & Ullen, F. (2005). Extensive piano practicing has regionally specific effects on white matter development. *Nat Neurosci*, *8*(9), 1148–50.

Benjamini, Y. & Hochberg, Y. (1995). Controlling the false discovery rate: a practical and powerful approach to multiple testing. *J R Statist Soc B*, *57*(1), 289–300.

Bermudez, P., Lerch, J. P., Evans, A. C., & Zatorre, R. J. (2009). Neuroanatomical correlates of musicianship as revealed by cortical thickness and voxel-based morphometry. *Cereb Cortex*, *19*(7), 1583–96.

Besson, M., Chobert, J., & Marie, C. (2011). Transfer of training between music and speech: common processing, attention, and memory. *Front Psychol*, *2*, 94.

Bidelman, G. M., Krishnan, A., & Gandour, J. T. (2011). Enhanced brainstem encoding predicts musicians' perceptual advantages with pitch. *Eur J Neurosci*, *33*(530-538).

Bilhartz, T. D., Bruhn, R. A., & Olson, J. E. (1999). The effect of early music training on child cognitive development. *J Appl Dev Psychol*, *20*, 615–636.

Binkofski, F., Amunts, K., Stephan, K. M., Posse, S., Schormann, T., Freund, H. J., ... Seitz, R. J. (2000). Broca's region subserves imagery of motion: a combined cytoarchitectonic and fMRI study. *Hum Brain Mapp*, *11*, 273–285.

Biswal, B., DeYoe, A., & Hyde, J. (1996). Reduction of physiological fluctuations in fMRI using digital filters. *Magn Reson Med*, *35*, 107–13.

Biswal, B., Yetkin, F., Haughton, V., & Hyde, J. (1995). Functional connectivity in the motor cortex of resting human brain using echo-planar MRI. *Magn Reson Med*, *34*, 537–41.

Blood, A. J., Zatorre, R. J., Bermudez, P., & Evans, A. C. (1999). Emotional responses to pleasant and unpleasant music correlate with activity in paralimbic brain regions. *Nat Neurosci*, *2*(4), 382–87.

Bonmassar, G., Hadjikhani, N., Ives, J. R., Hinton, D., & Belliveau, J. W. (2001). Influence of EEG electrodes on the BOLD fMRI signal. *Hum Brain Mapp*, *14*(2), 108–115.

Boyke, J., Driemeyer, J., Gaser, C., Buchel, C., & May, A. (2008). Training-induced brain structure changes in the elderly. *J Neurosci*, *28*(28), 7031–5.

Britz, J., Diaz Hernandez, L., Ro, T., & Michel, C. M. (2014). EEG-microstate dependent emergence of perceptual awareness. *Front Behav Neurosci*, *8*, 163.

Britz, J. & Michel, C. M. (2010). Errors can be related to pre-stimulus differences in ERP topography and their concomitant sources. *Neuroimage*, *49*(3), 2774–82.

Britz, J. & Michel, C. M. (2011). State-dependent visual processing. *Front Psychol*, *2*, 370.

Brochard, R., Dufour, A., & Després, O. (2004). Effect of musical expertise on visuospatial abilities: evidence from reaction times and mental imagery. *Brain Cogn*, *54*(2), 103–109.

Brodmann, K. (1909). Vergleichende Lokalisationslehre der Grosshirnrinde in ihren Prinzipien dargestellt auf Grund des Zellenbaues. *Barth, Leipzig*.

Bullmore, E. & Sporns, O. (2009). Complex brain networks: graph theoretical analysis of structural and functional systems. *Nat Rev Neurosci*, *10*(3), 186–98.

Busch, N. A., Dubois, J., & VanRullen, R. (2009). The phase of ongoing EEG oscillations predicts visual perception. *J Neurosci*, *29*(24), 7869–76.

Buschman, T. J. & Miller, E. K. (2009). Serial, covert shifts of attention during visual search are reflected by the frontal eye fields and correlated with population oscillations. *Neuron*, *63*(3), 386–96.

Buschman, T. J. & Miller, E. K. (2007). Top-down versus bottom-up control of attention in the prefrontal and posterior parietal cortices. *Science*, *315*(5820), 1860–2.

Cabeza, R. & Nyberg, L. (2000). Imaging cognition II: an empirical review of 275 PET and fMRI studies. *J Cogn Neurosci*, *12*(1), 1–47.

Catani, M., Jones, D. K., & ffytche, D. H. (2005). Perisylvian language networks of the human brain. *Ann Neurol*, *57*(1), 8–16.

Catani, M. & Mesulam, M. (2008). The arcuate fasciculus and the disconnection theme in language and aphasia: history and current state. *Cortex*, *44*(8), 953–61.

Chao-Gan, Y. & Yu-Feng, Z. (2010). DPARSF: a MATLAB Toolbox for Pipeline Data Analysis of Resting-State fMRI. *Front Syst Neurosci*, *4*, 13.

Chen, J., Dastjerdi, M., Foster, B. L., LaRocque, K. F., Rauschecker, A. M., Parvizi, J., & Wagner, A. D. (2013). Human hippocampal increases in low-frequency power during associative prediction violations. *Neuropsychologia*, *51*(12), 2344–51.

Chen, S. S., Tu, P. C., Su, T. P., Hsieh, J. C., Lin, Y. C., & Chen, L. F. (2008). Impaired frontal synchronization of spontaneous magnetoencephalographic activity in patients with bipolar disorder. *Neurosci Lett*, *445*(2), 174–8.

Crespo-Garcia, M., Cantero, J. L., & Atienza, M. (2012). Effects of semantic relatedness on age-related associative memory deficits: the role of theta oscillations. *Neuroimage*, *61*(4), 1235–48.

Creutzfeldt, O., Watanabe, S., & Lux, H. (1966). Relations between EEG phenomena and potentials of single cortical cells. *Electroencephalogr Clin Neurophysiol*, *20*, 19–37.

Cuadra, M. B., Cammoun, L., Butz, T., Cuisenaire, O. A., & Thiran, J. P. A. (2005). Comparison and validation of tissue modelization and statistical classification methods in T1-weighted MR brain images. *IEEE Trans Med Imaging*, *24*(12), 1548–1565.

Damoiseaux, J. S. & Greicius, M. D. (2009). Greater than the sum of its parts: a review of studies combining structural connectivity and resting-state functional connectivity. *Brain Struct Funct*, *213*(6), 525–33.

Damoiseaux, J. S., Rombouts, S. A., Barkhof, F., Scheltens, P., Stam, C. J., Smith, S. M., & Beckmann, C. F. (2006). Consistent resting-state networks across healthy subjects. *Proc Natl Acad Sci U S A*, *103*(37), 13848–53.

De Vico Fallani, F., Maglione, A., Babiloni, F., Mattia, D., Astolfi, L., Vecchiato, G., ... Micheloyannis, S. (2010). Cortical network analysis in patients affected by schizophrenia. *Brain Topogr*, *23*(2), 214–20.

Debener, S., Mullinger, K. J., Niazy, R. K., & Bowtell, R. (2008). Properties of the ballistocardiogram artefact as revealed by EEG recordings at 1.5, 3 and 7 Tesla static magnetic field strength. *Int J Psychophysiol*, *67*, 189–199.

Deco, G. & Corbetta, M. (2011). The dynamical balance of the brain at rest. *Neuroscientist*, *17*(1), 107–23.

Desikan, R. S., Ségonne, F., Fischl, B., Quinn, B. T., Dickerson, B. C., Blacker, D., ... Killiany, R. J. (2006). An automated labeling system for subdividing the human cerebral cortex on MRI scans into gyral based regions of interest. *Neuroimage*, *31*(3), 968–980.

Destrieux, C., Fischl, B., Dale, A., & Halgren, E. (2010). Automatic parcellation of human cortical gyri and sulci using standard anatomical nomenclature. *Neuroimage*, *53*(1), 1–15.

Di, X., Zhu, S., Jin, H., Wang, P., Ye, Z., Zhou, K., ... Rao, H. (2012). Altered resting brain function and structure in professional badminton players. *Brain Connect*, *2*(4), 225–33.

Douglas, K. M. & Bilkey, D. K. (2007). Amusia is associated with deficits in spatial processing. *Nat Neurosci*, *10*(7), 915–21.

Draganski, B., Gaser, C., Busch, V., Schuierer, G., Bogdahn, U., & May, A. (2004). Changes in grey matter induced by training. *Nature*, *427*(6972), 311–312.

Draganski, B., Gaser, C., Kempermann, G., Kuhn, H., Winkler, J., Büchel, C., & May, A. (2006). Temporal and spatial dynamics of brain structure changes during extensive learning. *J Neurosci*, *26*(23), 6314–6317.

Duan, X., Liao, W., Liang, D., Qiu, L., Gao, Q., Liu, C., ... Chen, H. (2012). Large-scale brain networks in board game experts: insights from a domain-related task and task-free resting state. *PLoS One*, *7*(3), e32532.

Elbert, T., Pantev, C., Wienbruch, C., Rockstroh, B., & Taub, E. (1995). Increased cortical representation of the fingers of the left hand in string players. *Science*, *270*(5234), 305–307.

Ellis, R. J., Norton, A. C., Overy, K., Winner, E., Alsop, D. C., & Schlaug, G. (2012). Differentiating maturational and training influences on fMRI activation during music processing. *Neuroimage*, *60*(3), 1902–12.

Elmer, S., Hänggi, J., & Jäncke, L. (2014a). Interhemispheric transcallosal connectivity between the left and right planum temporale predicts musicianship, performance in temporal speech processing, and functional specialization. *Brain Struct Funct*, [Epub ahead of print].

Elmer, S., Hänggi, J., & Jäncke, L. (2014b). Processing demands upon cognitive, linguistic, and articulatory functions promote grey matter plasticity in the adult multilingual brain: insights from simultaneous interpreters. *Cortex*, *54*, 179–89.

Elmer, S., Hänggi, J., Meyer, M., & Jäncke, L. (2013). Increased cortical surface area of the left planum temporale in musicians facilitates the categorization of phonetic and temporal speech sounds. *Cortex*, *49*(10), 2812–21.

Elmer, S., Klein, C., Kühnis, J., Liem, F., Meyer, M., & Jäncke, L. (2014). Music and language expertise influence the categorization of speech and musical sounds: behavioral and electrophysiological measurements. *J Cogn Neurosci*, *26*(10), 235–69.

Elmer, S., Meyer, M., & Jäncke, L. (2012). Neurofunctional and behavioral correlates of phonetic and temporal categorization in musically trained and untrained subjects. *Cereb Cortex*, *22*(3), 650–8.

Engel, A. K. & Fries, P. (2010). Beta-band oscillations–signalling the status quo? *Curr Opin Neurobiol*, *20*(2), 156–65.

Engel, A. K., Fries, P., & Singer, W. (2001). Dynamic predictions: oscillations and synchrony in top-down processing. *Nat Rev Neurosci*, *2*(10), 704–716.

Engel, A., Hijmans, B. S., Cerliani, L., Bangert, M., Nanetti, L., Keller, P. E., & Keysers, C. (2014). Inter-individual differences in audio-motor learning of piano melodies and white matter fiber tract architecture. *Hum Brain Mapp*, *35*(5), 2483–97.

Ergenoglu, T., Demiralp, T., Bayraktaroglu, Z., Ergen, M., Beydagi, H., & Uresin, Y. (2004). Alpha rhythm of the EEG modulates visual detection performance in humans. *Brain Res Cogn Brain Res*, *20*(3), 376–83.

Fauvel, B., Groussard, M., Chetelat, G., Fouquet, M., Landeau, B., Eustache, F., ... Platel, H. (2014). Morphological brain plasticity induced by musical expertise is accompanied by modulation of functional connectivity at rest. *Neuroimage*, *90*, 179–88.

Fedorenko, E., Duncan, J., & Kanwisher, N. (2012). Language-selective and domain-general regions lie side by side within broca's area. *Curr Biol*, *22*(21), 2059–62.

Ferguson, M. A., Nielsen, J. A., & Anderson, J. S. (2014). Altered resting functional connectivity of expressive language regions after speed reading training. *J Clin Exp Neuropsychol*, *36*(5), 482–93.

Fischl, B. & Dale, A. M. (2000). Measuring the thickness of the human cerebral cortex from magnetic resonance images. *Proc Natl Acad Sci U S A*, *97*(20), 11050–11055.

Fischl, B., Liu, A., & Dale, A. M. (2001). Automated manifold surgery: constructing geometrically accurate and topologically correct models of the human cerebral cortex. *IEEE Trans Med Imaging*, *20*(1), 70–80.

Fischl, B., Salat, D. H., Busa, E., Albert, M., Dieterich, M., Haselgrove, C., ... Dale, A. M. (2002). Whole brain segmentation: automated labeling of neuroanatomical structures in the human brain. *Neuron*, *33*(3), 341–355.

Fischl, B., Salat, D. H., van der Kouwe, A. J. W., Makris, N., Ségonne, F., Quinn, B. T., & Dale, A. M. (2004). Sequence-independent segmentation of magnetic resonance images. *Neuroimage*, *23*(Supplement 1), S69–S84.

Fischl, B., Sereno, M. I., & Dale, A. M. (1999). Cortical surface-based analysis. II: inflation, flattening, and a surface-based coordinate system. *Neuroimage*, *9*(2), 195–207.

Fischl, B., Sereno, M. I., Tootell, R. B. H., & Dale, A. (1999). High-resolution intersubject averaging and a coordinate system for the cortical surface. *Hum Brain Mapp*, *8*(4), 272–284.

Fischl, B., van der Kouwe, A., Destrieux, C., Halgren, E., Ségonne, F., Salat, D. H., ... Dale, A. M. (2004). Automatically parcellating the human cerebral cortex. *Cereb Cortex*, *14*(1), 11–22.

Flor, H., Elbert, T., Knecht, S., Wienbruch, C., Pantev, C., Birbaumer, N., ... Taub, E. (1995). Phantom-limb pain as a perceptual correlate of cortical reorganization following arm amputation. *Nature*, *375*(6531), 482–4.

Fox, M. D. & Raichle, M. E. (2007). Spontaneous fluctuations in brain activity observed with functional magnetic resonance imaging. *Nat Rev Neurosci*, *8*(9), 700–11.

Fox, M. D., Snyder, A. Z., Vincent, J. L., & Raichle, M. (2007). Intrinsic fluctuations within cortical systems account for intertrial variability in human behavior. *Neuron*, *56*(1), 171–84.

Foxe, J. J., Simpson, G. V., & Ahlfors, S. P. (1998). Parieto-occipital approximately 10Hz activity reflects anticipatory state of visual attention mechanisms. *Neuroreport*, *9*(17), 3929–3933.

Foxe, J. J. & Snyder, A. C. (2011). The role of alpha-band brain oscillations as a sensory suppression mechanism during selective attention. *Front Psychol*, *2*, 154.

Freunberger, R., Fellinger, R., Sauseng, P., Gruber, W., & Klimesch, W. (2009). Dissociation between phase-locked and nonphase-locked alpha oscillations in a working memory task. *Hum Brain Mapp*, *30*(10), 3417–25.

Freunberger, R., Holler, Y., Griesmayr, B., Gruber, W., Sauseng, P., & Klimesch, W. (2008). Functional similarities between the P1 component and alpha oscillations. *Eur J Neurosci*, *27*(9), 2330–40.

Freunberger, R., Werkle-Bergner, M., Griesmayr, B., Lindenberger, U., & Klimesch, W. (2011). Brain oscillatory correlates of working memory constraints. *Brain Res*, *1375*, 93–102.

Fries, P. (2009). Neuronal gamma-band synchronization as a fundamental process in cortical computation. *Annu Rev Neurosci*, *32*, 209–24.

Gaser, C. & Schlaug, G. (2003). Brain structures differ between musicians and non-musicians. *J Neurosci*, *23*(27), 9240–9245.

Geller, A. S., Burke, J. F., Sperling, M. R., Sharan, A. D., Litt, B., Baltuch, G. H., ... Kahana, M. J. (2014). Eye closure causes widespread low-frequency power increase and focal gamma attenuation in the human electrocorticogram. *Clin Neurophysiol*, *125*(9), 1764–73.

George, E. M. & Coch, D. (2011). Music training and working memory: an ERP study. *Neuropsychologia*, *49*(5), 1083–94.

Gladwin, T. E., Lindsen, J. P., & de Jong, R. (2006). Pre-stimulus EEG effects related to response speed, task switching and upcoming response hand. *Biol Psychol*, *72*(1), 15–34.

Gonzalez Andino, S. L., Michel, C. M., Thut, G., Landis, T., & Grave de Peralta, R. (2005). Prediction of response speed by anticipatory high-frequency (gamma band) oscillations in the human brain. *Hum Brain Mapp*, *24*(1), 50–8.

Good, C., Johnsrude, I. S., Ashburner, J., Henson, R. N. A., Friston, K. J., & Frackowiak, R. S. J. (2001). A voxel-based morphometric study of ageing in 465 normal adult human brains. *Neuroimage*, *14*(1), 21–36.

Gordon, E. E. (1989). Manual for the advanced measures of music education. *Chicago, G.I.A. Publications, Inc.*

Greicius, M. D., Krasnow, B., Reiss, A. L., & Menon, V. (2003). Functional connectivity in the resting brain: a network analysis of the default mode hypothesis. *Proc Natl Acad Sci U S A*, *100*(1), 253–8.

Greicius, M. D., Supekar, K., Menon, V., & Dougherty, R. F. (2009). Resting-state functional connectivity reflects structural connectivity in the default mode network. *Cereb Cortex*, *19*(1), 72–8.

Grewe, O., Kopiez, R., & Altenmüller, E. (2009). Chills as an indicator of individual emotional peaks. *Ann N Y Acad Sci*, *1169*, 351–4.

Grewe, O., Nagel, F., Kopiez, R., & Altenmüller, E. (2005). How does music arouse 'chills'? Investigating strong emotions, combining psychological, physiological, and psychoacoustical methods. *Ann N Y Acad Sci*, *1060*, 446–9.

Griffith, T. D. & Warren, J. D. (2002). The planum temporale as a computational hub. *Trends Neurosci*, *25*(7), 348–353.

Gross, J., Schmitz, F., Schnitzler, I., Kessler, K., Shapiro, K., Hommel, B., & Schnitzler, A. (2004). Modulation of long-range neural synchrony reflects temporal limitations of visual attention in humans. *Proc Natl Acad Sci U S A*, *101*(35), 13050–5.

Groussard, M., La Joie, R., Rauchs, G., Landeau, B., Chetelat, G., Viader, F., ... Platel, H. (2010). When music and long-term memory interact: effects of musical expertise on functional and structural plasticity in the hippocampus. *PLoS One*, *5*(10), e13225.

Gruber, M. J. & Otten, L. J. (2010). Voluntary control over prestimulus activity related to encoding. *J Neurosci*, *30*(29), 9793–800.

Haegens, S., Handel, B. F., & Jensen, O. (2011). Top-down controlled alpha band activity in somatosensory areas determines behavioral performance in a discrimination task. *J Neurosci*, *31*(14), 5197–204.

Haider, B., Duque, A., Hasenstaub, A., & McCormick, D. (2006). Neocortical network activity in vivo is generated through a dynamic balance of excitation and inhibition. *J Neurosci*, *26*, 4535–45.

Halwani, G. F., Loui, P., Ruber, T., & Schlaug, G. (2011). Effects of practice and experience on the arcuate fasciculus: comparing singers, instrumentalists, and non-musicians. *Front Psychol*, *2*, 156.

Hamann, J. M., Dayan, E., Hummel, F. C., & Cohen, L. G. (2014). Baseline frontostriatal-limbic connectivity predicts reward-based memory formation. *Hum Brain Mapp*, *35*(12), 5921–31.

Hamm, J. P., Dyckman, K. A., Ethridge, L. E., McDowell, J. E., & Clementz, B. A. (2010). Preparatory activations across a distributed cortical network determine production of express saccades in humans. *J Neurosci*, *30*(21), 7350–7.

Han, X., Jovicich, J., Salat, D., van der Kouwe, A., Quinn, B., Czanner, S., ... Fischl, B. (2006). Reliability of MRI-derived measurements of human cerebral cortical thickness: the effects of field strength, scanner upgrade and manufacturer. *Neuroimage*, *32*(1), 180–94.

Hänggi, J., Brütsch, K., Siegel, A. M., & Jäncke, L. (2014). The architecture of the chess player's brain. *Neuropsychologia*, *62*, 152–162.

Hanslmayr, S., Aslan, A., Staudigl, T., Klimesch, W., Herrmann, C. S., & Bauml, K. H. (2007). Prestimulus oscillations predict visual perception performance between and within subjects. *Neuroimage*, *37*(4), 1465–73.

Hanslmayr, S., Klimesch, W., Sauseng, P., Gruber, W., Doppelmayr, M., Freunberger, R., & Pecherstorfer, T. (2005). Visual discrimination performance is related to decreased alpha amplitude but increased phase locking. *Neurosci Lett*, *375*(1), 64–8.

Haslinger, B., Erhard, P., Altenmüller, E., Hennenlotter, A., Schwaiger, M., Grafin von Einsiedel, H., ... Ceballos-Baumann, A. O. (2004). Reduced recruitment of motor association areas during bimanual coordination in concert pianists. *Hum Brain Mapp*, *22*(3), 206–15.

Hebb, D. O. (1949). Organization of behavior: a neuropsychological theory. *John Wiley and Sons, New York*.

Herholz, S. C. & Zatorre, R. J. (2012). Musical training as a framework for brain plasticity: behavior, function, and structure. *Neuron*, *76*(3), 486–502.

Herrmann, C. S. & Debener, S. (2008). Simultaneous recording of EEG and BOLD responses: a historical perspective. *Int J Psychophysiol*, *67*(3), 161–8.

Ho, Y. C., Cheung, M. C., & Chan, A. S. (2003). Music training improves verbal but not visual memory: cross-sectional and longitudinal explorations in children. *Neuropsychology*, *17*(3), 439–450.

Honey, C., Kotter, R., Breakspear, M., & Sporns, O. (2007). Network structure of cerebral cortex shapes functional connectivity on multiple time scales. *Proc Natl Acad Sci U S A*, *104*(24), 10240–5.

Huang, Z., Zhang, J. X., Yang, Z., Dong, G., Wu, J., Chan, A. S., & Weng, X. (2010). Verbal memory retrieval engages visual cortex in musicians. *Neuroscience*, *168*(1), 179–89.

Humphries, M. D., Gurney, K., & Prescott, T. J. (2006). The brainstem reticular formation is a small-world, not scale-free, network. *Proc Biol Sci*, *273*(1585), 503–11.

Hutton, C., Bork, A., Josephs, O., Deichmann, R., Ashburner, J., & Turner, R. (2002). Image distortion correction in fMRI: a quantitative evaluation. *Neuroimage*, *16*(1), 217–40.

Hyde, K. L., Lerch, J., Norton, A., Forgeard, M., Winner, E., Evans, A. C., & Schlaug, G. (2009). Musical training shapes structural brain development. *J Neurosci*, *29*(10), 3019–25.

Imfeld, A., Oechslin, M. S., Meyer, M., Loenneker, T., & Jancke, L. (2009). White matter plasticity in the corticospinal tract of musicians: a diffusion tensor imaging study. *Neuroimage*, *46*(3), 600–7.

Jäncke, L. (2009a). Music drives brain plasticity. *F1000 Biol Rep*, *1*, 78.

Jäncke, L. (2013). Music making and the aging brain. *Zeitschrift für Neuropsychologie*, *24*(2), 113–121.

Jäncke, L. (2012). The dynamic audio-motor system in pianists. *Ann N Y Acad Sci*, *1252*, 246–52.

Jäncke, L. (2009b). The plastic human brain. *Restor Neurol Neurosci*, *27*(5), 521–38.

Jäncke, L. & Langer, N. (2011). A strong parietal hub in the small-world network of coloured-hearing synaesthetes during resting state EEG. *J Neuropsychol*, *5*(2), 178–202.

Jäncke, L., Langer, N., & Hänggi, J. (2012). Diminished whole-brain but enhanced peri-sylvian connectivity in absolute pitch musicians. *J Cogn Neurosci*, *24*(6), 1447–1461.

Jäncke, L., Specht, K., Mirzazade, S., Loose, R., Himmelbach, M., Lutz, K., & Shah, N. J. (1998). A parametric analysis of the 'rate effect' in the sensorimotor cortex: a

functional magnetic resonance imaging analysis in human subjects. *Neurosci Lett*, *252*(1), 37–40.

Jenkins, W. M., Merzenich, M. M., & Recanzone, G. (1990). Neocortical representational dynamics in adult primates: implications for neuropsychology. *Neuropsychologia*, *28*(6), 573–584.

Jensen, O. & Mazaheri, A. (2010). Shaping functional architecture by oscillatory alpha activity: gating by inhibition. *Front Hum Neurosci*, *4*, 186.

Jolles, D. D., van Buchem, M. A., Crone, E. A., & Rombouts, S. A. (2013). Functional brain connectivity at rest changes after working memory training. *Hum Brain Mapp*, *34*(2), 396–406.

Jones, M. W. & Wilson, M. A. (2005). Theta rhythms coordinate hippocampal-prefrontal interactions in a spatial memory task. *PLoS Biol*, *3*(12), 2187–2199.

Jung, T. P., Makeig, S., Humphries, C., Lee, T. W., Mckeown, M. J., Iragui, V., & Sejnowski, T. (2000). Removing electroencephalographic artifacts by blind source separation. *Psychophysiology*, *37*, 163–178.

Jung, W. H., Kim, S. N., Lee, T. Y., Jang, J. H., Choi, C. H., Kang, D. H., & Kwon, J. S. (2013). Exploring the brains of Baduk (Go) experts: gray matter morphometry, resting-state functional connectivity, and graph theoretical analysis. *Front Hum Neurosci*, *7*, 633.

Kaminski, J., Brzezicka, A., Gola, M., & Wrobel, A. (2012). Beta band oscillations engagement in human alertness process. *Int J Psychophysiol*, *85*(1), 125–8.

Kanai, R. & Rees, G. (2011). The structural basis of inter-individual differences in human behavior and cognition. *Nat Rev Neurosci*, *12*(4), 231–42.

Katscher, U. & Bornert, P. (2006). Parallel RF transmission in MRI. *NMR Biomed*, *19*(3), 393–400.

Katsuki, F. & Constantinidis, C. (2012). Unique and shared roles of the posterior parietal and dorsolateral prefrontal cortex in cognitive functions. *Front Integr Neurosci*, *6*, 17.

Kelly, A. M. & Garavan, H. (2005). Human functional neuroimaging of brain changes associated with practice. *Cereb Cortex*, *15*(8), 1089–102.

Kenet, T., Bibitchkov, D., Tsodyks, M., Grinvald, A., & Arieli, A. (2003). Spontaneously emerging cortical representations of visual attributes. *Nature*, *425*, 954–6.

Klimesch, W. (1999). EEG alpha and theta oscillations reflect cognitive and memory performance: a review and analysis. *Brain Res Rev*, *29*(2-3), 169–195.

Klimesch, W., Sauseng, P., & Hanslmayr, S. (2007). EEG alpha oscillations: the inhibition-timing hypothesis. *Brain Res Rev*, *53*(1), 63–68.

Koelsch, S. (2014). Brain correlates of music-evoked emotions. *Nat Rev Neurosci*, *15*(3), 170–80.

Koelsch, S., Fritz, T., v. Cramon, D. Y., Muller, K., & Friederici, A. D. (2006). Investigating emotion with music: an fMRI study. *Hum Brain Mapp*, *27*(3), 239–50.

Koelsch, S., Schulze, K., Sammler, D., Fritz, T., Muller, K., & Gruber, O. (2009). Functional architecture of verbal and tonal working memory: an fMRI study. *Hum Brain Mapp*, *30*(3), 859–73.

Koenig, T., Kottlow, M., Stein, M., & Melie-Garcia, L. (2011). Ragu: a free tool for the analysis of EEG and MEG event-related scalp field data using global randomization statistics. *Comput Intell Neurosci*, *2011*, 938925.

Koenig, T. & Melie-Garcia, L. (2010). A method to determine the presence of averaged event-related fields using randomization tests. *Brain Topogr*, *23*(3), 233–42.

Koenig, T., Melie-Garcia, L., Stein, M., Strik, W., & Lehmann, C. (2008). Establishing correlations of scalp field maps with other experimental variables using covariance analysis and resampling methods. *Clin Neurophysiol*, *119*(6), 1262–70.

Konorski, J. (1948). Conditioned reflexes and neuron organization. *Cambridge University Press, Cambridge, UK*.

Kottlow, M., Praeg, E., Leuthy, C., & Jäncke, L. (2011). Artist's advance: decreased upper alpha power while drawing in artists compared with non-artists. *Brain Topogr*, *23*, 392–402.

Kraus, N. & Chandrasekaran, B. (2010). Music training for the development of auditory skills. *Nat Rev Neurosci*, *11*(8), 599–605.

Krings, T., Töpper, R., Foltys, H., Erberich, S., Sparing, R., Willmes, K., & Thron, A. (2000). Cortical activation patterns during complex motor tasks in piano players and control subjects. A functional magnetic resonance imaging study. *Neurosci Lett*, *278*, 189–193.

Kubicki, S., Herrmann, W. M., Fichte, K., & Freund, G. (1979). Reflections on the topics: EEG frequency bands and regulation of vigilance. *Pharmakopsychiatr Neuropsychopharmakol*, *12*(2), 237–245.

Kühnis, J., Elmer, S., & Jäncke, L. (2014). Auditory evoked responses in musicians during passive vowel listening are modulated by functional connectivity between bilateral auditory-related brain regions. *J Cogn Neurosci*, 1–12.

Kühnis, J., Elmer, S., Meyer, M., & Jäncke, L. (2013). Musicianship boosts perceptual learning of pseudoword-chimeras: an electrophysiological approach. *Brain Topogr*, *26*(1), 110–25.

Kuperberg, G. R., Broome, M. R., McGuire, P. K., David, A. S., Eddy, M., Ozawa, F., ... Fischl, B. (2003). Regionally localized thinning of the cerebral cortex in schizophrenia. *Arch Gen Psychiatry*, *60*(9), 878–888.

Langer, N., Pedroni, A., Gianotti, L. R., Hänggi, J., Knoch, D., & Jäncke, L. (2012). Functional brain network efficiency predicts intelligence. *Hum Brain Mapp*, *33*(6), 1393–406.

Langer, N., von Bastian, C. C., Wirz, H., Oberauer, K., & Jäncke, L. (2013). The effects of working memory training on functional brain network efficiency. *Cortex*, *49*(9), 2424–38.

Lara, A. H. & Wallis, J. D. (2014). Executive control processes underlying multi-item working memory. *Nat Neurosci*, *17*(6), 876–83.

Lewis, C. M., Baldassarre, A., Committeri, G., Romani, G. L., & Corbetta, M. (2009). Learning sculpts the spontaneous activity of the resting human brain. *Proc Natl Acad Sci U S A*, *106*(41), 17558–63.

Logothetis, N. K., Pauls, J., Augath, M., Trinath, T., & Oeltermann, A. (2001). Neurophysiological investigation of the basis of the fMRI signal. *Nature*, *412*, 150–157.

Lotze, M., Scheler, G., Tan, H. R. M., Brain, C., & Birbaumer, N. (2003). The musician's brain: functional imaging of amateurs and professionals during performance and imagery. *Neuroimage*, *20*(3), 1817–29.

Loui, P. & Schlaug, G. (2009). Investigating musical disorders with diffusion tensor imaging: a comparison of imaging parameters. *Ann N Y Acad Sci*, *1169*, 121–5.

Luo, C., Guo, Z. W., Lai, Y. X., Liao, W., Liu, Q., Kendrick, K. M., ... Li, H. (2012). Musical training induces functional plasticity in perceptual and motor networks: insights from resting-state fMRI. *PLoS One*, *7*(5), e36568.

Luo, Q. & Glover, G. H. (2012). Influence of dense-array EEG cap on fMRI signal. *Magn Reson Med*, *68*(3), 807–15.

MacDonald, A. W. 3., Cohen, J. D., Stenger, V. A., & Carter, C. S. (2000). Dissociating the role of the dorsolateral prefrontal and anterior cingulate cortex in cognitive control. *Science*, *288*(5472), 1835–8.

Mackey, A. P., Miller Singley, A. T., & Bunge, S. A. (2013). Intensive reasoning training alters patterns of brain connectivity at rest. *J Neurosci*, *33*(11), 4796–803.

Maess, B., Koelsch, S., Gunter, T. C., & Friederici, A. D. (2001). Musical syntax is processed in Broca's area: an MEG study. *Nat Neurosci*, *4*(5), 540–45.

Maguire, E. A., Gadian, D. G., Johnsrude, I. S., Good, C. D., Ashburner, J., Frackowiak, R. S., & Frith, C. D. (2000). Navigation-related structural change in the hippocampi of taxi drivers. *Proc Natl Acad Sci U S A*, *97*(8), 4398–403.

Makuuchi, M. & Friederici, A. D. (2013). Hierarchical functional connectivity between the core language system and the working memory system. *Cortex*, *49*(9), 2416–23.

Maldjian, J. A., Laurienti, P. J., Kraft, R. A., & Burdette, J. H. (2003). An automated method for neuroanatomic and cytoarchitectonic atlas-based interrogation of fMRI data sets. *Neuroimage*, *19*(3), 1233–9.

Marie, C., Magne, C., & Besson, M. (2011). Musicians and the metric structure of words. *J Cogn Neurosci*, *23*, 294–305.

Marques, C., Moreno, S., Castro, S. L., & Besson, M. (2007). Musicians detect pitch violation in a foreign language better than nonmusicians: behavioral and electrophysiological evidence. *J Cogn Neurosci*, *19*(9), 1453–1463.

Mason, M., Norton, M., Van Horn, J., Wegner, D., Grafton, S., & Macrae, C. (2007). Wandering minds: the default mode network and stimulus-independent thought. *Science*, *315*(5810), 393–395.

Mathewson, K. E., Gratton, G., Fabiani, M., Beck, D. M., & Ro, T. (2009). To see or not to see: prestimulus alpha phase predicts visual awareness. *J Neurosci*, *29*(9), 2725–32.

Mazaheri, A., DiQuattro, N. E., Bengston, J., & Geng, J. J. (2011). Pre-stimulus activity predicts the winner of top-down vs. bottom up attentional selection. *PLoS One*, *6*(2), e16243.

Meeter, M., Murre, J. M., & Talamini, L. M. (2004). Mode shifting between storage and recall based on novelty detection in oscillating hippocampal circuits. *Hippocampus*, *14*(6), 722–41.

Meltzer, J. A., Negishi, M., Mayes, L. C., & Constable, R. T. (2007). Individual differences in EEG theta and alpha dynamics during working memory correlate with fMRI responses across subjects. *Clin Neurophysiol*, *118*(11), 2419–36.

Merzenich, M. M., Recanzone, G. H., Jenkins, W. M., & Grajski, K. A. (1990). Adaptive mechanisms in cortical networks underlying cortical contributions to learning and nondeclarative memory. *Cold Spring Harb Symp Quant Biol*, *55*, 873–887.

Meyer, M., Baumann, S., & Jancke, L. (2006). Electrical brain imaging reveals spatio-temporal dynamics of timbre perception in humans. *Neuroimage*, *32*(4), 1510–23.

Michel, C. M., Murray, M. M., Lantz, G., Gonzalez, S., Spinelli, L., & Grave de Peralta, R. (2004). EEG source imaging. *Clin Neurophysiol*, *115*(10), 2195–222.

Michels, L., Bucher, K., Lüchinger, R., Klaver, P., Martin, E., Jeanmonod, D., & Brandeis, D. (2010). Simultaneous EEG-fMRI during a working memory task: modulations in low and high frequency bands. *PLoS One*, *5*(4), e10298.

Milovanov, R. & Tervaniemi, M. (2011). The interplay between musical and linguistic aptitudes: a review. *Front Psychol*, *2*, 321.

Minkwitz, J., Trenner, M. U., Sander, C., Olbrich, S., Sheldrick, A. J., Schonknecht, P., ... Himmerich, H. (2011). Prestimulus vigilance predicts response speed in an easy visual discrimination task. *Behav Brain Funct*, *7*, 31.

Moreno, S., Bialystok, E., Barac, R., Schellenberg, E. G., Cepeda, N. J., & Chau, T. (2011). Short-term music training enhances verbal intelligence and executive function. *Psychol Sci*, *22*(11), 1425–33.

Moreno, S., Marques, C., Santos, A., Santos, M., Castro, S. L., & Besson, M. (2009). Musical training influences linguistic abilities in 8-year-old children: more evidence for brain plasticity. *Cereb Cortex*, *19*(3), 712–23.

Moreno, S., Wodniecka, Z., Tays, W., Alain, C., & Bialystok, E. (2014). Inhibitory control in bilinguals and musicians: event related potential (ERP) evidence for experience-specific effects. *PLoS One*, *9*(4), e94169.

Muente, T. F., Altenmueller, E., & Jaencke, L. (2002). The musician's brain as a model of neuroplasticity. *Nat Neurosci*, *3*, 473–478.

Mullinger, K., Debener, S., Coxon, R., & Bowtell, R. (2008). Effects of simultaneous EEG recording on MRI data quality at 1.5, 3 and 7 Tesla. *Int J Psychophysiol*, *67*(3), 178–88.

Noh, E., Herzmann, G., Curran, T., & de Sa, V. R. (2014). Using single-trial EEG to predict and analyze subsequent memory. *Neuroimage*, *84*, 712–23.

Nudo, R. J., Jenkins, W. M., & Merzenich, M. M. (1990). Repetitive microstimulation alters the cortical representation of movements in adult rats. *Somatosens Mot Res*, *7*(4), 463–483.

Oechslin, M. S., Imfeld, A., Loenneker, T., Meyer, M., & Jäncke, L. (2009). The plasticity of the superior longitudinal fasciculus as a function of musical expertise: a diffusion tensor imaging study. *Front Hum Neurosci*, *3*, 76.

Ohnishi, T., Matsuda, H., Asada, T., Aruga, M., Hirakata, M., Nishikawa, M., ... Imabayashi, E. (2001). Functional anatomy of musical perception in musicians. *Cereb Cortex*, *11*, 754–760.

Ott, C. G., Langer, N., Oechslin, M. S., Meyer, M., & Jäncke, L. (2011). Processing of voiced and unvoiced acoustic stimuli in musicians. *Front Psychol*, *2*(195).

Otten, L. J., Henson, R. N., & Rugg, M. D. (2002). State-related and item-related neural correlates of successful memory encoding. *Nat Neurosci*, *5*(12), 1339–44.

Otten, L. J., Quayle, A. H., Akram, S., Ditewig, T. A., & Rugg, M. D. (2006). Brain activity before an event predicts later recollection. *Nat Neurosci*, *9*(4), 489–91.

Otten, L. J., Quayle, A. H., & Puvaneswaran, B. (2010). Prestimulus subsequent memory effects for auditory and visual events. *J Cogn Neurosci*, *22*(6), 1212–1223.

Pantev, C., Lappe, C., Herholz, S. C., & Trainor, L. (2009). Auditory-somatosensory integration and cortical plasticity in musical training. *Ann N Y Acad Sci*, *1169*, 143–50.

Pantev, C., Roberts, L. E., Schulz, M., Engelien, A., & Ross, B. (2001). Timbre-specific enhancement of auditory cortical representations in musicians. *Neuroreport*, *12*(1), 169–174.

Papenberg, G., Hammerer, D., Muller, V., Lindenberger, U., & Li, S. C. (2013). Lower theta inter-trial phase coherence during performance monitoring is related to higher reaction time variability: a lifespan study. *Neuroimage*, *83*, 912–20.

Park, H. & Rugg, M. D. (2010). Prestimulus hippocampal activity predicts later recollection. *Hippocampus*, *20*(1), 24–8.

Parsons, L. M., Sergent, J., Hodges, D. A., & Fox, P. T. (2005). The brain basis of piano performance. *Neuropsychologia*, *43*(2), 199–215.

Pascual-Marqui, R. D. (2007a). Discrete, 3D distributed, linear imaging methods of electrical neuronal activity. Part 1: exact, zero error localization. *ArXiv*, *arXiv:0710.3341 [math-ph]*.

Pascual-Marqui, R. D. (2007b). Instantaneous and lagged measurements of linear and nonlinear dependence between groups of multivariate time series: frequency decomposition. *ArXiv*, *arXiv:0711.1455 [stat.ME]*(http://arxiv.org/abs/0711.1455).

Pascual-Marqui, R. D. (2002). Standardized low resolution brain electromagnetic tomography (sLORETA): technical details. *Methods Find Exp Clin Pharmacol*, *24*(500), 5–12.

Patel, A. D. (2011). Why would musical training benefit the neural encoding of speech? The OPERA hypothesis. *Front Psychol*, *2*, 142.

Peller, K. A. & Wagner, A. D. (2002). Observing the transformation of experience into memory. *Trends Cogn Sci*, *6*(2), 93–102.

Peretz, I. & Zatorre, R. J. (2005). Brain organization for music processing. *Annu Rev Psychol*, *56*, 89–114.

Peters, A., Payne, B. R., & Budd, J. (1994). A numerical analysis of the geniculocortical input to striate cortex in the monkey. *Cereb Cortex*, *215*(3), 215–29.

Poeppel, D. (2003). The analysis of speech in different temporal integration windows: cerebral lateralization as 'asymmetric sampling in time'. *Speech Communication*, *41*(1), 245–255.

Posner, M. I. & Dehaene, S. (1994). Attentional networks. *Trends Neurosci*, *17*(2), 75–79.

Proverbio, A. M., Calbi, M., Manfredi, M., & Zani, A. (2014). Audio-visuomotor processing in the musician's brain: an ERP study on professional violinists and clarinetists. *Sci Rep*, *4*, 5866.

Proverbio, A. M., Manfredi, M., Zani, A., & Adorni, R. (2013). Musical expertise affects neural bases of letter recognition. *Neuropsychologia*, *51*(3), 538–49.

Raichle, M. E., MacLeod, A. M., Snyder, A. Z., Powers, W. J., Gusnard, D. A., & Shulman, G. L. (2001). A default mode of brain function. *Proc Natl Acad Sci U S A*, *98*(2), 676–682.

Rihs, T. A., Michel, C. M., & Thut, G. (2007). Mechanisms of selective inhibition in visual spatial attention are indexed by alpha-band EEG synchronization. *Eur J Neurosci*, *25*(2), 603–10.

Ritter, P. & Villringer, A. (2006). Simultaneous EEG-fMRI. *Neurosci Biobehav Rev*, *30*(6), 823–38.

Rosas, H. D., Liu, A. K., Hersch, S., Glessner, M., Ferrante, R. J., Salat, D. H., ... Fischl, B. (2002). Regional and progressive thinning of the cortical ribbon in huntington's disease. *Neurology*, *58*(5), 695–701.

Rubinov, M. & Sporns, O. (2010). Complex network measures of brain connectivity: uses and interpretations. *Neuroimage*, *52*(3), 1059–69.

Sadaghiani, S. & Kleinschmidt, A. (2013). Functional interactions between intrinsic brain activity and behavior. *Neuroimage*, *80*, 379–86.

Sala-Llonch, R., Pena-Gomez, C., Arenaza-Urquijo, E. M., Vidal-Pineiro, D., Bargallo, N., Junque, C., & Bartres-Faz, D. (2012). Brain connectivity during resting state and subsequent working memory task predicts behavioural performance. *Cortex*, *48*(9), 1187–96.

Salat, D. H., Buckner, R. L., Snyder, A. Z., Greve, D. N., Desikan, R. S. R., Busa, E., ... Fischl, B. (2004). Thinning of the cerebral cortex in aging. *Cereb. Cortex*, *14*(7), 721–730.

Sauseng, P., Klimesch, W., Stadler, W., Schabus, M., Doppelmayr, M., Hanslmayr, S., ... Birbaumer, N. (2005). A shift of visual spatial attention is selectively associated with human EEG alpha activity. *Eur J Neurosci*, *22*(11), 2917–26.

Scheeringa, R., Petersson, K. M., Kleinschmidt, A., Jensen, O., & Bastiaansen, M. C. (2012). EEG alpha power modulation of fMRI resting-state connectivity. *Brain Connect*, *2*(5), 254–64.

Schlaug, G., Forgeard, M., Zhu, L., Norton, A., Norton, A., & Winner, E. (2009). Training-induced neuroplasticity in young children. *Ann N Y Acad Sci*, *1169*, 205–8.

Schlaug, G., Jäncke, L., Huang, Y., Staiger, J. F., & Steinmetz, H. (1995a). Increased corpus callosum size in musicians. *Neuropsychologia*, *33*(8), 1047–1055.

Schlaug, G., Jäncke, L., Huang, Y., & Steinmetz, H. (1995). In vivo evidence of structural brain asymmetry in musicians. *Science*, *267*(5198), 699–701.

Schmithorst, V. J. & Wilke, M. (2002). Differences in white matter architecture between musicians and non-musicians: a diffusion tensor imaging study. *Neurosci Lett*, *321*(1-2), 57–60.

Schneider, P., Scherg, M., Dosch, H. G., Specht, H. J., Gutschalk, A., & Rupp, A. (2002). Morphology of Heschl's gyrus reflects enhanced activation in the auditory cortex of musicians. *Nat Neurosci*, *5*(7), 688–94.

Schneider, P., Sluming, V., Roberts, N., Bleeck, S., & Rupp, A. (2005). Structural, functional, and perceptual differences in Heschl's gyrus and musical instrument preference. *Ann N Y Acad Sci*, *1060*, 387–94.

Schneider, R., Ritter, D., Haueisen, J., & Pfeuffer, J. (2013). B0-informed variable density trajectory design for enhanced correction of off-resonance effects in parallel transmission. *Magn Reson Med*, *71*(4), 1381–93.

Schon, D. & Francois, C. (2011). Musical expertise and statistical learning of musical and linguistic structures. *Front Psychol*, *2*, 167.

Schon, D., Magne, C., & Besson, M. (2004). The music of speech: music training facilitates pitch processing in both music and language. *Psychophysiology*, *41*(3), 341–9.

Schroeder, C. E. & Lakatos, P. (2009). Low-frequency neuronal oscillations as instruments of sensory selection. *Trends Neurosci*, *32*(1), 9–18.

Schulze, K. & Koelsch, S. (2012). Working memory for speech and music. *Ann N Y Acad Sci*, *1252*, 229–36.

Schulze, K., Mueller, K., & Koelsch, S. (2011). Neural correlates of strategy use during auditory working memory in musicians and non-musicians. *Eur J Neurosci*, *33*(1), 189–96.

Seither-Preisler, A., Parncutt, R., & Schneider, P. (2014). Size and synchronization of auditory cortex promotes musical, literacy, and attentional skills in children. *J Neurosci*, *34*(33), 10937–49.

Senkowski, D., Molholm, S., Gomez-Ramirez, M., & Foxe, J. J. (2006). Oscillatory beta activity predicts response speed during a multisensory audiovisual reaction time task: a high-density electrical mapping study. *Cereb Cortex*, *16*(11), 1556–65.

Sergent, J., Zuck, E., Terriah, S., & MacDonald, B. (1992). Distributed neural network underlying musical sight-reading and keyboard performance. *Science*, *257*(5066), 106–9.

Sluming, V., Brooks, J., Howard, M., Downes, J. J., & Roberts, N. (2007). Broca's area supports enhanced visuospatial cognition in orchestral musicians. *J Neurosci*, *27*(14), 3799–806.

Smith, S. M. & Nichols, T. E. (2009). Threshold-free cluster enhancement: addressing problems of smoothing, threshold dependence and localisation in cluster inference. *Neuroimage*, *44*(1), 83–98.

Song, X. W., Dong, Z. Y., Long, X. Y., Li, S. F., Zuo, X. N., Zhu, C. Z., ... Zang, Y. F. (2011). REST: a toolkit for resting-state functional magnetic resonance imaging data processing. *PLoS One*, *6*(9), e25031.

Sowell, E. R. (2004). Longitudinal mapping of cortical thickness and brain growth in normal children. *J Neurosci*, *24*(38), 8223–8231.

Sporns, O., Honey, C., & Kötter, R. (2007). Identification and classification of Hubs in brain networks. *PLoS One*, *2*(10), e1049.

Steele, C. J., Bailey, J. A., Zatorre, R. J., & Penhune, V. B. (2013). Early musical training and white-matter plasticity in the corpus callosum: evidence for a sensitive period. *J Neurosci*, *33*(3), 1282–90.

Strauss, A., Wostmann, M., & Obleser, J. (2014). Cortical alpha oscillations as a tool for auditory selective inhibition. *Front Hum Neurosci*, *8*, 350.

Tambini, A., Ketz, N., & Davachi, L. (2010). Enhanced brain correlations during rest are related to memory for recent experiences. *Neuron*, *65*(2), 280–90.

Taubert, M., Lohmann, G., Margulies, D. S., Villringer, A., & Ragert, P. (2011). Long-term effects of motor training on resting-state networks and underlying brain structure. *Neuroimage*, *57*(4), 1492–8.

Tenforde, T. S., Gaffey, C. T., Moyer, B. R., & Budinger, T. F. (1983). Cardiovascular alterations in Macaca monkeys exposed to stationary magnetic fields: experimental observations and theoretical analysis. *Bioelectromagnetics*, *4*(1), 1–9.

Tervaniemi, M., Castaneda, A., & Knoll, M., M.and Uther. (2006). Sound processing in amateur musicians and nonmusicians: event-related potential and behavioral indices. *Neuroreport*, *17*(11), 1225–1228.

Tervaniemi, M., Just, V., Koelsch, S., Widmann, A., & Schroger, E. (2005). Pitch discrimination accuracy in musicians vs nonmusicians: an event-related potential and behavioral study. *Exp Brain Res*, *161*(1), 1–10.

Thierry, G., Giroud, A. L., & Prica, C. (2003). Hemispheric dissociation in access to the human semantic system. *Neuron*, *38*, 499–506.

Thut, G., Nietzel, A., Brandt, S. A., & Pascual-Leone, A. (2006). Alpha-band electroencephalographic activity over occipital cortex indexes visuospatial attention bias and predicts visual target detection. *J Neurosci*, *26*(37), 9494–502.

Urner, M., Schwarzkopf, D. S., Friston, K., & Rees, G. (2013). Early visual learning induces long-lasting connectivity changes during rest in the human brain. *Neuroimage*, *77*, 148–56.

Vahdat, S., Darainy, M., Milner, T. E., & Ostry, D. J. (2011). Functionally specific changes in resting-state sensorimotor networks after motor learning. *J Neurosci*, *31*(47), 16907–15.

Vasios, C. E., Angelone, L. M., Purdon, P. L., Ahveninen, J., Belliveau, J. W., & Bonmassar, G. (2006). EEG/(f)MRI measurements at 7 Tesla using a new EEG cap ('InkCap'). *Neuroimage*, *33*(4), 1082–92.

Volberg, G., Kliegl, K., Hanslmayr, S., & Greenlee, M. W. (2009). EEG alpha oscillations in the preparation for global and local processing predict behavioral performance. *Hum Brain Mapp*, *30*(7), 2173–83.

von Stein, A., Chiang, C., & Koenig, P. (2000). Top-down processing mediated by interareal synchronization. *Proc Natl Acad Sci U S A*, *97*(26).

Waldmann, H. C. (2008). Kurzformen des HAWIK-IV: Statistische Bewertung in verschiedenen Anwendungsszenarien. *Diagnostica*, *54*(4), 202–210.

Wan, C. Y. & Schlaug, G. (2010). Music making as a tool for promoting brain plasticity across the life span. *Neuroscientist*, *16*(5), 566–77.

Ward, L. M. (2003). Synchronous neural oscillations and cognitive processes. *Trends Cogn Sci*, *7*(12), 553–559.

Wechsler, D. (1997). Wechsler Adult Intelligence Scale–3rd Edition (WAIS-III). *San Antonio, TX, Harcourt Assessment.*

Weissman-Fogel, I., Moayedi, M., Taylor, K. S., Pope, G., & Davis, K. D. (2010). Cognitive and default-mode resting state networks: do male and female brains 'rest' differently? *Hum Brain Mapp*, *31*(11), 1713–26.

Williamson, V. J., Baddeley, A. D., & Hitch, G. J. (2010). Musicians' and nonmusicians' short-term memory for verbal and musical sequences: comparing phonological similarity and pitch proximity. *Mem Cognit*, *38*(2), 163–75.

Wu, J., Srinivasan, R., Kaur, A., & Cramer, S. C. (2014). Resting-state cortical connectivity predicts motor skill acquisition. *Neuroimage*, *91*, 84–90.

Yarnykh, V. L. (2007). Actual flip-angle imaging in the pulsed steady state: a method for rapid three-dimensional mapping of the transmitted radiofrequency field. *Magn Reson Med*, *57*(1), 192–200.

Yekutieli, D. & Benjamini, Y. (1999). Resampling-based false discovery rate controlling multiple test procedures for correlated test statistics. *J Stat Plan Inf*, *82*, 171–196.

Zakrzewska, M. Z. & Brzezicka, A. (2014). Working memory capacity as a moderator of load-related frontal midline theta variability in Sternberg task. *Front Hum Neurosci*, *8*, 399.

Zalesky, A., Fornito, A., & Bullmore, E. T. (2010). Network-based statistic: identifying differences in brain networks. *Neuroimage*, *53*(4), 1197–207.

Zatorre, R. J. & Belin, P. (2001). Spectral and temporal processing in human auditory cortex. *Cereb Cortex*, *11*(10), 946–953.

Zatorre, R. J., Chen, J. L., & Penhune, V. B. (2007). When the brain plays music: auditory-motor interactions in music perception and production. *Nat Rev Neurosci*, *8*(7), 547–58.

Zuk, J., Benjamin, C., Kenyon, A., & Gaab, N. (2014). Behavioral and neural correlates of executive functioning in musicians and non-musicians. *PLoS One*, *9*(6), e99868.

List of Figures

List of Tables

APPENDIX A

Supplementary Figures

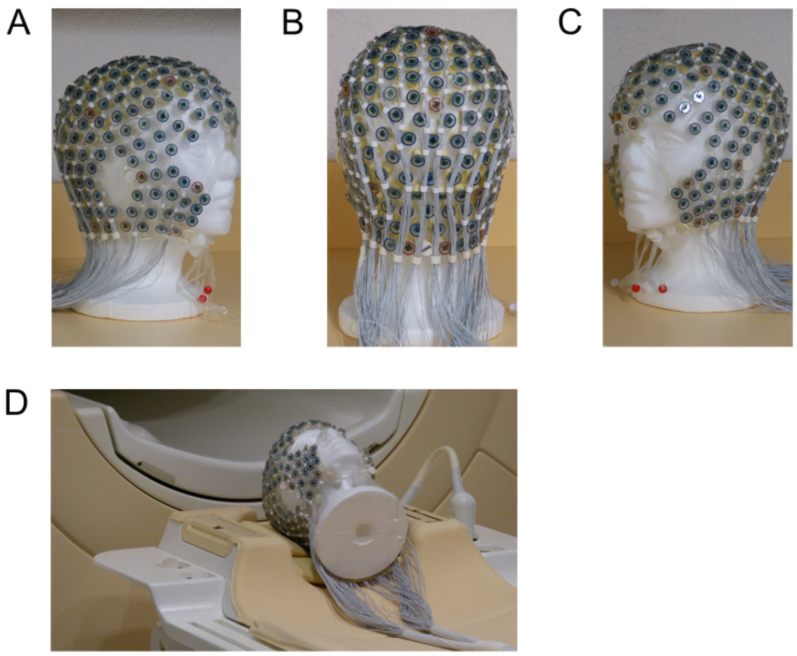

Figure A.1: The high-density EEG cap used in the present study from A) left, B) the back, C) right, and D) how it is placed in the scanner. The electrodes are distributed equally over the subject's head and the electrode wires are bundled posterior, leaving the scanner under the subject's back in two main bundles.

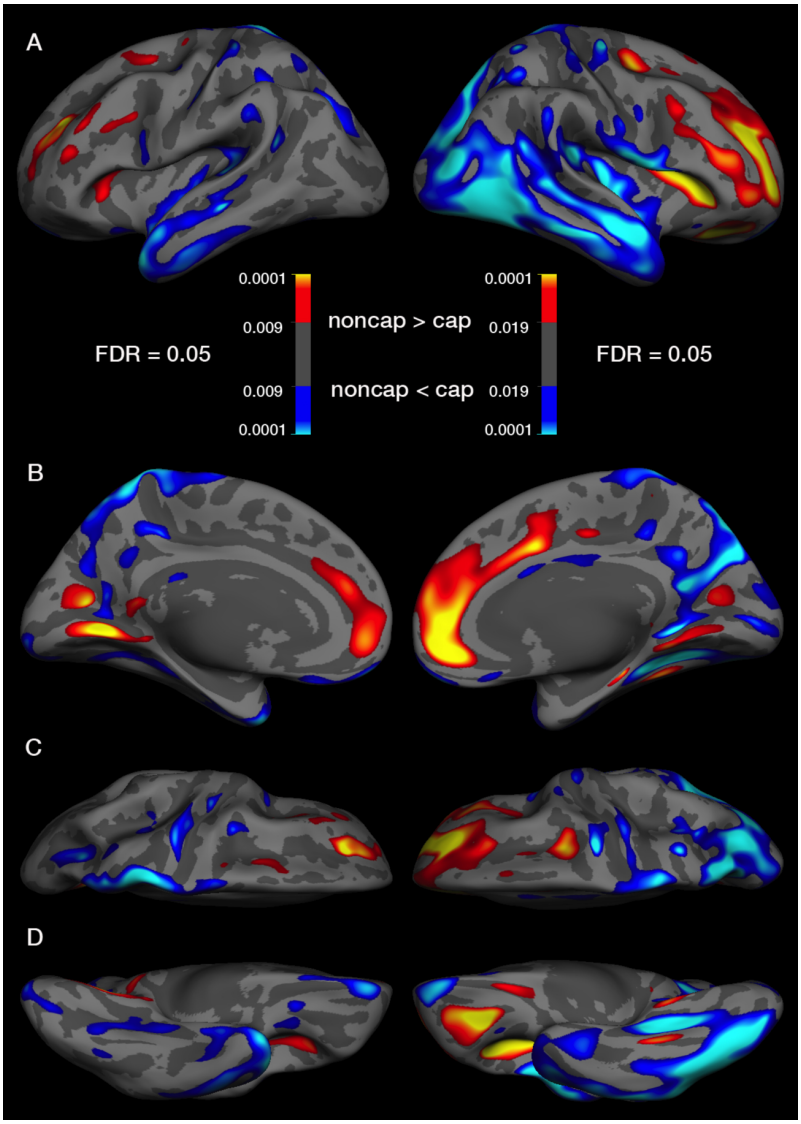

Figure A.2: The influence of the high-density EEG net on cortical surface area measurement derived from surface-based morphometry of T1-weighted images shown on A) lateral, B) medial, C) superior, and D) inferior view of the left (left column) and right (right column) hemisphere. Blue indicates an increased and yellow-red a decreased cortical surface area when subjects do wear the EEG cap in the scanner (paired t-test, FDR = 0.05 false discovery rate corrected). The color bar represents FDR corrected p-values.

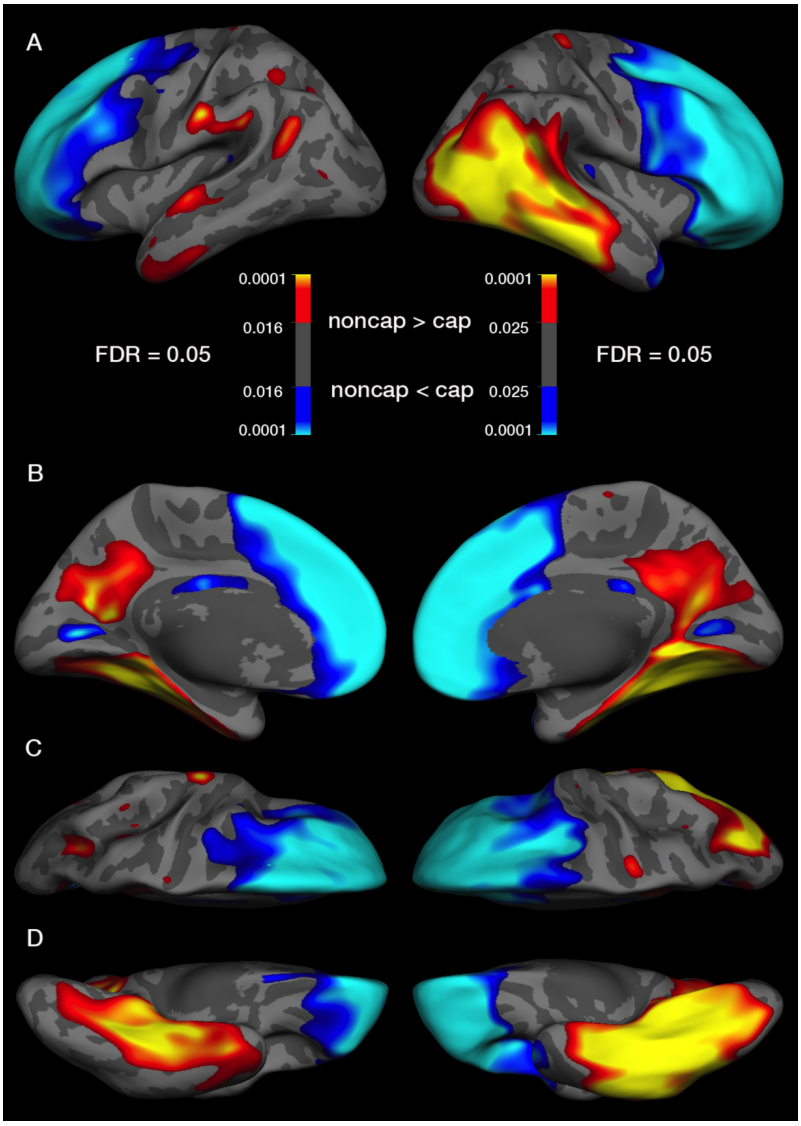

Figure A.3: The influence of the high-density EEG net on cortical volume measurement derived from surface-based morphometry of T1-weighted images shown on A) lateral, B) medial, C) superior, and D) inferior view of the left (left column) and right (right column) hemisphere. Blue indicates an increased cortical volume over the frontal lobe when subjects do wear the EEG cap in the scanner, whereas yellow-red regions indicate a decreased cortical volume (paired t-test, FDR $= 0.05$). The color bar represents FDR corrected p-values.

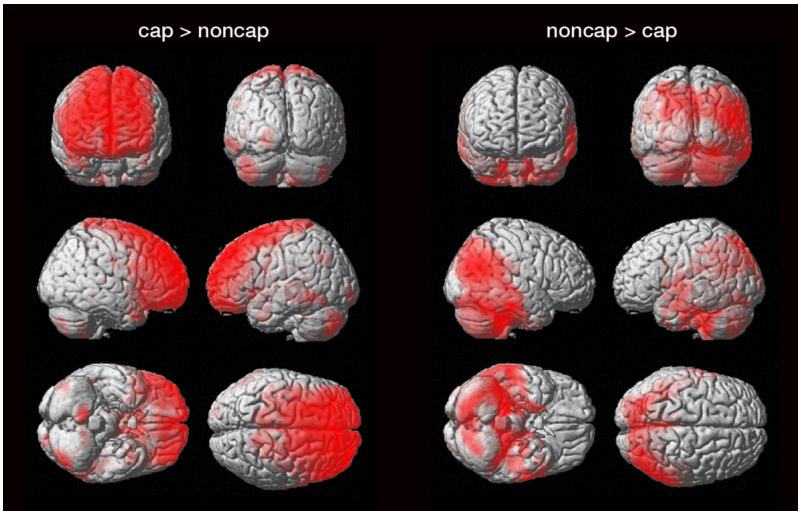

Figure A.4: Voxel-based morphometry; effects of grey matter density for the contrasts cap > noncap (left column) and noncap > cap (right column; paired *t*-test, $T_{12} = 3.93$, $p < 0.001$ uncorrected, $k > 20$ voxels).

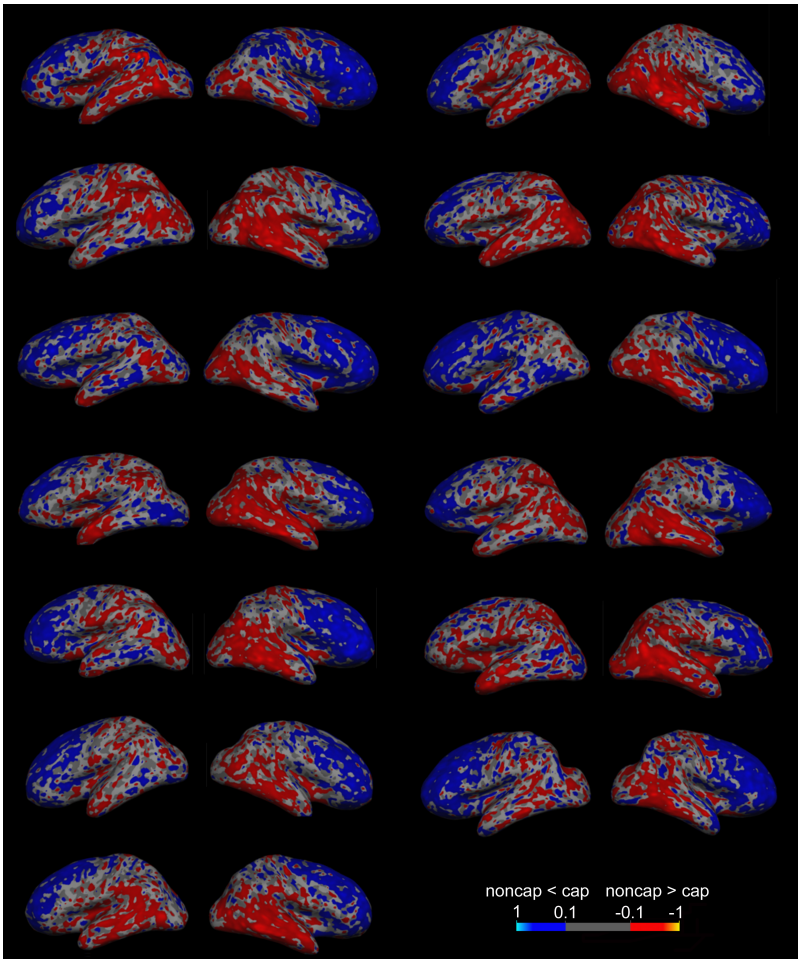

Figure A.5: The influence of the high-density EEG net on cortical thickness measurement derived from surface-based morphometry of T1-weighted images shown on lateral view of the left and right hemispheres per individual subject. Blue indicates increased cortical thickness over the frontal lobe when subjects do wear the EEG cap in the scanner, whereas yellow-red regions indicate decreased cortical thickness over the temporal, occipital, and parietal lobe. Color bar represents thickness differences in [mm].

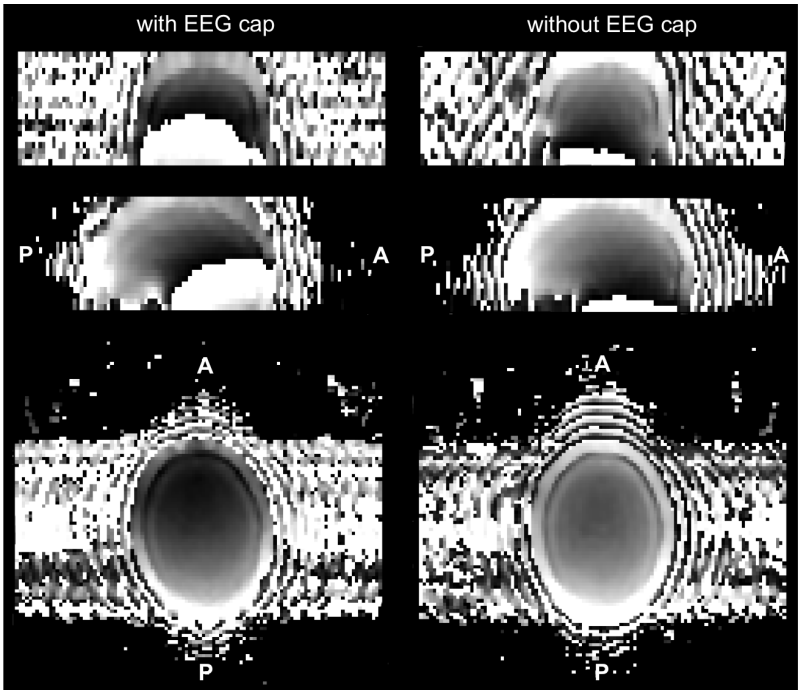

Figure A.6: Frontal B_1 field inhomogeneities (raw data) on the example of one subject caused by the high-density EEG cap (left) and without the EEG cap (right). Upper row: frontal view, middle row: sagittal view, lower row: horizontal view. The more homogenous the shade of grey, the more homogenous is the B_1 field.

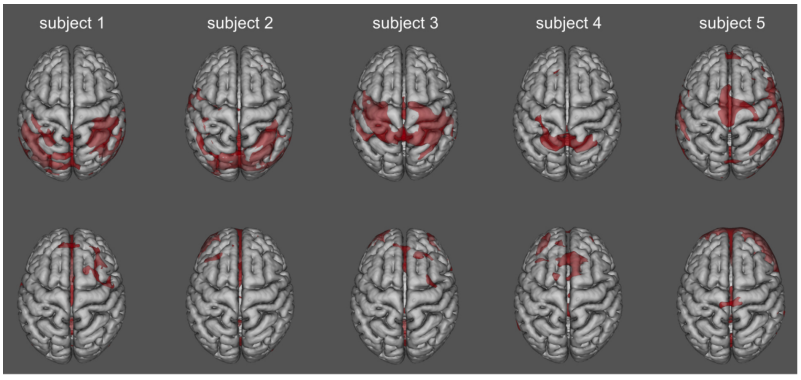

Figure A.7: z-transformed B_0 field maps of the five individual subjects who entered the group level analyses, reflecting the contrasts cap > noncap (upper row) and noncap > cap (lower row). z-maps are thresholded with z-value > 1.96 ($p < 0.05$).

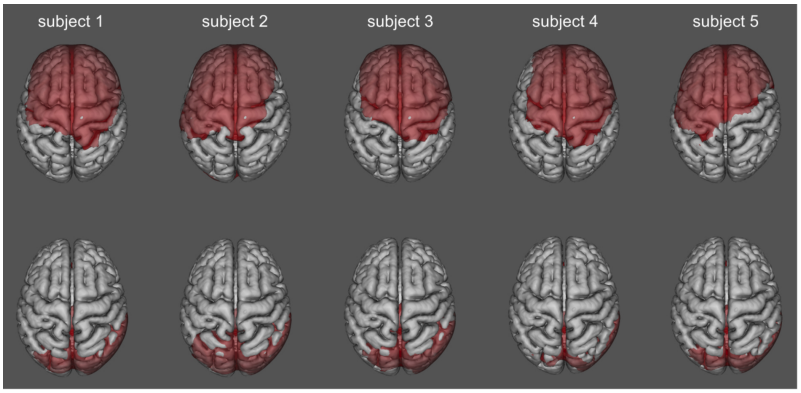

Figure A.8: z-transformed B_1 field maps of the five individual subjects who entered the group level analysis, representing the contrasts cap > noncap (upper row) and the noncap > cap (lower row). z-maps are thresholded with z-value > 1.96 ($p < 0.05$).

Table A.1: Global and subcortical volumes of the left hemisphere (in [cm^3]; paired *t*-test).

Structure [cm^3]	With EEG cap		Without EEG cap		p-value
	Mean	SD	Mean	SD	
Cerebral grey matter volume	237.65	17.21	236.81	18.05	0.51260
Cerebral white matter volume	245.04	21.88	241.99	21.09	0.00001
Cerebellar grey matter volume	50.59	4.76	14.48	1.52	0.00060
Cerebellar white matter volume	14.15	1.68	14.48	1.52	0.08220
Caudate nucleus	4.02	0.54	3.89	0.53	0.00003
Putamen	6.06	0.89	5.95	0.92	0.00680
Pallidum	1.80	0.22	1.83	0.21	0.03340
Hipppocampus	4.30	0.40	4.43	0.37	0.00030
Amygdala	1.54	0.19	1.72	0.22	0.00020
Nucleus accumbens	0.64	0.09	0.63	0.09	0.47880
Ventral diencephalon	4.05	0.42	4.03	0.38	0.54830
Lateral ventricle	7.16	2.91	6.76	2.92	0.00001
Inferior lateral ventricle	0.30	0.11	0.23	0.10	0.00070

Table A.2: Global and subcortical volumes of the right hemisphere (in [cm^3]; paired t-test).

Structure [cm^3]	With EEG cap		Without EEG cap		p-value
	Mean	SD	Mean	SD	
Cerebral grey matter volume	235.69	14.62	237.17	17.05	0.35500
Cerebral white matter volume	245.42	21.35	243.06	21.94	0.00310
Cerebellar grey matter volume	51.11	5.36	53.59	5.60	0.000000003
Cerebellar white matter volume	14.23	1.69	15.11	1.39	0.00610
Caudate nucleus	4.11	0.54	3.94	0.48	0.00020
Putamen	5.68	0.90	5.50	0.86	0.00050
Pallidum	1.64	0.24	1.67	0.26	0.00440
Hipppocampus	4.49	0.42	4.60	0.47	0.01000
Amygdala	1.74	0.23	1.83	0.22	0.00080
Nucleus accumbens	0.68	0.14	0.69	0.14	0.51710
Ventral diencephalon	3.92	0.38	3.88	0.35	0.07300
Lateral ventricle	6.42	1.99	6.02	1.99	0.00003
Inferior lateral ventricle	0.27	0.13	0.23	0.13	0.00002

Table A.3: Global, corpus callosum, brain stem, and cerebrospinal fluid volumes (in [cm^3]; paired t-test).

Structure [cm^3]	With EEG cap		Without EEG cap		p-value
	Mean	SD	Mean	SD	
Supratentorial volume	1070.08	79.77	1064.55	82.09	0.06
Total grey matter volume	655.51	41.35	660.97	45.53	0.06
Subcortical grey matter volume	182.17	15.52	186.98	16.00	0.0000001
Total white matter volume	490.45	43.18	485.05	42.96	0.00002
Corpus callosum posterior	0.90	0.14	0.89	0.14	0.46230
Corpus callosum mid-posterior	0.39	0.09	0.39	0.08	0.77510
Corpus callosum central	0.41	0.09	0.42	0.09	0.00520
Corpus callosum mid-anterior	0.41	0.06	0.42	0.06	0.00050
Corpus callosum anterior	0.86	0.10	0.87	0.09	0.45590
3rd-Ventricle	0.96	0.17	0.92	0.14	0.00760
4th-Ventricle	1.98	0.41	1.86	0.37	0.00060
Brain-Stem	21.28	2.00	21.69	2.06	0.00004
CSF	1.26	0.15	1.26	0.14	0.95070

Curriculum Vitae

Personal Information

Name	Carina Klein
Date of birth	08.04.1987
Nationality	German

Education

02/12 - 05/15	**Ph.D. Student** University of Zurich (Switzerland) Prof. Dr. Lutz Jäncke, Institute of Psychology, Division Neuropsychology Funded by the Swiss National Science Foundation (SNSF)
Graduate School	Neuroscience Center Zurich (ZNZ) International Ph.D. Program in Neuroscience
09/09 - 10/11	**Master of Science in Biology** ETH Zurich (Swiss Federal Institute of Technology, Switzerland)
10/06 - 06/09	**Bachelor of Science in Biology** Technische Universität Kaiserslautern (Germany)
03/06	**Abitur** Burggymnasium Kaiserslautern (Germany)

Publications

Bachmann, V., **Klein, C.**, Bodenmann, S., Schäfer, N., Berger, W., Brugger, P., Landolt, H.P. (2012). The BDNF Val66Met polymorphism modulates sleep intensity: EEG frequency- and state-specificity. *Sleep*, 35(3):335-44. doi: 10.5665/sleep.1690.

Elmer, S.*, **Klein, C.***, Kühnis, J., Liem, F., Meyer, M., Jäncke, L. (2014). Music and language expertise influence the categorization of speech and musical sounds: Behavioural and electrophysiological measurements. *Journal of Cognitive Neuroscience*, 26(10):2356-2369. doi: 10.1162/jocn_a_00632.

Klein, C.*, Hänggi, J.*, Luechinger, R., Jäncke, L. (2015). MRI with and without a high-density EEG cap–what makes the difference? *NeuroImage*, 106:189-197. doi: 10.1016/j.neuroimage.2014.11.053.

Klein, C., Diaz-Hernandez, L., Koenig, T., Elmer, S., Kottlow, M., Jäncke, L. (2015). The influence of pre-stimulus EEG activity on reaction time during a verbal Sternberg task is related to musical expertise. (accepted for publication in *Brain Topography*. doi: 10.1007/s10548-015-0433-7).

Klein, C., Liem, F., Hänggi, J., Elmer, S., Jäncke, L. (2015). The 'silent' imprint of musical training. (under review)

*These authors contributed equally to the study.